(19) OFICIUL DE STAT
PENTRU INVENŢII ŞI MĂRCI
Bucureşti

ROMÂNIA

(11) **RO 134513 A2**
(51) **Int.Cl.**
F25B 15/06 (2006.01)

(12) # CERERE DE BREVET DE INVENŢIE

(21) Nr. cerere: **a 2019 00229**

(22) Data de depozit: **09/04/2019**

(41) Data publicării cererii:
30/10/2020 BOPI nr. **10/2020**

(71) Solicitant:
• **UNIVERSITATEA TEHNICĂ "GHEORGHE ASACHI" DIN IAŞI**, *STR. PROF. DR. DOC. DIMITRIE MANGERON NR. 67, IAŞI, IS, RO*

(72) Inventatori:
• **VERDEŞ MARINA**, *STR. TEASCULUI, NR.44, IAŞI, IS, RO;*
• **BURLACU ANDREI**, *STR. NECULAU NR.14, BL.578, SC.A, PARTER, AP.1, IAŞI, IS, RO;*
• **ATANASIU MARIUS-VASILE**, *STR. TĂTĂRAŞI NR.70, IAŞI, IS, RO;*
• **BALAN MARIUS- COSTEL**, *STR.TUDOR VLADIMIRESCU NR.15, CÂMPULUNG MOLDOVENESC, SV, RO*

(54) # SISTEM DE RĂCIRE CU ABSORBŢIE ACŢIONAT CU ENERGIE SOLARĂ

(57) Rezumat:

Invenţia se referă la un sistem de răcire cu absorbţie acţionat cu energie solară care poate fi integrat în sistemele de climatizare care echipează clădirile rezidenţiale, putând fi asistat şi de o sursă auxiliară der energie, pe gaze naturale sau electricitate. Sistemul de răcire, conform invenţiei, are capacitatea frigorifică de circa 5 kW, valoare care poate satisface cererea de confort pe piaţa rezidenţială, agentul de încălzire pentru acţionarea procesului de absorbţie fiind preparat cu un colector (**7**) solar, iar şi schimbătoarele de căldură cu plăci, un generator (**5**) de vapori, un vaporizator (**1**) şi un economizor (**4**), dar, în special, schimbătoarele de căldură cu minicanale, un absorbitor (**3**) şi un condensator (**2**) care intră în alcătuirea sistemului, sunt compacte contribuind esenţial la reducerea dimensiunilor maşinii frigorifice, a cantităţii de materiale şi a cantităţii de agent frigorific, implicit la creşterea eficienţei frigorifice, îndeobşte fiind cunoscut faptul că aceste schimbătoare de căldură sunt şi eficiente energetic.

Revendicări: 1
Figuri: 1

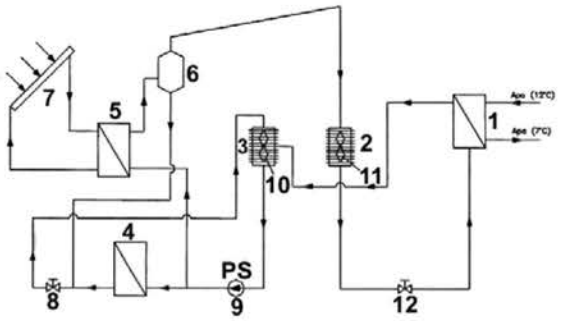

RO 134513 A2

6.

SISTEM DE RĂCIRE CU ABSORBŢIE ACŢIONAT CU ENERGIE SOLARĂ

Invenţia se referă la un sistem de răcire cu absorbţie, cu soluţie hidroamoniacală, acţionat cu energie solară ce poate fi integrat în sistemele de climatizare care echipează clădirile rezidenţiale. Sistemul poate fi asistat şi de o sursă auxiliară de energie, pe gaze naturale sau electricitate.

Sunt cunoscute sistemele pentru climatizarea locală care utilizează instalaţii frigorifice cu comprimare mecanică de vapori, cu compresoare mecanice, acţionate integral cu energie electrică, cu răcire directă, model split sau multisplit.

Utilizarea acestor sisteme prezintă dezavantajul că, în perioadele calde ale anului, când sarcinile de răcire sunt maxime, acestea conduc atât la o supraîncărcare a reţelelor electrice cât şi la costuri de exploatare mari cu efecte nedorite asupra mediului ambiant. Totodată, cea mai mare parte a instalaţiilor frigorifice cu absorbţie care se găsesc, în prezent pe piaţă, sunt de capacităţi mari, de ordinul zecilor, sutelor sau chiar miilor de kW iar, parte din echipamentele care le compun sunt voluminoase şi complexe ca alcătuire, sectorul rezidenţial nebeneficiind de oportunitatea utilizării unui sistem de răcire cu absorbţie compact şi eficient are să acopere cerinţele de confort

Problema pe care o rezolvă invenţia este realizarea unui sistem frigorific cu absorbţie, de capacitate mică, cu putere nominală de circa 5 kW, ce poate fi integrat instalaţiilor de climatizare aferente clădirilor unifamiliale. Sistemul utilizează ca agent de lucru soluţia hidroamoniacală, are un consum de energie, în exploatare, mult redus comparativ cu sistemele care folosesc comprimarea mecanică de vapori, este prietenoas cu mediul ambiant deoarece utilizează un agent frigorific natural, este compact şi poate fi considerat o alternativă atractivă pentru beneficiarii rezidenţiali.

Sistem de răcire cu absorbţie acţionat cu energie solară, de capacitate frigorifică redusă, cu agent de lucru soluţia hidroamoniacală, conform invenţiei, înlătură dezavantajele enumerate mai sus, prin aceea că, este echipat cu schimbătoare de căldură compacte, două dintre acestea, absorbitorul şi condensatorul, fiind schimbătoare cu microcanale. Propunerea de compactizare a componentelor principale are ca rezultat atât reducerea dimensiunii sistemului în ansamblu, cât şi diminuarea cantităţii de agent frigorific utilizat.

Invenţia prezintă următorul avantaj major:

- Poate asigura cerinţa de confort în perioadele calde din an pentru consumatorii rezidenţiali care necesită capacităţi de frig reduse, 4-5 kW, prin intermediul unui sistem frigorific acţionat solar care integrează schimbătoare de căldură compacte, cu minicanale şi plăci aspect ce conduce la reducerea dimensiunilor maşinii frigorifice, a cantităţii de materiale înglobate în structura sa şi a cantităţii de agent frigorific, implicit la creşterea eficienţei frigorifice, îndeobşte fiind cunoscut faptul că aceste schimbătoare de căldură sunt şi eficiente energetic.

Se prezintă în continuare un exemplu de realizare a invenţiei în legătură cu figura 1 care reprezintă schema generală de funcţionare a sistemului de răcire.

Sistem frigorific cu absorbţie acţionat cu energie solară, conform invenţiei, are puterea frigorifică nominală de circa 5 kW şi utilizează ca agent de lucru soluţia hidroamoniacală iar agentul de încălzire pentru acţionarea procesului de absorbţie, conform invenţiei, este preparat prin intermediul colectorului solar **(7)** sau printr-un echipament ce utilizează enegia convenţională dacă cea solară nu este disponibilă.

În schimbătorul de căldură în plăci, numit generator de vapori **(5),** are loc fierberea soluţiei hidroamoniacale care este o soluţie bogată în amoniac şi care devine săracă în amoniac prin traversarea separatorului de lichid **(6)**, astfel încât, în schimbătorul de căldură cu minicanale, condensatorul **(2),** ajung vapori puri de amoniac ce condensează, iar lichidul rezultat este apoi laminat în ventilul de laminare **(12)** şi ajunge, după aceea, în schimbătorul de căldura cu plăci, vaporizatorul **(1),** unde vaporizează.

Vaporii rezultaţi din vaporizatorul **(1)** sunt absorbiţi în schimbătorul de căldură cu minicanale, absorbitorul **(3),** unde se reface soluţia bogată în amoniac, care este apoi preîncălzită în schimbătorul de căldură în plăci, economizorul **(4)** fiind preluată după aceea, de pompa de soluţie **(9)** şi refulată în generatorul de vapori **(5)**.

Soluţia bogată, este răcită în economizorul **(4)**, apoi laminată în ventilul de laminare **(8)** şi absorbită în absorbitorul **(3)** unde se combină cu vaporii de amoniac, refăcându-se astfel soluţia bogată.

Pentru eliminarea căldurii de absorbţie şi de condensare se foloseşte, ca agent de răcire, aerului activat de ventilatoarele **(10)** şi **(11).**

Bibliografie

1. Roberto Best Y Brown - ADVANCED SOLAR COOLING SYSTEM (SOLAR-GAX CYCLE)., Brevet Nr. MXPA03006027, 2014

2. M.Verdeş, A.Şerban, A.Verdeş, MC.Balan – ANALIZA ŞI INGINERIA VALORII ÎN CLIMATIZAREA DE CONFORT, Ed.Tehnopress, ISBN978-606-687-343-7

Revendicare

1. Sistemul frigorific cu absorbţie acţionat cu energie solară se **caracterizată prin aceea că** are capacitatea frigorifică de circa 5 kW, valoare care poate satisface cererea de confort pe piaţa rezidenţială, agentul de încălzire pentru acţionarea procesului de absorbţie fiind preparat cu colectorul solar **(7)** iar şi schimbătoarele de căldură cu plăci, generatorul de vapori **(5)**, vaporizatorul **(1)** şi economizorul **(4)** dar, în special, schimbătoarele de căldură cu minicanale, absorbitorul **(3)** şi condensatorul **(2)** care intră în alcătuirea sistemului, sunt compacte contribuind esenţial la reducerea dimensiunilor maşinii frigorifice, a cantităţii de materiale şi a cantităţii de agent frigorific, implicit la creşterea eficienţei frigorifice, îndeobşte fiind cunoscut faptul că aceste schimbătoare de căldură sunt şi eficiente energetic.

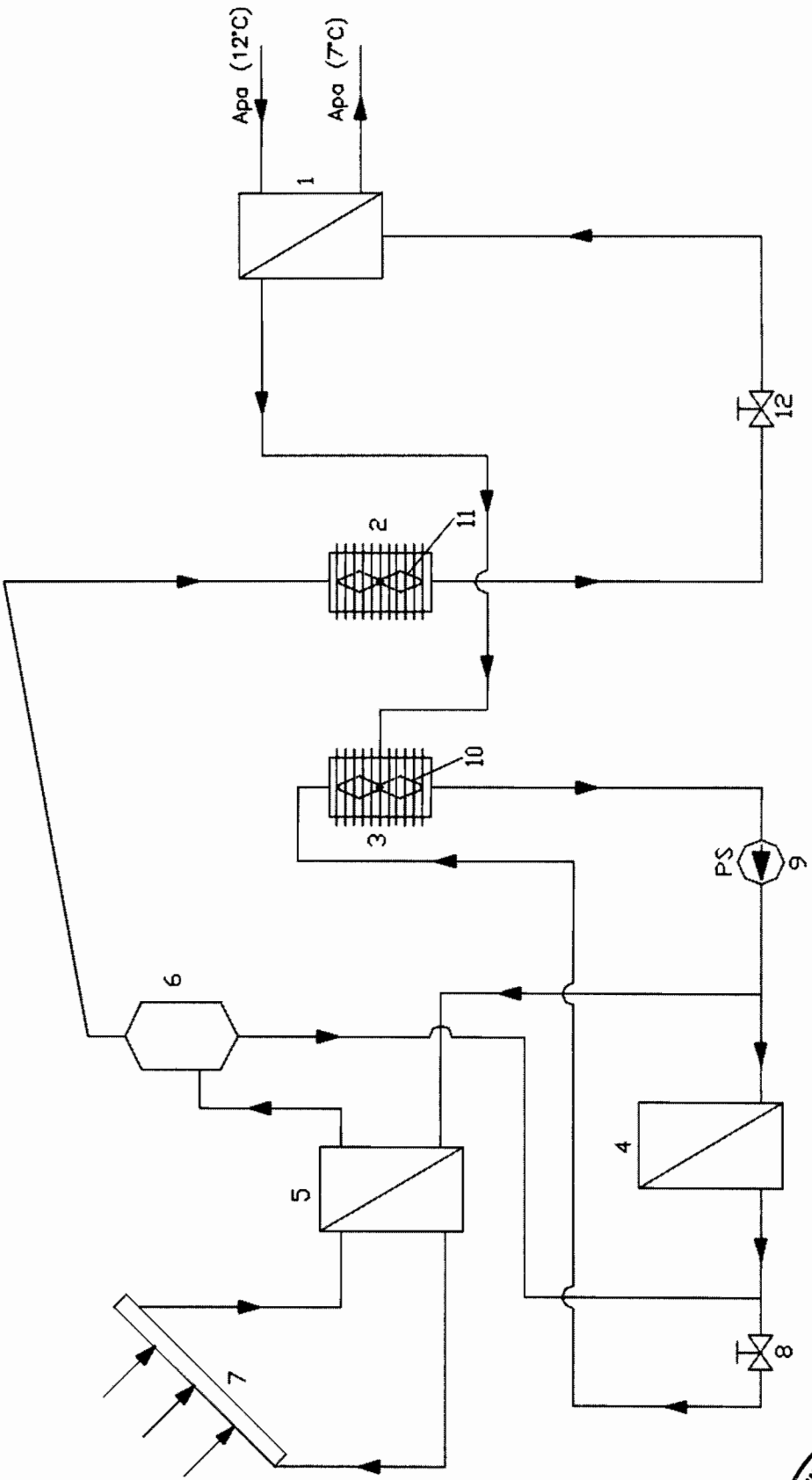

Figura 1

sustainability

MDPI

Article

Strategic Optimization of Operational Parameters in a Low-Temperature Waste Heat Recovery System: A Numerical Approach

Ștefănica Eliza Vizitiu [1,*], Chérifa Abid [2], Andrei Burlacu [1], Robert Ștefan Vizitiu [1] and Marius Costel Balan [1]

[1] Faculty of Civil Engineering and Building Services, "Gheorghe Asachi" Technical University of Iasi, 700050 Iasi, Romania; andrei.burlacu@academic.tuiasi.ro (A.B.); robert-stefan.vizitiu@academic.tuiasi.ro (R.Ș.V.); marius-costel.balan@academic.tuiasi.ro (M.C.B.)

[2] CNRS Centre National de la Recherche Scientifique (National Centre for Scientific Research), IUSTI Institut Universitaire des Systèmes Thermiques Industriels (University Institute of Industrial Thermal Systems), UMR 7343, Aix-Marseille Université, 13453 Marseille, France; cherifa.abid@univ-amu.fr

* Correspondence: stefanica-eliza.vizitiu@student.tuiasi.ro

Abstract: In the transition to sustainable energy consumption, waste heat recovery and storage systems become key to advancing Europe's energy efficiency and reducing carbon emissions, especially by harnessing thermal energy from low-temperature sources like wastewater. This study focuses on optimizing a heat recovery system that uses heat pipes for effective heat extraction and coconut oil as a phase change material for efficient thermal storage. A total of 12 numerical simulations were conducted to analyze the outcomes of varying operational parameters, including the diameter of the heat pipe, condenser size, secondary agent flow rate, coil length, and primary agent inlet temperature. The numerical findings indicate that reduced flow rates, in combination with smaller condenser diameters and increased primary agent temperatures, greatly improve the efficiency of heat absorption and transfer. Following a 4 h test period, the most successful outcome resulted in a melting fraction of 98.8% and a temperature increase of 18.95 °C in the output temperature of the secondary agent. In contrast, suboptimal conditions resulted in only a 2.21 °C rise and a 30.80% melting fraction. The study highlights the importance of component sizing and optimization, noting that strategic modifications and appropriate phase change materials can lead to highly efficient and scalable systems.

Keywords: waste heat recovery; thermal energy storage; optimization

Citation: Vizitiu, Ș.E.; Abid, C.; Burlacu, A.; Vizitiu, R.Ș.; Balan, M.C. Strategic Optimization of Operational Parameters in a Low-Temperature Waste Heat Recovery System: A Numerical Approach. *Sustainability* **2024**, *16*, 7013. https://doi.org/10.3390/su16167013

Academic Editors: Dalia Patino-Echeverri, Isaac Dyner and Camila Ochoa

Received: 14 June 2024
Revised: 26 July 2024
Accepted: 13 August 2024
Published: 15 August 2024

1. Introduction

The necessity to shift towards more sustainable energy consumption is growing in light of the challenges presented by economic expansion and environmental constraints [1]. Both national and European levels acknowledge decarbonizing the energy system as an essential objective in the fight against climate change. Reducing emissions, increasing energy efficiency, and moving Europe toward at least 40% final energy consumption from renewable sources are among the energy sector's main goals by 2030 [2]. In light of the increasing global emphasis on clean energy and improved energy management, it is essential to underscore the significance of these approaches, especially in the European Union. Within this particular context, buildings play a substantial role in both energy consumption and carbon dioxide (CO_2) emissions, accounting for 40% of energy consumption and contributing significantly to 36% of emissions across the entire area [3]. The idea of recovering waste heat has been a prominent focus in current energy-related approaches, indicating an increasing level of attention and acknowledgment of its potential to capture, utilize, and reuse excess thermal energy [4]. Furthermore, the ongoing investigation and development of waste heat

recovery systems are currently at the forefront of research efforts, as underscored by the studies conducted by [5–8]. Current research underscores the significant potential of waste heat recovery systems; yet, there are specific knowledge gaps in optimizing these systems for low-temperature applications, enhancing energy storage efficiency, and integrating multiple components for both heat recovery and storage. While recovering energy from buildings and the industrial sector has received a lot of interest, the process of water heating contributes to an important amount of energy usage [8]. The discharge of wastewater from various sources, including residential, commercial, and industrial activities, offers an important amount of thermal energy. This energy is typically overlooked as a potential source of heat loss in terms of energy recovery, but it presents promising opportunities for improving energy efficiency while making a valuable contribution to global efforts against climate change [9].

As noted by [10], several technologies, ranging from economizers to waste heat boilers and heat pipe systems, have demonstrated the potential to capture, recover, and exchange significant amounts of thermal energy that would normally be lost in different processes. Heat pipes, recognized for their remarkable efficiency and versatility, hold a pivotal position in heat recovery technologies [11]. Functioning as thermal superconductors, they facilitate rapid heat transfer with additional benefits such as low operational costs and easy maintenance [12]. From isothermal processes to heat flux transformation, the diverse applications of heat pipes make them a preferred choice across various industries for efficient heat recovery and management [13,14]. Heat pipes have undergone significant advancements and are now considered essential elements for successfully integrating into heat exchangers, due to their numerous advantages and capabilities. Heat pipe heat exchangers usually have a small design that is both cost-effective and allows for the effective recuperation of thermal energy without requiring additional power sources. Moreover, the distinct benefit of heat pipe heat exchangers lies in their nearly uniform temperature distribution, emphasizing their substantial value in a wide range of applications [14]. Furthermore, their compact design facilitates the efficient adjustment of heat flux transfer, allowing for versatility in applications like preheating or heating air in conditioning systems and generating domestic hot water [10,11]. As researchers continue to focus on optimizing heat pipe heat exchangers, numerous studies provide important insights that could enhance these systems for a wide variety of applications.

In their study, ref. [15] conducted a CFD (Computational Fluid Dynamics) heat transfer analysis for a heat pipe system designed for waste heat recovery in buildings. The study focused on developing an innovative heat exchanger utilizing the return of the existing heating system, demonstrating its adaptability to varying secondary agent flow rates and different primary agent temperatures. The system exhibited successful performance, achieving favorable secondary agent temperatures even with increased flow rates and lower temperatures for the primary agent. Additionally, the introduction of heat transfer rings further enhanced heat transfer efficiency. Ref. [16] explored the optimization of a water-to-water heat pipe heat exchanger for effective waste heat recovery in the steel industry. Notably, they found that an increase in wastewater flow rate from 0.83 m^3/h to 1.87 m^3/h enhanced exergy efficiency from 34% to 41%, despite a decrease in system effectiveness. The findings not only revealed the impact of varying wastewater mass flow rates but also identified optimal flow rates at 1.20 m^3/h for wastewater and 3.00 m^3/h for fresh water. Their research not only underlines the intricate balance between flow rates and system efficiency but also points towards the importance of maintenance and structural optimization in sustaining the system's performance. Building upon this, the subsequent study [17] further analyzed heat pipe heat exchangers (HPHE) in the steel industry, particularly focusing on slag cooling. Consistent with the previous findings, increasing the wastewater flow rate improves effectiveness but reduces exergy efficiency, pinpointing optimal flow rates of wastewater at 1.40 m^3/h and cold-water mass flow rates and 2.90 m^3/h. Both studies confirm that online cleaning devices have a significant role in enhancing heat transfer performance, reinforcing the importance of maintenance for

optimal HPHE operation. Expanding the application of heat pipe heat exchangers, a distinct study successfully integrated an HPHE into the aluminum industry, recovering 97 kW with a notable 35-month return on investment. Although the theoretical model exhibited a 20% deviation, it suggests the potential for widespread adoption of HPHE, significantly reducing primary energy consumption (476 MWh/year) and estimated CO_2 emissions (86 tCO_2/year) [18]. Another study conducted by [19] highlighted the benefits of incorporating a heat-pipe heat exchanger in a window-type air-conditioning system. The HPHE significantly reduced compressor power consumption, resulting in substantial power savings of 2.01% to 1.33% for different working fluids. This emphasizes the significant role of HPHEs in enhancing air conditioning efficiency and promoting energy savings. To improve overall energy efficiency even more, incorporating advanced energy storage technologies becomes crucial.

As highlighted in the study by [20], efficient thermal energy storage systems, such as those utilizing latent heat, contribute significantly to storing and utilizing industrial waste heat effectively. Studies, such as those by [21,22], emphasize the efficacy of incorporating heat pipes and increasing the number of heat transfer tubes in a phase change material (PCM) for enhancing heat transfer rates in latent heat thermal energy storage systems. The integration of these techniques proves advantageous, with heat pipes demonstrating a two-fold increase in energy transfer during solidification and multitube arrangements, as demonstrated by [22], showcasing faster PCM melting. In their study, ref. [23] developed a low-cost, in-house method for manufacturing heat pipes, achieving an average melting enhancement coefficient of 135% with coconut oil as the PCM, further underscoring the potential for cost-effective heat recovery applications. Furthermore, ref. [24] investigated dynamic thermal management for industrial waste heat recovery using PCM thermal storage and achieved a reduction in daily fossil fuel consumption from 6.81 tons to 6.34 tons and optimized fuel consumption ratios, underscoring the effectiveness of advanced optimization algorithms. Expanding on the insights gained from earlier research, particularly highlighting the importance of effective thermal energy storage systems leveraging latent heat, a recent investigation led by [25] delves into the exploration of an innovative two-stage heat recovery–storage system aimed at mitigating thermal energy losses in industrial settings. By employing heat pipes for recovery and an eco-friendly phase change material for storage, the system demonstrated a peak efficiency of 78.1%, showcasing its substantial capacity for thermal energy recovery. Additionally, a novel triplex-tube heat exchanger proposed by [26] further underscores the potential of new configurations in enhancing storage and recovery processes. Their design, featuring a dual-PCM configuration, significantly improved the rate of melting and solidification. The optimized arrangement achieved 23.43% and 18.87% enhancements in energy storage and recovery, respectively, compared to conventional single-PCM systems. This study highlights the importance of innovative designs and configurations in maximizing the efficiency of these systems intended for heat recovery and storage.

Despite progress in refining these systems to boost heat transfer and energy storage capabilities, ongoing challenges persist in achieving optimal efficiency for low-temperature applications. The current literature often focuses on optimizing single components of heat recovery systems, neglecting the potential benefits of a comprehensive multicomponent approach. At the same time, studies in the literature on waste heat recovery systems predominantly employ heat pipes, neglecting the possibility of storage. Nonetheless, these studies demonstrate the significant potential of heat recovery in various industrial sectors [27–29]. Our study aims to fill this gap by optimizing a waste heat recovery and storage system that utilizes heat pipes and coconut oil as a PCM, focusing on improving heat transfer efficiency for low-temperature applications. Employing numerical simulations, we explored various configurations of the system to identify the most efficient setup for improved performance. Integrating techniques like heat pipes, as investigated by [20,21,30,31], and optimizing the number of heat transfer tubes in PCM and arrangement, as highlighted by [22,32], further accentuates the potential to enhance heat transfer rates in latent heat thermal energy

storage systems. Additionally, an experimental investigation underscores the importance of optimizing temperature gradients to improve efficiency, as the increase of temperature in thermal energy storage systems can effectively enhance heat transfer [33].

The unique contribution of our study lies in the detailed optimization of these components and configurations, providing a comprehensive analysis of their effects on the system. This approach not only addresses challenges in existing systems but also offers a practical framework for improving waste heat recovery and storage. In alignment with these principles, our study aims to contribute to ongoing advancements in efficiently recovering and storing waste thermal energy for sustainable energy consumption. Within the context of the European energy system, the optimization of these systems is particularly relevant. Given the substantial role of buildings in energy consumption and emissions, our research addresses a critical need for efficient heat recovery solutions in residential, commercial, and industrial settings. Specifically, our system can be developed for use in residential settings, coupled with solar thermal panels. The heat pipe heat recovery system can utilize the hot water generated by the solar thermal panels for heat recovery, producing instant hot water for domestic use and storing excess heat within a phase change material for prolonged hot water availability. Additionally, it can be applied in industrial settings, such as in the steel and aluminum industries, to recover heat from wastewater resulting from various processes, providing instant hot water for other processes while also offering storage capabilities, improving overall efficiency in industrial processes, and significantly reducing primary energy consumption and CO_2 emissions. We anticipate that the insights gained from this study will offer valuable guidance for optimizing the geometrical design and operational parameters of heat pipe heat recovery and storage systems.

2. Materials and Methods

2.1. The Design of the Heat Pipe Heat Recovery System

This study focuses on the optimization of a heat pipe heat recovery and storage system to enhance heat transfer performance and address the imperative need for energy efficiency. We developed 3D behavioral models to optimize the system's design and gain useful insights into its behavior. We used the educational version of ANSYS 2022 for numerical simulations and Autodesk Inventor 2023 for 3D modeling. Numerical simulations were employed for investigating alternate coil placement and secondary agent flow rates, as well as various design and operating scenarios. The SIMPLE algorithm was applied for efficient pressure-velocity coupling, and second-order upwind schemes were used for the discretization of momentum and energy equations. Our analysis involved several steps to systematically evaluate the system's performance under various conditions. Initially, we developed 3D behavioral models of the heat pipe heat recovery system and then employed numerical simulations to explore different operational scenarios. These simulations were categorized based on varying single parameters to isolate their effects on the system's thermal behavior. Finally, we analyzed the simulation results to identify the most promising design and operational settings.

During this phase of simulations, we conducted the tests on a system comprised of two key sections: the evaporation zone and the condensation zone, both traversed vertically by a single heat pipe. The evaporation zone has a height of 400 mm and a width of 100 mm, while the cylindrical condensation zone reaches a height of 600 mm with a diameter of 150 mm. Both zones are vertically penetrated by a heat pipe, with a diameter of 15 mm and a length of 1000 mm. At first, in our research, we examined two distinct designs. In the first one (Design 1), the coil measures 1916 mm in length, with a total height of 474 mm, featuring 10 turns and a diameter of 15 mm. In contrast, in the second design (Design 2), the coil is 1096 mm long, with a height of 244 mm, a reduced turn count of 5, and a diameter of 15 mm. These designs with different coil lengths help understand how coil dimensions affect the PCM melting behavior and the end temperature of the secondary agent. The heat pipe, which serves as a crucial component in the system, is crafted from copper. The phase change material used is coconut oil, distinguished by its melting point of 25 °C. The coil is

made of copper, while the housings for the evaporator and condenser are made of stainless steel. The system operates by transferring thermal energy from the primary agent in the evaporator to the heat pipe, which subsequently transfers the heat to the condenser zone. Simultaneously, the secondary agent flows through the coil in the condenser, extracting heat from the melted PCM within the condenser. This dual-functionality ensures efficient heat recovery and storage while simultaneously producing warm water that can be utilized for a range of purposes, including domestic hot water supply. The constructive details are illustrated in Table 1.

Table 1. Constructive details of the components.

Design No.	Component Specifications								
	Evaporator		Condenser		Heat Pipe		Coil		
	Height [mm]	Width [mm]	Height [mm]	Diameter [mm]	Length [mm]	Diameter [mm]	Height [mm]	Length [mm]	Diameter [mm]
Design 1	400	100	600	150	1000	15	1916	474	15
Design 2							1096	244	
Design 3						25	1916	474	
Design 4				100					
Design 5				85					

A visual representation of the first two designs and their components is presented in Figure 1.

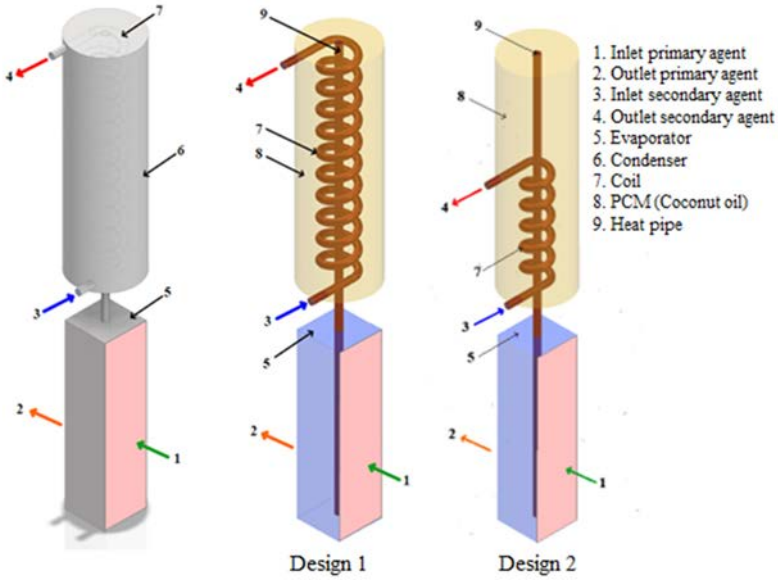

Figure 1. The 3D design of the heat recovery and storage system for Design 1 and Design 2.

After our initial simulations on Design 1 and Design 2, we refined our approach, making adjustments to the condenser and heat pipe dimensions, resulting in three additional constructive models represented in Figure 2. In Design 3, we kept the diameter of 150 mm for the condenser, and simultaneously, we increased the heat pipe diameter from 15 mm to 25 mm, for enhanced heat transfer. Next, we optimized the heat exchange efficiency by reducing the condenser diameter from 150 mm to 100 mm, resulting in what we denote as Design 4. This reduction was anticipated to increase the rate of heat exchange, resulting in faster and more uniform melting by concentrating the thermal energy transfer. In Design 5, we pushed the boundaries by further decreasing the condenser diameter from 100 mm to 85 mm, aiming to achieve higher thermal efficiency and heat transfer by concentrating the thermal energy within a smaller volume. These adjustments reflect our commitment to

refining the system's performance under varying conditions, with Design 1 serving as the baseline for our subsequent optimizations and explorations.

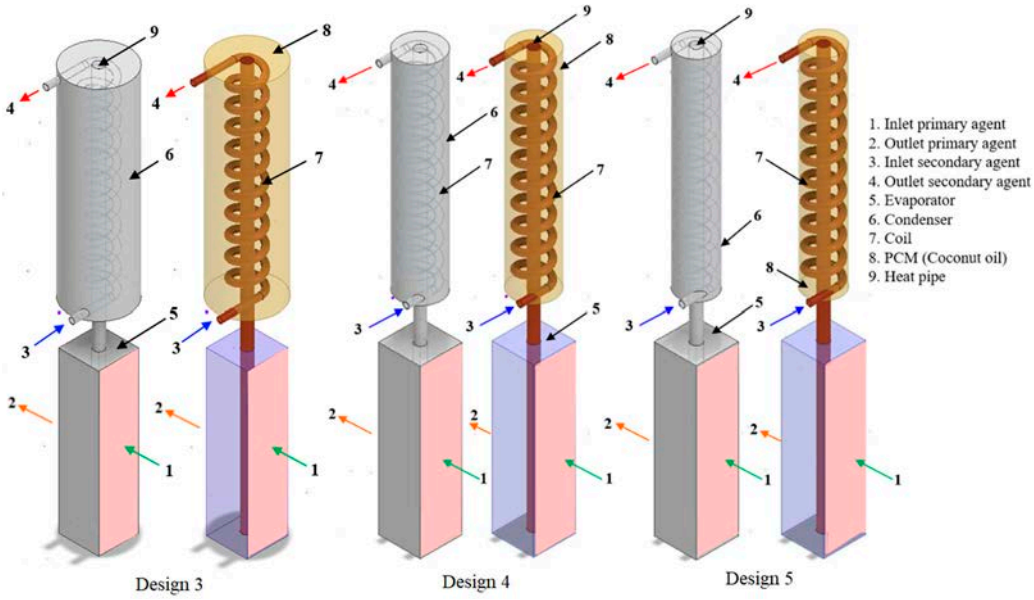

Figure 2. The 3D design of the heat recovery and storage system for Design 3, Design 4, and Design 5.

To systematically evaluate the impact of each design and operational parameter, simulations were grouped based on single-variable variation, allowing for a clear analysis of each parameter's influence on system performance. Group A investigated how varying the secondary agent flow rate affected system melting behavior and heat transfer characteristics, while Groups B and C examined the impact of different coil lengths on the system. Group D assessed how changing the heat pipe diameter influenced thermal transfer within the system, while Group E evaluated the effect of different condenser diameters on the system's heat exchange efficiency. Groups F and G examined the thermal response of the system to varying primary agent inlet temperatures. These groups and their corresponding details are presented in Section 2.5 along with the relevant tables and parameters.

The criteria for evaluating the performance of each design were primarily based on two key metrics: the melting percentage of the phase change material and the outlet temperature of the secondary agent. A higher melting percentage of the PCM signifies higher thermal storage capacity, while elevated outlet temperatures of the secondary agent demonstrate more efficient heat transfer and absorption.

2.2. Numerical Approach

In the simulation stage, we imported the three-dimensional geometries that were initially created using Autodesk Inventor into the Ansys-Fluent framework so that we could perform precise analyses. The meshing process, essential for numerical simulations, unfolded within the constraints of the academic version, limited to 500,000 elements. Our mesh networks, consisting of 130,000–200,000 nodes, were created using a progressive refinement approach. This was carried out by initially generating a mesh with a lower element count and subsequently increasing the density in critical areas as needed. The aim was to create a high-quality mesh that guarantees accurate representation of thermal behavior while also considering computational efficiency. In our computational analysis, the nodal distribution within the Ansys-Fluent environment was meticulously defined to capture the intricate thermal behaviors in both the evaporation and condensation zones. Specifically, the nodes were concentrated in critical regions within the heat recovery system where temperature gradients, phase change, or fluid flow were expected to exhibit significant variations or complexities. Particular attention was given to areas around the heat pipe and coil interfaces due to their critical roles in heat transfer processes. In areas

where finer details were crucial, such as around bends or junctions where heat and fluid flow might experience abrupt changes, the mesh was refined to increase node density, enhancing the local resolution of the simulation results. Given the different configurations in our study—Design 1 with a longer coil and more turns, and Design 2 with a shorter coil and fewer turns—the nodal distribution was adjusted to reflect the geometric complexities of each design. The node distribution plays an essential part in our simulation method, allowing us to obtain detailed and accurate insights into the heat transfer performance of the heat pipe system under different conceptual and operational scenarios.

2.3. Initial and Boundary Conditions

Our primary objective was to assess the system's thermal dynamics and identify optimal configurations under varying operational conditions. The next step in initiating our simulations involved selecting the appropriate materials and setting the boundary conditions. We chose steel for the evaporator and condenser casings, and copper for the coil and heat pipe due to its large thermal conductivity. Recognizing the computational constraints and the broad scope of our investigation, we opted not to simulate the internal phase change processes. Thus, the heat pipe was modeled as a cylindrical material with a very high thermal conductivity to simulate its heat transfer capabilities within the overall system. The focus was on ensuring that the heat pipe's role in transferring heat between system components was accurately represented, thereby simplifying the model while still capturing the essential functionality needed for our analysis. The working fluids, designated as primary and secondary agents, were both modeled as water to accurately simulate the flow dynamics within the system. Additionally, coconut oil was introduced as a phase change material (PCM) within the condenser.

Given the absence of coconut oil's properties in the Fluent database, we customized its material profile based on the recent literature [34], ensuring an accurate representation of its thermophysical properties. For our simulations, a transient, pressure-based solver was employed to capture the time-dependent responses of the system to various operational scenarios. A laminar flow model was chosen, aligning with the expected flow conditions and the system's physical scale. Boundary conditions were applied, with velocity inlets specified for the primary agent entering the evaporator and the secondary agent flowing through the condenser coil. The inlet parameters—velocity magnitude and temperature—were set for each simulation design to reflect different operational states, as shown in Table 2.

Table 2. Testing parameters.

Design No.	Simulation No.	Boundary Conditions					
		Primary Agent—Water		Secondary Agent—Water		Phase Change Material—Coconut Oil	
		Inlet Temp. [°C]	Flow Rate [L/min]	Inlet Temp. [°C]	Flow Rate [L/min]	Melting Temp. [°C]	Solidification Temp. [°C]
Design 1	S1	70	24	15	1	25	15
	S2				0.1		
	S3				0.05		
Design 2	S4	70			1		
	S5				0.1		
Design 3	S6	70					
	S7						
Design 4	S8	90					
Design 5	S9	50			0.05		
	S10	70					
	S11	50					
	S12	90					

Pressure outlets were defined for both the evaporator and condenser, allowing the fluids to exit the system under controlled conditions. We conducted our analytical exploration across five distinct designs, varying the flow rate of the secondary agent and the inlet temperature of the primary agent. This approach enabled us to systematically evaluate the system's performance across a spectrum of conditions, from higher flow rates and temperatures to more conservative settings. The consistency of the secondary agent's temperature at 15 °C and the primary agent's flow rate at 24 L/min provided a stable baseline for our investigations. The numerical methods chosen ensured a balance between computational efficiency and the accuracy needed to discern the subtle impacts of design and operational adjustments on system behavior.

2.4. Mathematical Modeling

Our study utilizes ANSYS Fluent to simulate dynamic heat transfer and phase change within a heat recovery and storage system. To model our system, we can break it down into three main components (see Figure 2):

- The evaporator: In this part, the hot fluid, known as the primary fluid, circulates. The hot fluid flows at a specified flow rate of 24 L/min, enters at a given temperature (the temperature of the heat source), and exits at a temperature T_0 °C;
- The condenser: This section is filled with PCM and is traversed by the upper part of the heat pipe. A coil, immersed in the PCM and surrounding the heat pipe, allows cold water to enter and absorb energy from both the heat pipe and the PCM, thus heating up;
- Heat Pipe: To simplify the calculations, we modeled the heat pipe as a solid cylinder with very high thermal conductivity of 5000 W/m·K to simulate a heat transfer as efficient as that of a heat pipe;

This assembly is insulated; the thermal losses from the walls to the outside are negligible.

The fundamental equations of fluid mechanics and heat transfer serve as the foundation for the Ansys-Fluent simulations that we conducted as part of our analytical framework. The governing equations for these processes are derived and adapted from existing methodologies, such as fixed domain methods and the enthalpy method for phase change.

In fixed domain simulations, the computational domain remains constant, even as the phase changes occur. The primary governing equation for energy within these systems, accounting for the phase change, is given by:

$$\rho[\frac{\partial h}{\partial t} + \nabla\cdot(\vec{v}h)] = \nabla\cdot q - S \quad (1)$$

where:

$\frac{\partial h}{\partial t}$—unsteady term;

$\nabla\cdot\left(\vec{v}h\right)$—convective transport of energy;

q—diffusive heat flux;

S—source term;

The Voller [35] enthalpy method is commonly used for modeling phase change and integrated in ANSYS. This approach simplifies the problem by considering the enthalpy as the sum of sensible and latent heat, eliminating the need for interface conditions. This approach reduces complexities, transforming the governing equation into one that is equivalent to a single-phase equation and allowing precise tracking of fusion and solidification fronts.

- The mass conservation equation is fundamental in fluid dynamics simulations and is expressed as:

$$\frac{\partial \rho}{\partial t} + \nabla\cdot\left(\rho\vec{v}\right) = 0 \quad (2)$$

where ρ is the density of the fluid and $\vec{v}$ represents the velocity field.

- Conservation of Momentum:

$$\rho\left(\frac{\partial v_x}{\partial t} + \nabla\cdot\left(\vec{v}v_x\right)\right) = \nabla\cdot(\mu\nabla v_x) - \frac{\partial P}{\partial x} + S_x \tag{3}$$

$$\rho\left(\frac{\partial v_y}{\partial t} + \nabla\cdot\left(\vec{v}v_y\right)\right) = \nabla\cdot\ (\mu\nabla v_y) - \frac{\partial P}{\partial y} + S_y \tag{4}$$

$$\rho\left(\frac{\partial v_z}{\partial t} + \nabla\cdot\left(\vec{v}v_z\right)\right) = \nabla\cdot\ (\mu\nabla v_z) - \frac{\partial P}{\partial y} + S_z \tag{5}$$

where $\vec{S}$ includes source terms due to the phase change. These source terms are particularly influenced by the mushy zone model, where the PCM transitions between solid and liquid states. The source term $\vec{S}$ can be specifically expressed as:

$$\vec{S} = \frac{M(1-f)^2}{f^3 + c}\vec{v} \tag{6}$$

Here, f is the liquid fraction, M is the mushy zone constant, and c is a small number preventing division by zero, ensuring numerical stability.

- Energy Conservation in the PCM:

$$\rho\frac{\partial h}{\partial t} = \nabla\cdot\vec{q} - \rho\Lambda\ \frac{\partial f}{\partial t} \tag{7}$$

where ρ represents the density of the phase change material, $\frac{\partial h}{\partial t}$ is the rate of change of enthalpy over time, and $\frac{\partial f}{\partial t}$ represents the rate of change of the phase fraction.

For systems undergoing phase transitions, the total enthalpy is the sum of the sensible heat ($h_{sensible}(T)$) and the latent heat ($h_{latent}(T)$). This relationship is defined by the following equations:

$$h(T) = h_{sensible}(T) + h_{latent}(T) \tag{8}$$

The sensible heat represents the energy accumulated due to the temperature increase of the material, whether in solid or liquid state. It is calculated as:

$$h_{sensible}(T) = \int_{T_{initial}}^{T_{fusion}} C_p, S^{dT} + \int_{T_{fusion}}^{T_{final}} C_p,\ L^{dT} \tag{9}$$

The latent heat component represents the energy absorbed or released during the phase transition. It is expressed as:

$$h_{latent}(T) = f(T)\Delta h_{S-L} \tag{10}$$

Here, Δh_{S-L} is the latent heat of fusion and $f(T)$ is the temperature-dependent liquid fraction, which varies between 0 and 1 as the material transitions from solid to liquid, being defined as follows:

$f(T) = 0$, when the material is in a solid state, if $T < T_{solid}$;
$f(T) = 1$, when the material is in a liquid state, if $T > T_{liquid}$;
$0 < f(T) = \frac{T - T_{solid}}{T_{liquid} - T_{solid}} < 1$, when the material changes the phase, if $T_{solid} < T < T_{liquid}$;

Combining the sensible and latent heat equations, the energy conservation equation for a system experiencing phase change is given by:

$$\rho\left[\frac{\partial h_{sensible}(T)}{\partial t} + \nabla\cdot\left(\vec{v}h_{sensible}(T)\right) + \Delta h_{S-L}\frac{\partial f(T)}{\partial t} + \Delta h_{S-L}\nabla\cdot\left(\vec{v}f(T)\right)\right] \tag{11}$$

2.5. Simulation Parameters and Grouping Overview

To facilitate a nuanced understanding of how individual parameters affect system behavior, we strategically organized the simulations into categories based on a singularly varying parameter. Figure 3 illustrates the organized simulations and their respective groups, enhancing clarity through systematic categorization. The rationale for this approach was to isolate the influence of each variable on the system, which allowed us to draw precise conclusions about the impact of each varied parameter. Our results are presented in the format of comparative groups, reflecting the one-variable-at-a-time approach.

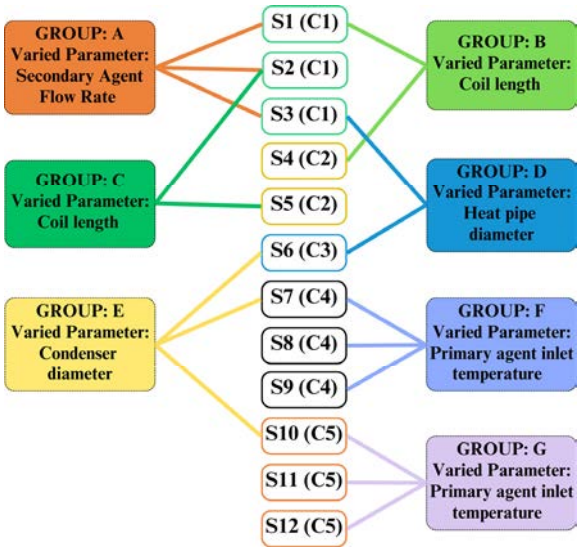

Figure 3. Schematic Diagram of Simulation Groups.

The organization of these simulation data is summarized in the accompanying tables, which outline the groups based on the varying parameters.

Our simulation study commenced with the establishment of a baseline scenario, denoted as simulation S1, and this initial setup is presented in Table 3.

Table 3. Characteristics of Secondary Agent Flow Rate Variations in Group A Simulations.

Comparison Group	ID	Parameter Variation and Values		Constant Parameters			
				Coil Height [mm]	Condenser Diameter [mm]	HP Diameter [mm]	T_{pin} [°C]
Group A	S1	Secondary Agent Flow Rate (Q_{sa} [L/min])	1	1916	150	15	70
	S2		0.1				
	S3		0.05				

Building upon the foundational parameters of S1, simulations S2 and S3 were systematically conducted with the sole variation of the secondary agent flow rate (Q_{sa}). These modifications allowed for a focused investigation into the effects of flow rate changes on system efficiency and heat transfer characteristics, while maintaining all other system parameters constant to isolate the impact of this single variable. Extending from Group A's findings, we examined coil length variations in Groups B and C to discern their effects on the system's performance. The specific parameters that remained fixed and those that were varied are systematically detailed in Table 4.

Table 4. Characteristics of Coil Length Variations in Group B and Group C Simulations.

Comparison Group	ID	Parameter Variation and Values		Constant Parameters			
				Q_{sa} [L/min]	Condenser Diameter [mm]	HP Diameter [mm]	T_{pin} [°C]
Group B	S1	Coil length [mm]	1916	1	150	15	70
	S4		1096				
Group C	S2		1916	0.1			
	S5		1096				

Following the assessment of coil lengths, our attention in Group D shifted towards the diameter of the heat pipe. Simulations S3 and S6 in Group D explore the system's behavior with a smaller and larger heat pipe diameter and a temperature of 70 °C for the primary agent (T_{pin}). The constant parameters across these groups, including condenser diameter, coil height, and secondary agent flow rate, ensure a targeted analysis of the heat pipe's influence. Table 5 presents the specific constants and varied parameters for clarity.

Table 5. Characteristics of Heat Pipe Diameter Variations in Group D Simulations.

Comparison Group	ID	Parameter Variation and Values		Constant Parameters			
				T_{pin} [°C]	Condenser Diameter [mm]	Coil Height	Q_{sa} [L/min]
Group D	S3	HP diameter [mm]	15	70	150	1916	0.05
	S6		25				

Building on the insights from the heat pipe diameter analysis in Group D, Table 6 presents Group E, where we focus on the effects of varying condenser diameters. Retaining the optimized heat pipe diameter of 25 mm from the previous comparisons, we evaluated how the system performance adjusts to condenser diameters of 150 mm, 100 mm, and 85 mm in Simulations S6, S7, and S10, respectively, while all other variables were held constant.

Table 6. Characteristics of Condenser Diameter Variations in Group E Simulations.

Comparison Group	ID	Parameter Variation and Values		Constant Parameters			
				Coil Height [mm]	Q_{sa} [L/min]	HP Diameter [mm]	T_{pin} [°C]
Group E	S6	Condenser diameter [mm]	150	1916	0.05	25	70
	S7		100				
	S10		85				

Groups F and G, detailed in Table 7, explore the impact of varying primary agent inlet temperatures. With condenser diameters of 100 mm for Group F and 85 mm for Group G carried forward from previous studies, these groups investigate the thermal response of the system to inlet temperatures ranging from 50 °C to 70 °C and 90 °C, respectively, keeping all other system parameters constant. Simulations S8, S7, and S9 constitute Group F, while S12, S10, and S11 form Group G. These groups presented below enable us to isolate and examine the impact of the primary agent inlet temperature variations on the system's thermal efficiency.

Table 7. Characteristics of Primary Agent Inlet Temperature Variations in Group F and Group G Simulations.

Comparison Group	ID	Parameter Variation and Values		Constant Parameters			
				Condenser Diameter [mm]	Q_{sa} [L/min]	HP Diameter [mm]	Coil Height [mm]
Group F	S8	Primary agent inlet temperature (T_{pin} [°C])	90	100	0.05	25	1916
	S7		70				
	S9		50				
Group G	S12		90	85			
	S10		70				
	S11		50				

3. Results and Discussion

The results of the 12 numerical simulations conducted to assess our heat recovery and storage system are analyzed based on specific boundary conditions and configurations from Tables 1 and 2. The figures presented below offer a visual depiction of the melting progression (MF) and temperature variations (T) across the system, captured through cross-sectional views, after 4 h of operation. Although the simulations we ran did not reach a stable state within the 4 h real-time duration, we deliberately chose this time frame with consideration of both computational efficiency and the scope of our study, which encompassed numerous designs. The 4 h window provided sufficient time to discern the effects of each parameter on the system's early thermal response, providing valuable insights while managing the extensive computational demand required for multiple long-duration simulations.

In the forthcoming discussions, we will analyze the results according to the groups outlined in Tables 3–7 from the previous section, examining the specific effects of individual parameter changes on system performance. Graphical representations will be provided for each group to accompany these discussions, illustrating the percentage of melted phase change material and the temperature of the secondary agent at the coil's outlet. In order to properly understand the flow characteristics within our system, we determined the Reynolds numbers for each simulated scenario. The results are presented in Table 8, showing that every scenario maintains a laminar flow profile, as the Reynolds number is smaller than 2300.

Table 8. Reynolds number.

Simulation No.	Secondary Agent			
	Temperature [°C]	Volume Flow Rate [L/min]	Reynolds	Regime
S1	15	1	1240.6	Laminar
S2	15	0.1	124.1	Laminar
S3	15	0.05	62.0	Laminar
S4	15	1	1240.6	Laminar
S5	15	0.1	124.1	Laminar
S6	15	0.05	62.0	Laminar
S7	15	0.05	62.0	Laminar
S8	15	0.05	62.0	Laminar
S9	15	0.05	62.0	Laminar
S10	15	0.05	62.0	Laminar
S11	15	0.05	62.0	Laminar
S12	15	0.05	62.0	Laminar

3.1. Comparative Analysis: Secondary Agent Flow Rate Variation in Group A

Figure 4 showcases cross-sectional views that capture the system's thermal behavior and melting progression after 14,400 s of real flow time, highlighting the thermal behavior and melting patterns for this group's simulations.

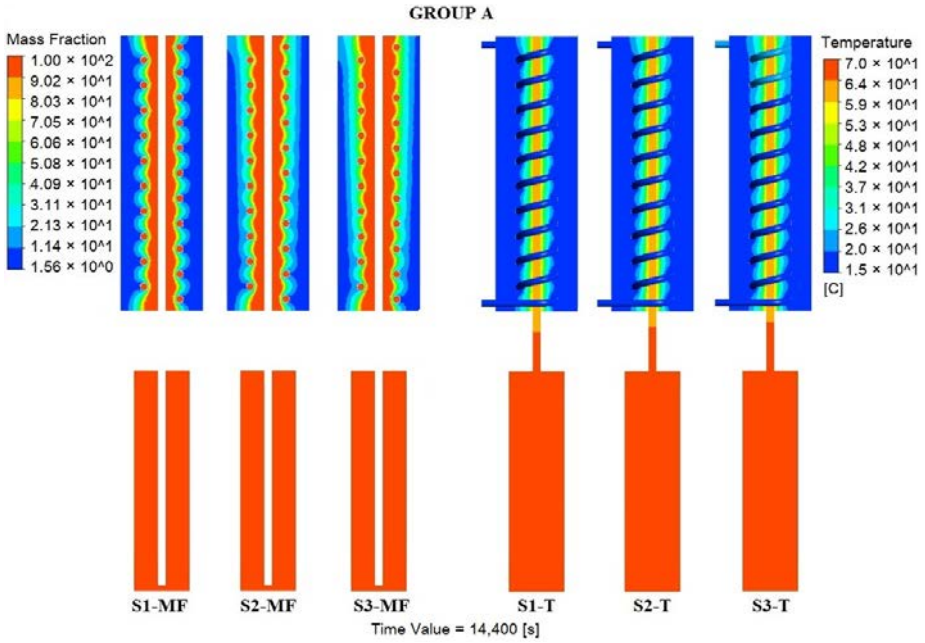

Figure 4. Cross-sectional melting fraction (MF) and temperature (T) contours of Group A.

In Group A, the variations in secondary agent flow rate yield insightful trends regarding the melting fraction of the phase change material (PCM) and the outlet temperature of the system. As shown in the provided data in Figure 5a,b, a clear dependency is observed between the flow rate and the system's thermal performance. The melting fraction of the PCM, represented as a percentage of total mass, demonstrates a progressive increase over the 4 h duration for all flow rates. Notably, the simulation with the lowest flow rate, S3-MF (0.05 L/min), exhibits a significantly higher melting fraction, reaching 30.71% at 14,400 s, compared to 20.49% for S1-MF (1 L/min).

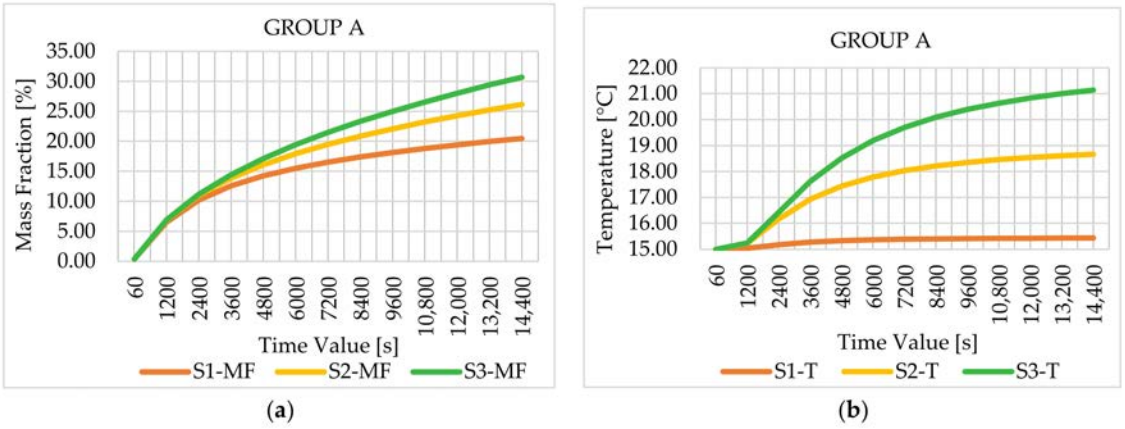

Figure 5. (**a**) Melting fraction percentage over time for Group A simulations; (**b**) Secondary agent outlet temperature profile over time in Group A simulations.

Consistent with the melting fraction observations, the outlet temperatures of the secondary agent also display an increase as the flow rate diminishes, as can be seen in Figure 5b. The S1-T's output temperature, which slightly exceeds the initial temperature,

indicates limited heat transfer. Conversely, S3-T reaches an outlet temperature of 21.15 °C, demonstrating a substantially more effective heat transfer process. This elevated temperature is indicative of the secondary agent's greater thermal absorption, aligning with the system's goal to maximize heat extraction.

3.2. Comparative Analysis: Coil Length Variation in Group B and Group C

Figure 6 provides cross-sectional views that depict the system's thermal behavior and melting trends over 4 h of real flow time, accentuating the impact of coil length on melting patterns and thermal dynamics in Group B's simulations.

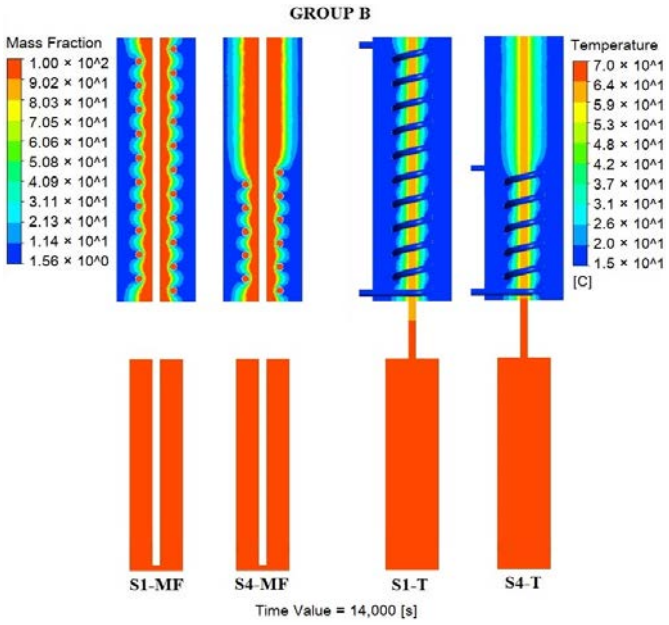

Figure 6. Cross-sectional melting fraction (MF) and temperature (T) contours of Group B.

The data for Group B indicate that the half-length coil in Simulation S4 leads to a higher melting fraction over time compared to the full-length coil in Simulation S1. At the 4 h mark, S4-MF achieves a melting fraction of 30.64%, which is significantly greater than the 20.49% seen in S1-MF. In contrast to the melting fraction data in Figure 7a, the final temperature of the secondary agent indicates that S1-T operates slightly better than S4-T, with a recorded temperature of 15.43 °C compared to 15.24 °C after 4 h, as shown in Figure 7b, suggesting that a longer coil may be more effective in transferring heat to the secondary agent.

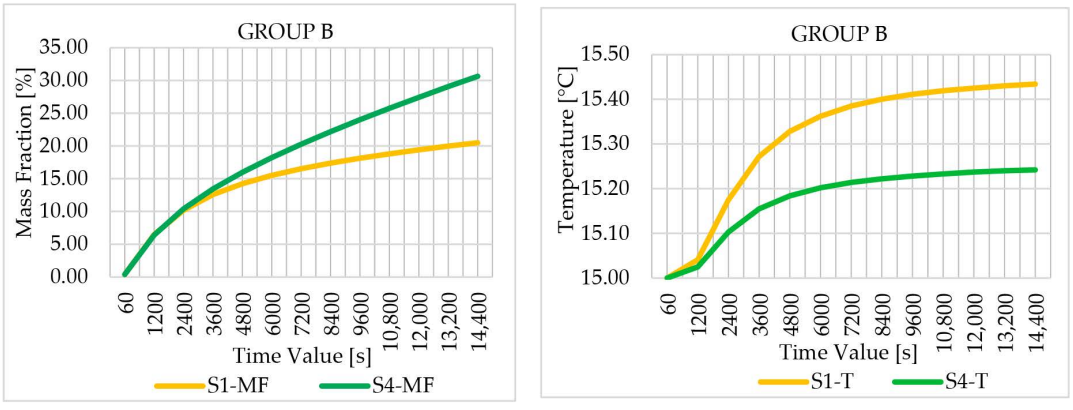

Figure 7. (**a**) Melting fraction percentage over time for Group B simulations; (**b**) Secondary agent outlet temperature profile over time in Group B simulations.

Figure 8 presents the cross-sectional melting fraction (MF) and temperature (T) contours for Group C, where the secondary agent flow rate is set at 0.1 L/min, contrasting a full-length coil in S2 with a half-length coil in S5 to visualize their respective impacts on the system's thermal efficiency and PCM melting behavior.

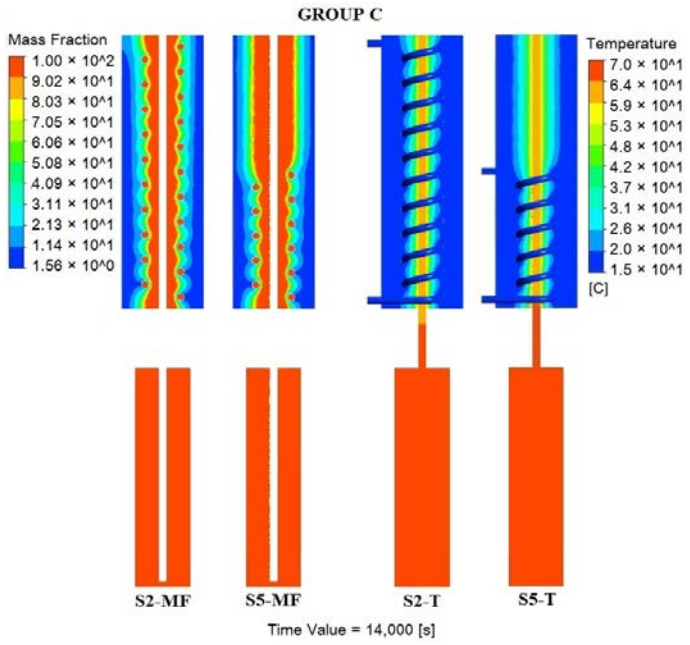

Figure 8. Cross-sectional melting fraction (MF) and temperature (T) contours of Group C.

The data in Figure 9a illustrate that reducing the flow rate to 0.1 L/min impacts the melting fraction of the PCM. In S5-MF, with the half-length coil, we see a higher melting fraction across the time spectrum, peaking at 30.80% after 4 h, compared to 26.17% in S2-MF with the full-length coil. Upon examining the outlet temperatures for S2-T and S5-T, it becomes evident that the half-length coil of S5-T does not achieve a significant temperature increase at the outlet as the full-length coil of S2-T does. After 4 h, S5-T reaches an outlet temperature of 17.21 °C, whereas S2-T attains a marginally higher temperature of 18.67 °C. Using a half-length coil at a lower flow rate can increase the amount of phase change material that melts. However, a full-length coil may be more effective in heating the secondary agent to a higher exit temperature, which is advantageous in systems that require higher exit temperatures.

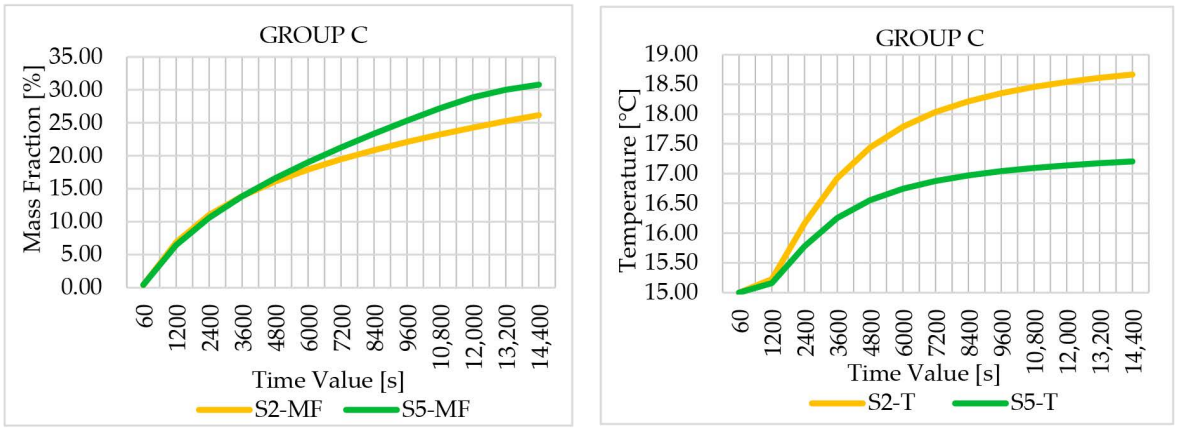

Figure 9. (**a**) Melting fraction percentage over time for Group C simulations; (**b**) Secondary agent outlet temperature profile over time in group C simulations.

3.3. Comparative Analysis: Heat Pipe Diameter Variation in Group D

Figure 10 delves into a comparative analysis of heat pipe diameter variation in Group D. We have retained the optimized secondary agent flow rate of 0.05 L/min and the full-length coil from prior simulations while investigating the impact of enlarging the heat pipe diameter from 15 mm in S3 to 25 mm in S6.

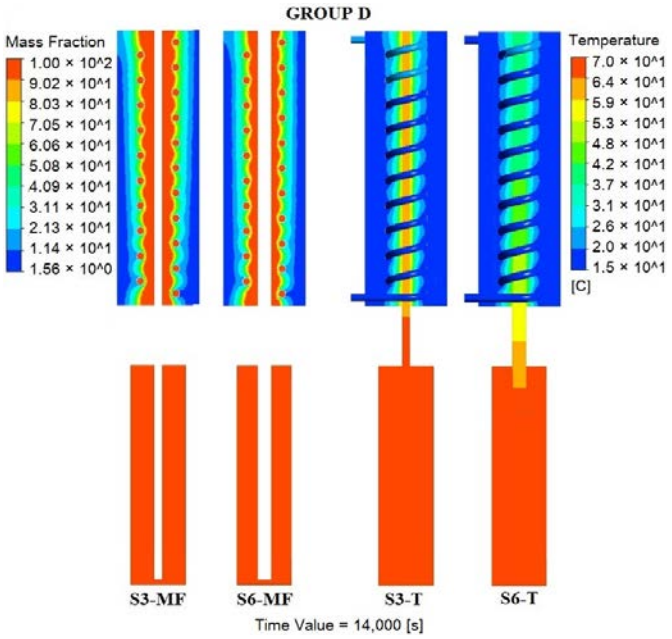

Figure 10. Cross-sectional melting fraction (MF) and temperature (T) contours of Group D.

The melting fraction data for Group D in Figure 11a show a distinct increase when using a heat pipe with a larger diameter. Simulation S6-MF, with a 25 mm diameter heat pipe, exhibits a consistently lower melting fraction compared to S3-MF, which has a 15 mm diameter. At the end of the 4 h period, S3-MF achieves a higher melting fraction of 30.71%, suggesting that the smaller diameter pipe is more effective in transferring heat to the PCM. The outlet temperature trends for S3-T and S6-T reveal that the secondary agent's temperature is consistently higher in S3-T throughout the 4 h period. Ending at 21.15 °C, S3-T's temperature is higher than S6-T's (20.47 °C). This indicates that the heat pipe with the smaller diameter is more effective at heating the secondary agent within the given flow rate and coil configuration.

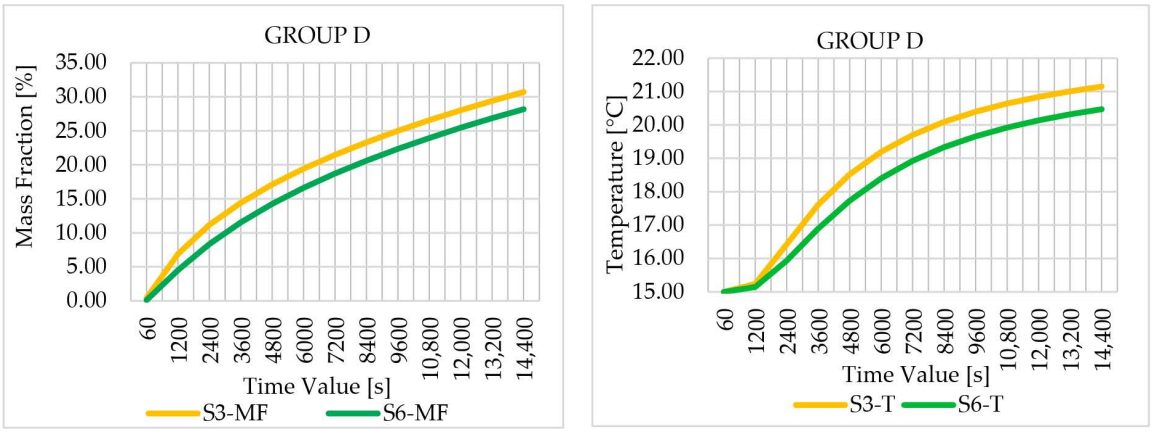

Figure 11. (**a**) Melting fraction percentage over time for Group D simulations; (**b**) Secondary agent outlet temperature profile over time in Group D simulations.

3.4. Comparative Analysis: Condenser Diameter Variation in Group E

Figure 12 shifts our focus to a comparative analysis of condenser diameter variation in Group E. Maintaining the previously optimized flow rate of 0.05 L/min and the full-length coil configuration, alongside a 25 mm heat pipe, we now examine the implications of condenser diameter changes. This group compares the effects of varying the condenser diameter from an initial 150 mm in S6 to 100 mm in S7 and finally to 85 mm in S10.

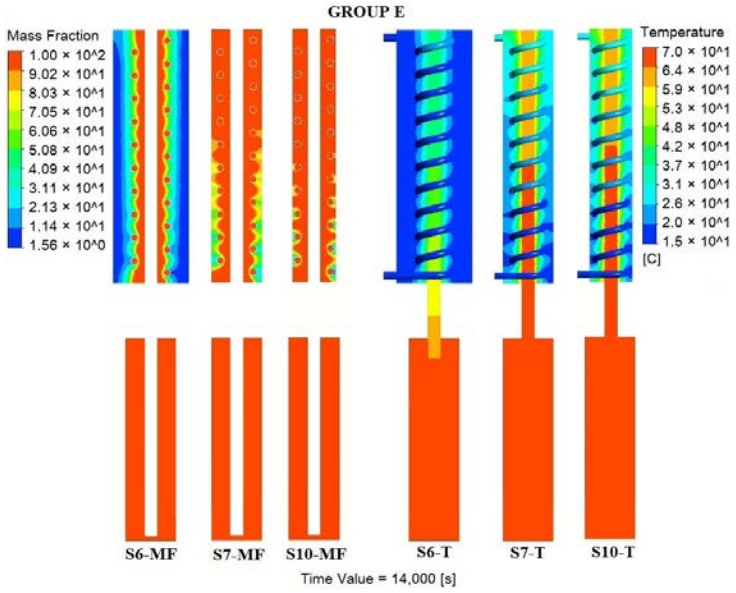

Figure 12. Cross-sectional melting fraction (MF) and temperature (T) contours of Group E.

The data in Figure 13a for Group E show a pronounced effect of condenser diameter on the melting fraction. As the diameter decreases, there is a notable increase in the melting fraction percentage. By the end of the 4 h period, S10-MF with the smallest diameter (85 mm) reaches the highest melting fraction of 95.24%, followed by S7-MF (100 mm) with 88.32%, and S6-MF (150 mm) with 28.19%. The outlet temperatures represented in Figure 13b correspondingly reflect the effects of condenser diameter reduction. S10-T demonstrates the greatest increase in outlet temperature, concluding at 28.85 °C, indicative of the most significant heat absorption by the secondary agent. The final temperatures of S7-T and S6-T are 27.95 °C and 20.47 °C, respectively, demonstrating that the secondary agent leaves the system at a higher temperature after taking greater amounts of heat when the condenser diameter decreases.

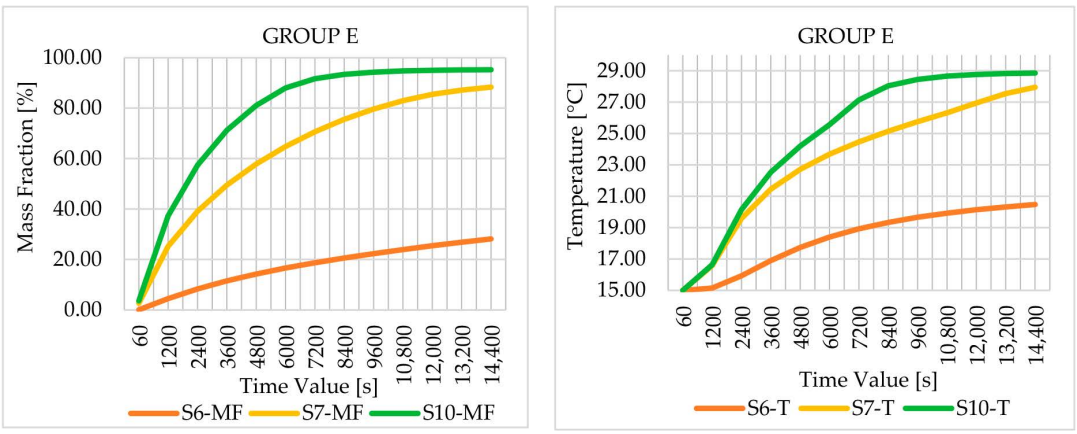

Figure 13. (**a**) Melting fraction percentage over time for Group E simulations; (**b**) Secondary agent outlet temperature profile over time in Group E simulations.

3.5. Comparative Analysis: Primary Agent Inlet Temperature Variation in Group F and Group G

In Group F represented in Figure 14, we extend our examination by keeping constant the optimized parameters from previous groups: a secondary agent flow rate of 0.05 L/min, a full-length coil, a heat pipe diameter of 25 mm, and a condenser diameter of 100 mm. We shifted our focus to explore the impact of the primary agent's inlet temperature variation, observing the effects at 70 °C in S7, increasing to 90 °C in S8, and decreasing to 50 °C in S9.

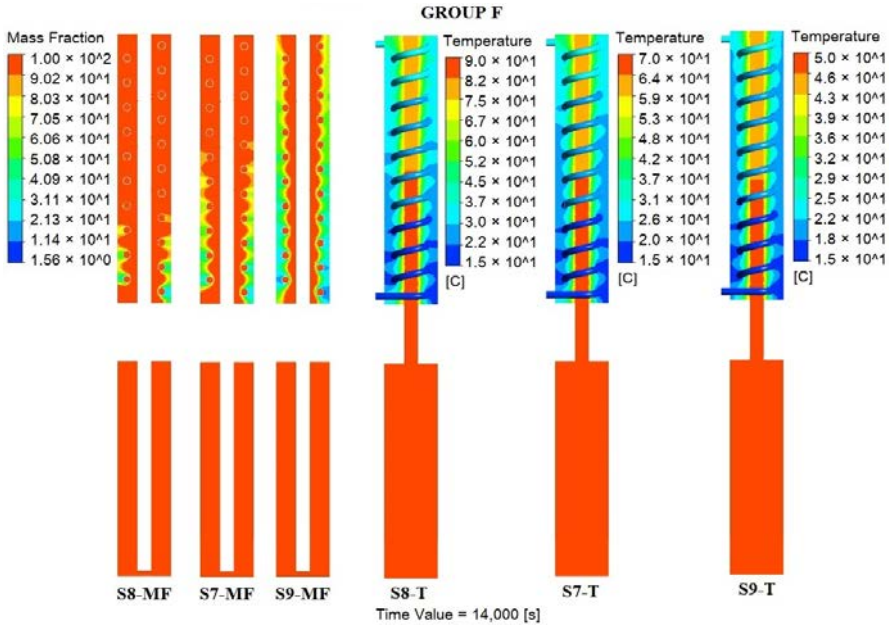

Figure 14. Cross-sectional melting fraction (MF) and temperature (T) contours of Group F.

The melting fraction data in Figure 15a illustrate a clear trend: higher inlet temperatures facilitate a greater degree of the phase change material's melting over time. Simulation S8-MF, operating at a 90 °C inlet temperature, achieves a significantly higher melting fraction, peaking at 95.22% after 4 h. This is in contrast to S7-MF, which reaches 88.32% at a 70 °C inlet temperature, and Simulation S9-MF, which only attains 68.64% at the lower 50 °C temperature. These results indicate that the phase change process is highly sensitive to the temperature of the primary agent, with higher temperatures accelerating the melting substantially.

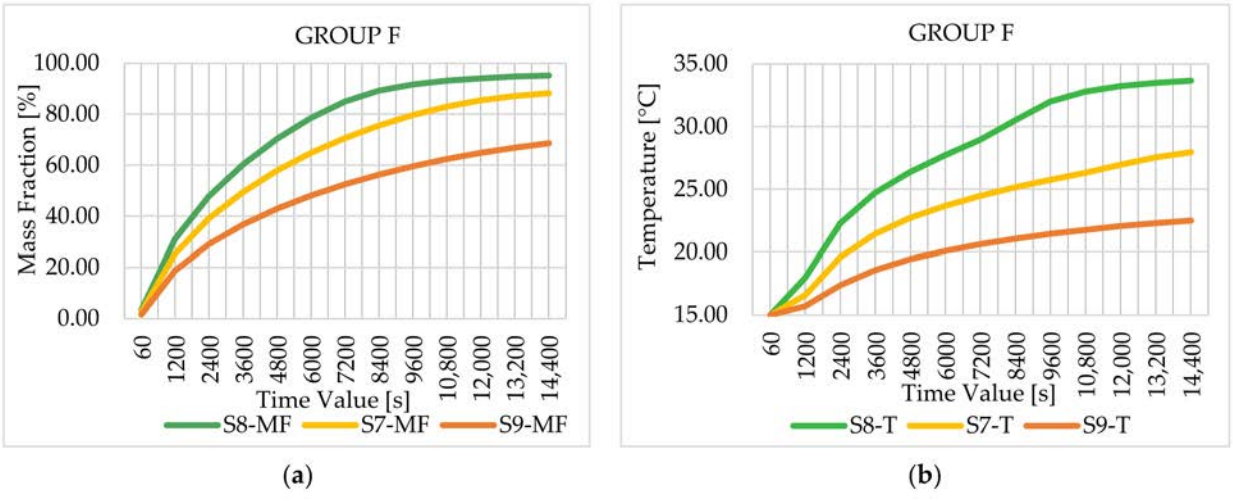

Figure 15. (**a**) Melting fraction percentage over time for Group F simulations; (**b**) Secondary agent outlet temperature profile over time in group F simulations.

As shown in Figure 15b, the outlet temperature trends follow a similar pattern. Simulation S8-T exhibits the greatest secondary agent outlet temperature, peaking at 33.66 °C, due to its higher inlet temperature for the primary agent. This is significantly higher compared to S7-T's 27.95 °C and S9-T's 22.51 °C, concluding that the temperature of the primary agent directly influences the secondary agent's heat absorption capabilities. Notably, S8-T's elevated outlet temperature suggests that the system is highly effective in transferring heat from the primary agent to the secondary agent, maximizing the potential for heat recovery.

Group G extends our systematic exploration by maintaining a condenser diameter of 85 mm and assessing the system's response to varied primary agent inlet temperatures. This analysis explores the thermal efficiency and phase change behavior at three different inlet temperatures: 70 °C for S10, 90 °C for S12, and 50 °C for S11. The corresponding thermal effects and phase change process are visually captured in Figure 16, which presents the cross-sectional melting fraction (MF) and temperature (T) contours for Group G.

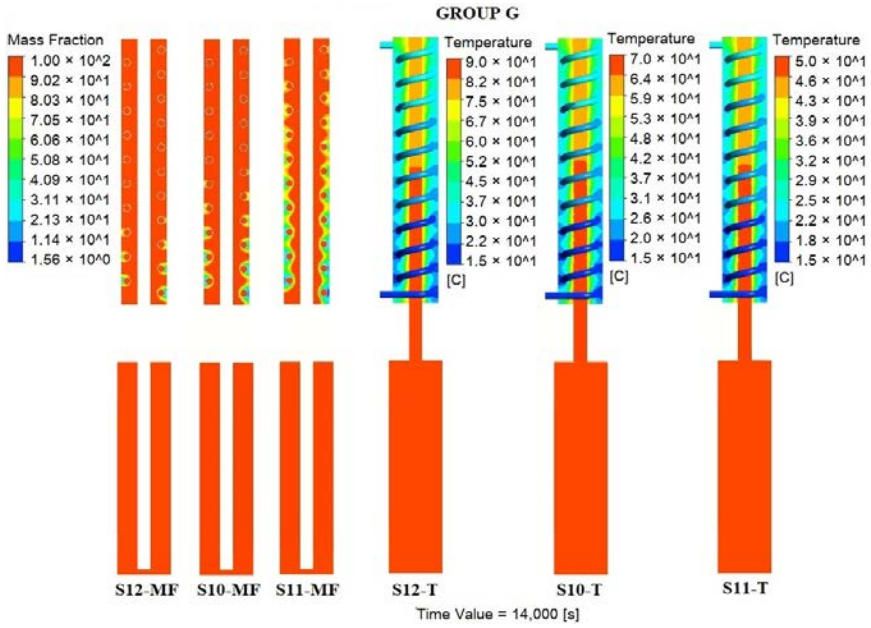

Figure 16. Cross-sectional melting fraction (MF) and temperature (T) contours of Group G.

The melting fraction data for Group G in Figure 17a reveal that the PCM melting is significantly influenced by the primary agent's inlet temperature, particularly within the smaller 85 mm condenser diameter.

Simulation S12-MF, with the highest inlet temperature of 90 °C, consistently exhibits the greatest melting fraction, achieving near completion with 98.80% melted after 4 h. Simulation S10-MF, at a moderate 70 °C, shows a substantial melting fraction as well, but Simulation S11-MF with the lowest temperature of 50 °C, reached only 84.14%. This clearly demonstrates that higher inlet temperatures are more conducive to the phase change process, especially when combined with a smaller condenser diameter. Addressing the outlet temperatures of the secondary agent, Simulation S12-T outperforms the others, achieving an ending temperature of 33.95 °C, as shown in Figure 17b. This suggests that the secondary agent is capable of absorbing greater amounts of heat at higher primary temperatures, regardless of the assembly's smaller dimensions. Simulations S10-T and S11-T conform to the aforementioned pattern, concluding at temperatures of 28.85 °C and 23.46 °C, respectively. The findings indicate that using an 85 mm condenser diameter is effective in transferring the thermal energy of the primary agent to the secondary agent. Higher inlet temperatures lead to greater heat gain, which is advantageous for systems that aim to achieve higher outlet temperatures for the secondary agent.

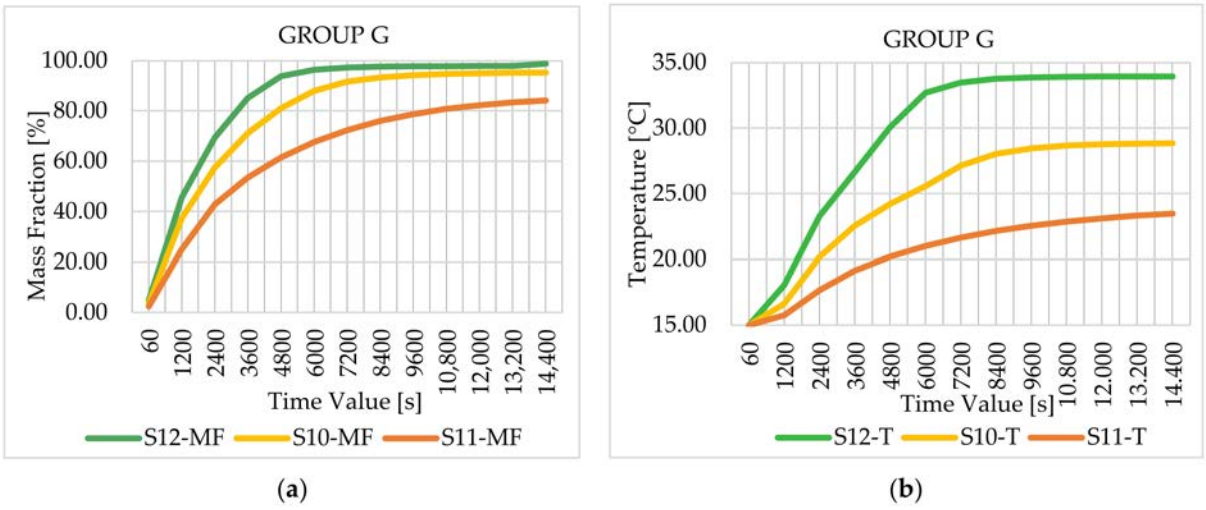

Figure 17. (**a**) Melting fraction percentage over time for Group G simulations; (**b**) Secondary agent outlet temperature profile over time in Group G simulations.

3.6. Summary of Findings

Upon analyzing Group A, it is evident that varying the flow rate of the secondary agent significantly impacts the thermal dynamics of the system. A lower flow rate results in a higher melting fraction and elevated outlet temperatures, indicating improved heat absorption and transport capacity. Although a steady state was not reached within the 4 h simulation, the observed patterns provide valuable insights for enhancing the early stage effectiveness of the heat recovery system. Results from Group B demonstrate that while a shorter coil enables more energy storage by melting more PCM, it does not necessarily improve the system's ability to efficiently transfer this stored energy to the secondary agent as effectively as a longer coil. Therefore, when both high energy storage and efficient heat transfer are desired, the coil length becomes a critical consideration. Balancing the melting fraction and heat transfer rate is essential for optimizing system performance. Group C's simulations show that combining a lower secondary agent flow rate with a half-length coil enhances PCM melting, indicating improved energy storage efficiency. However, the longer coil proves more effective at raising the outlet temperature of the secondary agent, highlighting its superior heat transfer capabilities. This suggests that while a half-length coil maximizes phase change and storage, a full-length coil excels at heat transfer, requiring a balance to optimize both thermal storage and heat delivery.

In Group D, findings emphasize the importance of selecting the appropriate heat pipe diameter to balance effective heat absorption from the primary agent and efficient heat transfer to both the PCM and the secondary agent. A reduced diameter increases heat transfer efficiency, underscoring the need for careful consideration of this parameter during the design phase to maximize system effectiveness. The findings from Group E highlight the significant impact of condenser diameter on heat recovery system performance. Smaller diameters improve both PCM melting and secondary agent outlet temperatures. However, balancing these benefits with the overall system design is crucial, particularly concerning PCM volume, which affects energy storage capacity. Optimizing system performance without compromising energy storage requires careful consideration of both condenser diameter and PCM volume. Group F reveals that higher primary agent inlet temperatures substantially increase PCM melting efficiency and secondary agent outlet temperatures. This underscores the importance of selecting an appropriate temperature range for the primary heat source, considering the specific needs and capabilities of the heat recovery equipment. Using a higher temperature source maximizes thermal output and enhances overall heat transfer performance, emphasizing the need for proper primary agent temperature selection. Results from Groups F and G demonstrate that the primary agent's inlet temperature is crucial in optimizing PCM melting and enhancing heat extraction

capabilities. The correlation between primary agent inlet temperature and an optimized condenser diameter significantly amplifies the system's heat transfer capacity, highlighting the importance of these parameters in maximizing system performance.

In general, it can be concluded that lower secondary agent flow rates, higher primary agent inlet temperatures, and smaller condenser diameters consistently enhance the system's thermal efficiency. These findings can be generalized to similar heat recovery systems aiming for improved heat absorption and transfer efficiency. However, specific design parameters such as coil length and heat pipe diameter need to be carefully selected based on the particular configuration and operational conditions of the system. These specific findings may not be universally applicable without considering the unique aspects of each system's design, operation, and intended application.

3.7. Limitations of the Study and Future Research Directions

While our study provides valuable insights into the optimization of heat recovery systems, several limitations should be acknowledged. The scope of our numerical simulations was limited to specific parameters and configurations, which may not encompass all real-world scenarios. Additionally, the study currently lacks experimental validation, as the ongoing experimental work will be presented in subsequent research. Our numerical model includes necessary assumptions and simplifications, such as imposed conditions and not including internal phase change processes within the heat pipe, to streamline the analysis. Furthermore, the academic version of ANSYS used in this study posed limitations on the element count. Despite these considerations, our results offer a robust framework for further exploration and development in heat recovery system optimization.

There are several research questions that remain unanswered, necessitating further investigation. Future studies should focus on experimentally validating the numerical findings to confirm the model's accuracy and reliability under real-world conditions. Including the internal phase change processes within heat pipes in the overall system analysis could provide a more comprehensive understanding of heat transfer dynamics and improve model precision. Additionally, exploring a broader range of parameters and configurations can help generalize the findings and enhance their applicability to various domestic and industrial settings. Assessing the long-term performance and durability of the optimized heat recovery systems under continuous operation is important for understanding their practical viability and maintenance needs. Exploring other phase change materials with superior thermal storage properties could lead to improved thermal performance and efficiency. Moreover, integrating heat recovery systems with renewable energy sources, such as solar thermal panels, can enhance sustainability and overall energy efficiency. Finally, conducting a detailed economic analysis, including cost-benefit and return-on-investment studies, can provide insights into the financial feasibility and attractiveness of implementing these systems.

Future studies addressing these questions will contribute to a more comprehensive understanding and development of efficient heat recovery systems, facilitating the development of practical applications in both the residential and industrial sectors.

4. Conclusions

A comprehensive heat recovery system was systematically analyzed through a series of 12 simulations, with each one optimizing various operating parameters. The thermal performance of the system was analyzed by methodically changing variables such as the flow rate of the secondary agent (1 L/min, 0.1 L/min, and 0.05 L/min), the length of the coil (474 mm and 244 mm), the diameter of the heat pipe (15 mm and 25 mm), and the size of the condenser (150 mm, 100 mm, and 85 mm). This analysis concluded with an investigation of the primary agent's inlet temperature (90 °C, 70 °C, and 50 °C). This methodical approach provided insight into the effects of the aforementioned variables on the efficiency of the system, both individually and collectively. Empirical data from numerical simulations

established a robust framework for evaluating the system's performance, revealing the following key insights:

- By varying the secondary agent's flow rate, it was possible to observe that slower rates greatly improve heat absorption and transfer, as shown by higher final temperatures and melting fractions;
- Similarly, the choice of coil length was shown to affect energy storage and heat transfer, as shorter coils enhance the melting of PCM while longer coils facilitate superior heat transfer;
- Furthermore, optimizing the heat pipe and condenser diameters was found to be important, as smaller diameters facilitated better heat transfer and increased the melting fraction, though careful attention must be paid to the overall volume of PCM to avoid limiting energy storage capacity;
- The temperature of the primary agent also played an important role, with higher temperatures leading to more efficient melting of the PCM and enhanced thermal output;
- Among all the simulations conducted, Simulation S12 demonstrated the most promising results after a 4 h flow time, achieving a remarkable melting fraction of 98.8% and an increase of 18.95 °C in the secondary agent's outlet temperature. In contrast, Simulation S5 highlighted areas for potential enhancement, achieving only a 30.80% melting fraction and a relatively small temperature gain of 2.21 °C for the secondary agent;

In summary, the study highlights the need for optimizing components in heat recovery systems. Strategic adjustments can lead to significant improvements in thermal efficiency. Such systems are beneficial in industrial applications, where they can recover thermal energy from wastewater processes, store surplus thermal energy in phase change materials, and use this energy to prepare domestic hot water or for other purposes, thereby providing prolonged hot water availability. Further investigations could explore the integration of multiple high-performance heat pipes and superior phase change materials to advance the system's design. Adjusting constructive dimensions and experimenting with innovative materials could lead to systems that are not only highly efficient but also scalable and suitable for industrial or domestic applications. Moreover, employing advanced experimental design methods such as the Taguchi method could further enhance our ability to efficiently optimize these systems. This comprehensive approach will ensure that future heat recovery systems are optimized for real-world settings, offering cost-effectiveness and environmental sustainability.

To maximize the benefits of these systems, it is recommended that policymakers introduce incentives for the adoption of optimized waste heat recovery systems in both residential and industrial sectors. Such policies could drive the implementation of these efficient technologies, resulting in increased energy savings, reduced operational costs, and significant environmental advantages.

Author Contributions: Conceptualization, Ș.E.V., A.B. and C.A.; methodology, Ș.E.V., R.Ș.V. and A.B.; software, M.C.B. and R.Ș.V.; validation, Ș.E.V., M.C.B. and A.B.; formal analysis, C.A. and Ș.E.V.; investigation, Ș.E.V., R.Ș.V. and M.C.B.; resources, M.C.B. and A.B.; data curation, R.Ș.V., C.A. and Ș.E.V.; writing—original draft preparation, Ș.E.V. and R.Ș.V.; writing—review and editing, C.A. and A.B.; visualization, Ș.E.V. and M.C.B.; supervision, C.A., A.B. and R.Ș.V. All authors have read and agreed to the published version of the manuscript.

Funding: This research received no external funding.

Institutional Review Board Statement: Not applicable.

Informed Consent Statement: Not applicable.

Data Availability Statement: The data presented in this study are available on request from the corresponding author.

Conflicts of Interest: The authors declare no conflicts of interest.

Nomenclature

HP	Heat pipe
HPHE	Heat pipe heat exchanger
MF	Melting fraction [%]
PCM	Phase change material
Q_{sa}	Secondary agent flow rate [L/min]
T	Temperature [°C]
T_{pin}	Inlet temperature of the primary agent [°C]

References

1. Söderholm, P. The Green Economy Transition: The Challenges of Technological Change for Sustainability. *Sustain. Earth* **2020**, *3*, 6. [CrossRef]
2. Directorate-General for Energy Renewable Energy Targets-European Commission. Available online: https://energy.ec.europa.eu/topics/renewable-energy/renewable-energy-directive-targets-and-rules/renewable-energy-targets_en (accessed on 12 June 2024).
3. European Commission. *A Renovation Wave for Europe-Greening Our Buildings, Creating Jobs, Improving Lives*; European Commission: Brussels, Belgium, 2020.
4. Xu, Z.Y.; Wang, R.Z.; Yang, C. Perspectives for Low-Temperature Waste Heat Recovery. *Energy* **2019**, *176*, 1037–1043. [CrossRef]
5. Akbari, A.; Kouravand, S.; Chegini, G. Experimental Analysis of a Rotary Heat Exchanger for Waste Heat Recovery from the Exhaust Gas of Dryer. *Appl. Therm. Eng.* **2018**, *138*, 668–674. [CrossRef]
6. Du, W.-J.; Yin, Q.; Cheng, L. Experiments on Novel Heat Recovery Systems on Rotary Kilns. *Appl. Therm. Eng.* **2018**, *139*, 535–541. [CrossRef]
7. Slimani, H.; Filali Baba, Y.; Ait Ousaleh, H.; Elharrak, A.; El Hamdani, F.; Bouzekri, H.; Al Mers, A.; Faik, A. Horizontal Thermal Energy Storage System for Moroccan Steel and Iron Industry Waste Heat Recovery: Numerical and Economic Study. *J. Clean. Prod.* **2023**, *393*, 136176. [CrossRef]
8. Wehbi, Z.; Taher, R.; Faraj, J.; Lemenand, T.; Mortazavi, M.; Khaled, M. Waste Water Heat Recovery Systems Types and Applications: Comprehensive Review, Critical Analysis, and Potential Recommendations. *Energy Rep.* **2023**, *9*, 16–33. [CrossRef]
9. Nagpal, H.; Spriet, J.; Murali, M.K.; McNabola, A. Heat Recovery from Wastewater—A Review of Available Resource. *Water* **2021**, *13*, 1274. [CrossRef]
10. Jouhara, H.; Khordehgah, N.; Almahmoud, S.; Delpech, B.; Chauhan, A.; Tassou, S.A. Waste Heat Recovery Technologies and Applications. *Therm. Sci. Eng. Prog.* **2018**, *6*, 268–289. [CrossRef]
11. Abdelkareem, M.A.; Maghrabie, H.M.; Sayed, E.T.; Kais, E.-C.A.; Abo-Khalil, A.G.; Radi, M.A.; Baroutaji, A.; Olabi, A.G. Heat Pipe-Based Waste Heat Recovery Systems: Background and Applications. *Therm. Sci. Eng. Prog.* **2022**, *29*, 101221. [CrossRef]
12. Delpech, B.; Milani, M.; Montorsi, L.; Boscardin, D.; Chauhan, A.; Almahmoud, S.; Axcell, B.; Jouhara, H. Energy Efficiency Enhancement and Waste Heat Recovery in Industrial Processes by Means of the Heat Pipe Technology: Case of the Ceramic Industry. *Energy* **2018**, *158*, 656–665. [CrossRef]
13. Jouhara, H.; Chauhan, A.; Nannou, T.; Almahmoud, S.; Delpech, B.; Wrobel, L.C. Heat Pipe Based Systems-Advances and Applications. *Energy* **2017**, *128*, 729–754. [CrossRef]
14. Faghri, A. HEAT PIPES: REVIEW, OPPORTUNITIES AND CHALLENGES. *Front. Heat Pipes* **2014**, *5*, 1–48. [CrossRef]
15. Burlacu, A.; Sosoi, G.; Vizitiu, R.Ș.; Bărbuță, M.; Lăzărescu, C.D.; Ciocan, V.; Șerbănoiu, A.A. Energy Efficient Heat Pipe Heat Exchanger for Waste Heat Recovery in Buildings. *Procedia Manuf.* **2018**, *22*, 714–721. [CrossRef]
16. Ma, H.; Yin, L.; Shen, X.; Lu, W.; Sun, Y.; Zhang, Y.; Deng, N. Experimental Study on Heat Pipe Assisted Heat Exchanger Used for Industrial Waste Heat Recovery. *Appl. Energy* **2016**, *169*, 177–186. [CrossRef]
17. Ma, H.; Du, N.; Zhang, Z.; Lyu, F.; Deng, N.; Li, C.; Yu, S. Assessment of the Optimum Operation Conditions on a Heat Pipe Heat Exchanger for Waste Heat Recovery in Steel Industry. *Renew. Sustain. Energy Rev.* **2017**, *79*, 50–60. [CrossRef]
18. Jouhara, H.; Nieto, N.; Egilegor, B.; Zuazua, J.; González, E.; Yebra, I.; Igesias, A.; Delpech, B.; Almahmoud, S.; Brough, D.; et al. Waste Heat Recovery Solution Based on a Heat Pipe Heat Exchanger for the Aluminium Die Casting Industry. *Energy* **2023**, *266*, 126459. [CrossRef]
19. Eidan, A.; Alshukri, M.; Alfahham, M.; Al Sahlani, A.; Abdulridha, D. Optimizing the Performance of the Air Conditioning System Using an Innovative Heat Pipe Heat Exchanger. *Case Stud. Therm. Eng.* **2021**, *26*, 101075. [CrossRef]
20. Amini, A.; Miller, J.; Jouhara, H. An Investigation into the Use of the Heat Pipe Technology in Thermal Energy Storage Heat Exchangers. *Energy* **2017**, *136*, 163–172. [CrossRef]
21. Robak, C.W.; Bergman, T.L.; Faghri, A. Enhancement of Latent Heat Energy Storage Using Embedded Heat Pipes. *Int. J. Heat Mass Transf.* **2011**, *54*, 3476–3484. [CrossRef]
22. Agyenim, F.; Eames, P.; Smyth, M. Heat Transfer Enhancement in Medium Temperature Thermal Energy Storage System Using a Multitube Heat Transfer Array. *Renew. Energy* **2010**, *35*, 198–207. [CrossRef]
23. Rogowski, M.; Fabrykiewicz, M.; Szymański, P.; Andrzejczyk, R. The In-House Method of Manufacturing a Low-Cost Heat Pipe with Specified Thermophysical Properties and Geometry. *Appl. Sci.* **2023**, *13*, 8415. [CrossRef]

24. Li, D.; Wang, J.; Ding, Y.; Yao, H.; Huang, Y. Dynamic Thermal Management for Industrial Waste Heat Recovery Based on Phase Change Material Thermal Storage. *Appl. Energy* **2019**, *236*, 1168–1182. [CrossRef]
25. Vizitiu, R.S.; Burlacu, A.; Abid, C.; Balan, M.C.; Vizitiu, S.E.; Branoaea, M.; Kaba, N.E. Investigating the Efficiency of a Heat Recovery–Storage System Using Heat Pipes and Phase Change Materials. *Materials* **2023**, *16*, 2382. [CrossRef]
26. Mozafari, M.; Lee, A.; Cheng, S. A Novel Dual-PCM Configuration to Improve Simultaneous Energy Storage and Recovery in Triplex-Tube Heat Exchanger. *Int. J. Heat Mass Transf.* **2022**, *186*, 122420. [CrossRef]
27. Jouhara, H.; Almahmoud, S.; Chauhan, A.; Delpech, B.; Bianchi, G.; Tassou, S.A.; Llera, R.; Lago, F.; Arribas, J.J. Experimental and Theoretical Investigation of a Flat Heat Pipe Heat Exchanger for Waste Heat Recovery in the Steel Industry. *Energy* **2017**, *141*, 1928–1939. [CrossRef]
28. Jouhara, H.; Bertrand, D.; Axcell, B.; Montorsi, L.; Venturelli, M.; Almahmoud, S.; Milani, M.; Ahmad, L.; Chauhan, A. Investigation on a Full-Scale Heat Pipe Heat Exchanger in the Ceramics Industry for Waste Heat Recovery. *Energy* **2021**, *223*, 120037. [CrossRef]
29. Geum, G.; Kang, S.; Cho, S.; Kong, D.; Lee, S.; Seo, J.; Shin, D.H.; Lee, S.H.; Lee, J.; Lee, H. Thermal Performance Analysis of Heat Pipe Heat Exchanger for Effective Waste Heat Recovery. *Int. Commun. Heat Mass Transf.* **2024**, *151*, 107223. [CrossRef]
30. Lohrasbi, S.; Miry, S.Z.; Gorji-Bandpy, M.; Ganji, D.D. Performance Enhancement of Finned Heat Pipe Assisted Latent Heat Thermal Energy Storage System in the Presence of Nano-Enhanced H2O as Phase Change Material. *Int. J. Hydrogen Energy* **2017**, *42*, 6526–6546. [CrossRef]
31. Tiari, S.; Qiu, S.; Mahdavi, M. Discharging Process of a Finned Heat Pipe–Assisted Thermal Energy Storage System with High Temperature Phase Change Material. *Energy Convers. Manag.* **2016**, *118*, 426–437. [CrossRef]
32. Vikas; Yadav, A.; Samir, S. Melting Dynamics Analysis of a Multi-Tube Latent Heat Thermal Energy Storage System: Numerical Study. *Appl. Therm. Eng.* **2022**, *214*, 118803. [CrossRef]
33. Ullah, F. Performance Assessment of Convective Heat Transfer in Tubes with a Temperature Difference in the High-Temperature Solar Power Generation System. *J. Food Process. Preserv.* **2021**, *45*, e16010. [CrossRef]
34. Saleel, C.A. A Review on the Use of Coconut Oil as an Organic Phase Change Material with Its Melting Process, Heat Transfer, and Energy Storage Characteristics. *J. Therm. Anal. Calorim.* **2022**, *147*, 4451–4472. [CrossRef]
35. Soupart-Caron, A.S. Stockage de Chaleur dans les Matériaux à Changement de Phase. Ph.D. Thesis, Université Grenoble Alpes, Grenoble, France, 2015.

sustainability

MDPI

Article

Experimental Investigation of a Water–Air Heat Recovery System

Robert Ștefan Vizitiu [1], Ștefănica Eliza Vizitiu [1,*], Andrei Burlacu [1,*], Chérifa Abid [2], Marius Costel Balan [1] and Nicoleta Elena Kaba [3]

[1] Faculty of Civil Engineering and Building Services, "Gheorghe Asachi" Technical University of Iasi, 700050 Iasi, Romania; robert-stefan.vizitiu@academic.tuiasi.ro (R.Ș.V.); marius-costel.balan@academic.tuiasi.ro (M.C.B.)
[2] CNRS, IUSTI UMR 7343, Aix-Marseille Université, 13453 Marseille, France; cherifa.abid@univ-amu.fr
[3] Faculty of Civil Engineering, Politehnica University of Timisoara, 300223 Timișoara, Romania; nicoleta_vox@yahoo.com
* Correspondence: stefanica-eliza.vizitiu@student.tuiasi.ro (Ș.E.V.); andrei.burlacu@academic.tuiasi.ro (A.B.)

Abstract: The implementation of energy-saving measures has a substantial and beneficial impact on the preservation of energy resources as well as the reduction of carbon dioxide emissions. This study focuses on the design and experimental analysis of a water-to-air heat recovery system aimed at capturing waste heat from wastewater and transferring it to a fresh cold air stream using heat pipe technology. The research problem addressed in this study is the efficient recovery of low-grade thermal energy from wastewater, which is often underutilized. The prototype heat recovery unit was designed, manufactured, and tested in the laboratory to assess its performance across various operating conditions. The experimental setup included a system where the primary agent, hot water, was heated to 60 °C and circulated through the evaporator section of the heat recovery unit, while the secondary agent, fresh air, was forced through the condenser section. The system's performance was evaluated under different air velocities, ranging from 3.5 m/s to 4.5 m/s, corresponding to airflow rates of 207.1 m^3/h and 268.6 m^3/h, respectively. The study employed analytical methods alongside empirical testing to determine the effectiveness of the heat recovery system, with the global heat transfer coefficient calculated for different scenarios. The efficiency of the system varied between 25% and 51.6%, depending on the temperature and speed of the fresh air stream. The most significant temperature difference observed between the inflow and outflow of the fresh air stream was 16.8 °C, resulting in a thermal output of 1553 W. Additionally, the average (mean) overall heat transfer coefficient of the unit was calculated to be 49 W/m^2 K, which aligns with values reported in the literature for similar systems. The results demonstrate the potential of the designed system for practical applications in energy conservation and carbon emission reduction.

Keywords: waste heat recovery; heat pipe; energy saving; heat exchanger; heat transfer

Citation: Vizitiu, R.Ș.; Vizitiu, Ș.E.; Burlacu, A.; Abid, C.; Balan, M.C.; Kaba, N.E. Experimental Investigation of a Water–Air Heat Recovery System. *Sustainability* **2024**, *16*, 7686. https://doi.org/10.3390/su16177686

Academic Editor: Andrea Nicolini

Received: 24 July 2024
Revised: 31 August 2024
Accepted: 2 September 2024
Published: 4 September 2024

1. Introduction

In the context of finding sustainable solutions to mitigate the impact of climate change, reducing global carbon dioxide (CO_2) emissions to net zero by 2050 is an urgent issue that requires immediate attention. A recent analysis conducted by the IEA in 2022 revealed that energy-related CO_2 emissions escalated to an all-time high in 2021, soaring by 6% compared to the previous year [1]. As pointed out in the IEA's 2021 investigation, major changes are needed in the production of energy, transportation, as well as consumption if we are going to achieve this ambitious objective by 2050 [2]. In other words, to accomplish this objective, a comprehensive and strategic approach is required that encompasses all aspects of the energy sector, from production to consumption. Waste heat recovery has been highlighted as a viable strategy for lowering carbon emissions and supporting sustainability [3]. This approach not only lowers carbon emissions but also increases energy efficiency and contributes to the system's overall sustainability by capturing wasted heat

from various industrial operations and converting it back into useful energy [4]. The increasing popularity of waste heat recovery systems is reflected in the numerous studies that have focused on improving their efficiency and effectiveness in capturing and repurposing surplus heat [5].

To capture, recover, and exchange heat in industrial processes, various systems have been developed, such as plate heat exchangers [6], waste heat boilers [7], heat pipe systems [8], and others [9]. These types of technologies play an important role in increasing long-term sustainability and energy efficiency in a variety of industries as they allow thermal waste from ongoing operations to be recovered and converted into use for other purposes like heating and the production of energy.

Due to their superior features when it comes to heat pipes, heat pipe heat exchangers stand out among these technologies [10]. Heat-pipe-based heat recovery systems have been extensively investigated in recent years for their potential to recover waste heat in various sectors. Successful applications have been reported in areas such as heating, ventilation and air conditioning [11–13], photovoltaic–thermal systems [14,15], the steel industry [16,17], the ceramic kiln industry [18], the aluminum industry [19], thermal storage [20], and other sectors.

In light of the aforementioned, heat pipes possess vast potential for implementation in various applications of waste heat recovery. Numerous studies have offered valuable insights into the effective utilization of heat pipes for this purpose, highlighting their versatility. As identified in the literature, a broad variety of heat pipe heat exchangers are available, each adapted to a particular application.

In a recent study, ref. [21] evaluated the performance of a heat pipe flue gas waste heat utilization system installed in front of the inlet of an electrostatic precipitator of a boiler. The results showed that the heat exchanger achieved an average flue gas temperature drop of 26.3 °C, a reduced temperature deviation of 8.1 °C, and had the potential to reduce coal consumption by 1.3 g/(kW h) through increased condensate temperature. In a relevant study, ref. [22] performed research aiming to design and construct a heat pipe heat exchanger to recover waste energy from flue gas in a city gate station and to evaluate the resulting energy savings. The results showed that the use of heat pipes reduced natural gas consumption by 510,132 SCM per year and prevented 756 tons of CO_2 from being emitted from the city gate station annually.

Given the extensive potential demonstrated by heat pipes in waste heat recovery applications, it is worth noting a study conducted by [23] that focused on the development and analysis of a heat pipe inserted plate air–air heat exchanger. The experimental results highlighted the improved heat transfer performance and high temperature effectiveness achieved by the heat exchanger. The maximum temperature effectiveness of the heat exchanger reached 70% in summer conditions and the average annual energy efficiency ratio while running in different cities was between 3.67 and 12.72.

In the ETKINA project [24], heat pipe heat exchangers (HPHEs) are identified as a suitable solution for heat recovery in various industrial applications, including aluminum, steel, and ceramics. The project focuses on achieving a 40% waste heat recovery from exhaust streams, ensuring a quick payback period. The anticipated results include annual recoveries of up to 597 MWh, 3020 MWh, and 4003 MWh in each industry, resulting in a substantial decrease in CO_2 emissions. Building upon previous work in the ceramic industry, ref. [25] further investigated the thermal performance of a heat pipe heat exchanger in a ceramic kiln. Their comprehensive study, combining theoretical, experimental, and numerical analyses, confirms the effectiveness of the system in recovering 876 MWh per year. The results demonstrate quick response times and great thermal performance, proving the heat recovery system's potential even further.

Heat pipes offer superior heat transfer performance and have been integrated into solar systems to overcome limitations [26] as a result of numerous studies showing their advantages. Also, by combining heat pipes with phase change materials (PCM), overall

heat transfer rates can be enhanced, leading to greater efficiency and performance in various thermal energy applications [27].

In their study, [28] designed a new solar air collection system that uses flat-plate micro heat pipe arrays and evaluated its thermal performance. The experiments were conducted at different volume flow rates to analyze the energy and exergy aspects. The key findings indicated that the system exhibited good heat storage and release performance, with an average collection efficiency of 35.8% and average storage efficiencies of 67.5% and 87.5% for latent heat storage units I and II, respectively.

In another study, [29] designed and tested a combined thermal storage system using solar Fresnel lenses, heat pipes, and phase change materials (PCM) for efficient heat transfer and long-term heat storage. The findings demonstrated the system's efficacy in efficiently storing heat energy using paraffin wax as the PCM, achieving a maximum energy storage of 730 kJ and over 6 h of heat retention. To optimize the system's performance, the study suggests insulating the heat collector and increasing the number of heat pipes to enhance heat transfer rates and reduce solidification time for the paraffin wax.

The potential of wastewater in terms of its thermal energy content, ranging from 10 to 25 °C [30], has been emphasized in a series of review papers. In line with this perspective, ref. [31] conducted a comprehensive literature review on wastewater heat recovery (WWHR) throughout the sewer system, exploring temperature dynamics, environmental impact, and legal regulations. While specific heat exchanger design and performance aspects are covered in related review papers [32,33], all these studies consistently underscored the significant potential of harnessing heat energy from wastewater for preheating water or space heating purposes in buildings.

In a study conducted by [13], researchers employed Computational Fluid Dynamics (CFD) Heat Transfer Analysis to examine the performance of an innovatively designed HPHE for efficient waste heat recovery in buildings. The primary objective was to develop a heat exchanger capable of preparing domestic hot water and thermal agents while effectively preheating or heating ventilation air. The experimental results showcased the proposed device's notable advantages, including exceptional heat recovery efficiency, cost-effective manufacturing, ease of installation, and user-friendly operation. The analysis demonstrated the effectiveness of the heat pipe heat exchanger, achieving high temperatures for the secondary agent and showcasing the feasibility of the design.

The extraction and utilization of waste heat has generally relied on commercially accessible devices like heat exchangers and heat pumps. According to the aforementioned research in this paper, there is tremendous potential for using waste heat by integrating PCMs into heat transfer systems. This innovative technique revolutionizes waste heat use by separating the heat capturing process from wastewater and integrating heat transfer and storage within a single device. This advancement not only enhances the efficiency of heat harnessing but also introduces a new level of flexibility in utilizing this waste heat, surpassing the limitations of current commercial technologies.

Exploring the topic, ref. [34] introduced a two-stage heat recovery–storage system that holds great potential for minimizing thermal energy losses in the industry. Their system incorporates heat pipes for energy recovery from wastewater and an environmentally friendly phase change material (PCM) for storage. Experimental tests revealed a peak efficiency of 78.1% and significant thermal energy recovery. This study highlights the potential of the system to address the industry's thermal energy losses and emphasizes the need for further research to achieve sustainable energy consumption.

In the non-industrial sector, researchers proposed a unique method for converting low-grade heat from greywater into cold water by integrating a phase change material into a single heat exchanger. The study presented a methodology for optimal PCM selection and heat transfer enhancement. The results showed that the installation of this PCM-HE in a four-member UK household can result in substantial energy savings and a payback time of 4.44 years [35].

In this comprehensive study, our aim was to design and investigate the performance of a water-to-air heat recovery unit that uses heat pipes to extract heat energy from wastewater and transfer it to a fresh air stream. The prototype of the heat recovery unit was designed and manufactured in the laboratory of the Faculty of Civil Engineering and Building Services at the Technical University "Gheorghe Asachi" of Iasi, Romania. To evaluate the performance of the system, the equipment was subjected to experimental investigations confirmed by an analytical approach.

While previous research has explored similar concepts, our study contributes to the ongoing research efforts by providing a comprehensive analysis of analytical data and experimental data. This approach enhances our understanding of the system's performance and its potential for real-world applications. Through this research, we aim to promote heat recovery from wastewater and inspire further advancements in the field of heat recovery systems that take advantage of the complementary advantages of heat pipes. Moreover, our findings underscore the importance of continued research in this domain to refine system designs and unlock its full potential across diverse applications.

2. Materials and Methods

2.1. The Design of the Heat Pipe Heat Recovery System

The water-to-air heat recovery unit is purposefully designed to harness the thermal energy present in wastewater and effectively transfer it to a fresh air stream.

This equipment comprises two distinct zones: the evaporator and the condenser. To ensure complete segregation of the two fluid streams, a separating flange is strategically placed between the two zones, preventing cross-contamination. Inside the heat recovery unit, a set of fourteen vertically oriented heat pipes acts as a highly effective heat conductor, optimizing heat transfer from the heat source. The evaporator, condenser, and separation flange are made of stainless steel and the heat pipes are made of copper. Utilizing water as the working fluid, these gravitational heat pipes have been designed and optimized through extensive experimental testing [36]. Detailed construction specifications of the heat recovery unit can be found in Table 1.

Table 1. Constructive details of the components.

Component	Height [m]	Diameter [m]
Evaporator	0.400	0.250
Condenser	0.645	0.250
Separation flange	0.010	0.300
Heat pipes	1.000	0.015
Diameter inlet/outlet primary agent	-	0.015
Diameter inlet/outlet secondary agent	-	0.150

The 3D model was designed using Autodesk Inventor 2021 software. A visual representation of the heat recovery system components described can be observed in Figure 1, providing a schematic overview.

2.2. Experimental Setup

The water-to-air heat recovery unit has been constructed, and an experimental test stand has been established for precise testing and evaluation. The primary agent used in the experiment is hot water, generated by an 8-kW electric heating unit set to the required temperature for the experiment. To facilitate the flow of hot water, a pump is integrated into the electric heating unit, ensuring efficient circulation throughout the system. The primary circuit comprises thermally insulated stainless steel pipes with a diameter of 0.02 m, connecting the evaporator to the heating unit. For the secondary agent circuit, the air circuit, a stainless-steel pipe with a diameter of 0.125 m, is utilized, supported by a 9-speed fan to ensure optimal air circulation. The air velocity for each stage was measured using a digital anemometer, placed at the inlet of the condenser. The mean air velocity in

the circular duct was determined using the Insize 9331-40 digital anemometer (Suzhou, China), which features an integrated function for calculating the average air velocity and has a precision of ±2%.

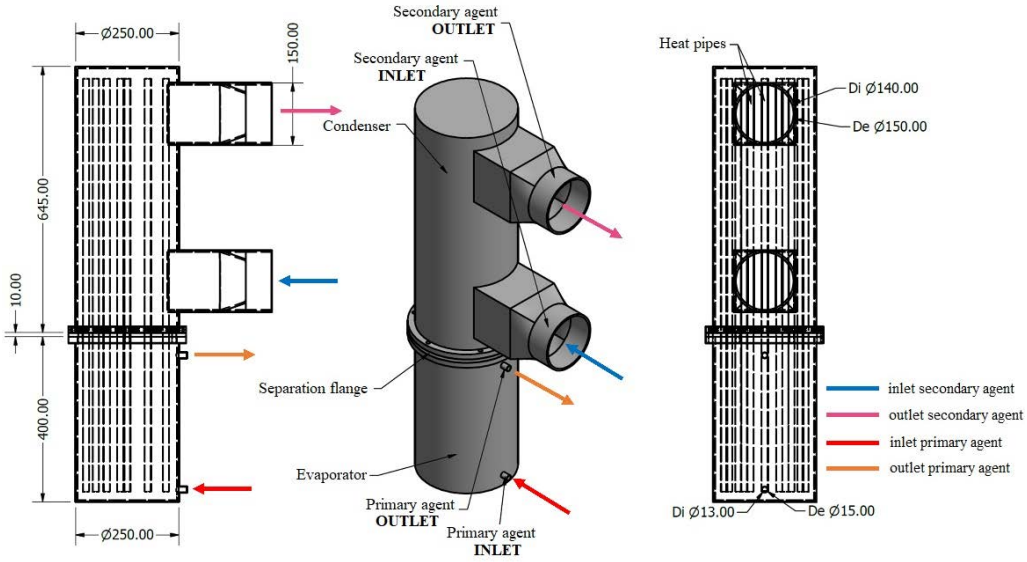

Figure 1. The 3D design of the HPHE.

Given that the Insize 9331-40 digital anemometer's impeller has a smaller diameter than the air duct, a potential error in measuring the average flow velocity was anticipated. To mitigate this, the anemometer was centrally positioned in the duct where the flow is most uniform, and additional measurements were taken at various points across the duct's cross-section. The anemometer's built-in averaging function, which records and averages the air velocity over time, was utilized to ensure accurate measurements. Furthermore, a correction factor based on the cross-sectional area difference between the duct and the impeller was applied to the recorded velocities. This approach, combined with the device's precision, provided a reliable estimate of the average air velocity within the duct. The recorded values are presented in Table 2. The air inlet of the ductwork is located outside the building, allowing the air temperature to vary with atmospheric conditions. The temperatures were measured using an LT BTM-420SD electronic thermometer (Coopersburg, PA, USA), which has a precision of ±0.4%. The temperature sensors were strategically placed at the inlet and outlet of both the evaporator and the condenser to ensure accurate monitoring and data collection during the performance evaluation of the heat recovery system.

Table 2. Average temperature of air at the inlet/outlet of the condenser.

Test No.	Fan Speed 3.5 [m/s]		Fan Speed 4.5 [m/s]	
	$T_{1,air}$—Inlet [°C]	$T_{2,air}$—Outlet [°C]	$T_{1,air}$—Inlet [°C]	$T_{2,air}$—Outlet [°C]
Test 1	−2.9	13.9	−3.9	12.2
Test 2	−0.4	15.0	2.4	16.7
Test 3	1.7	16.3	4.1	17.2
Test 4	2.6	17.2	5.0	17.2
Test 5	3.8	17.6	5.9	18.2
Test 6	4.8	18.1	8.2	18.9
Test 7	5.7	18.8	12.9	20.9
Test 8	6.6	19.3	14.6	22.6
Test 9	7.5	19.6	15.7	23.2

The equipment's primary objective is to preheat or warm the air introduced into the building during cold periods, enhancing comfort and energy efficiency. For a visual

representation, Figure 2 illustrates the detailed model of the experimental stand as currently present in the laboratory.

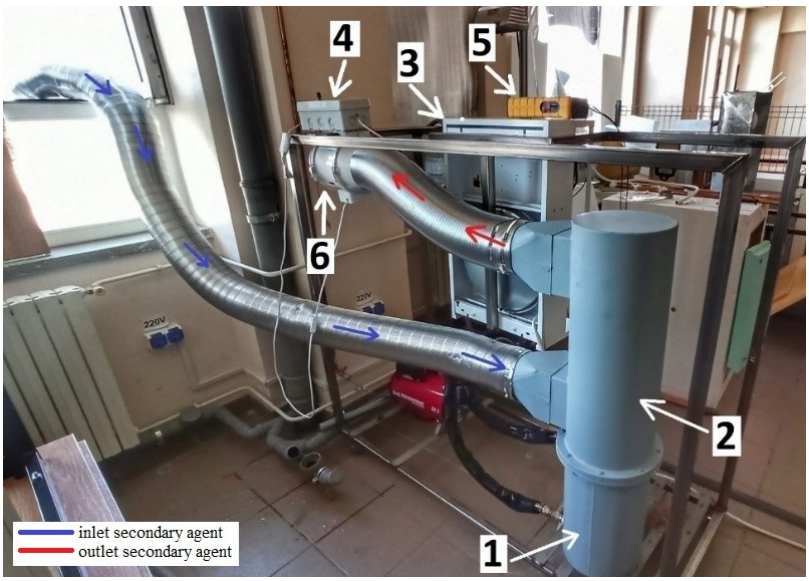

Figure 2. The laboratory experimental stand: 1—Evaporator, 2—Condenser, 3—Electric heater, 4—Fan speed control switch, 5—LT BTM-420SD electronic thermometer, 6—Fan.

2.3. Tests Performed

In the following stage, the air-to-water heat exchanger was subjected to a comprehensive series of tests to evaluate its efficiency. The water temperature and velocity at the inlet of the evaporator were maintained constantly at 60 °C and 2.25 m/s, respectively. The air velocity at the condenser's inlet is determined by the fan's setting. Measurements were taken for two fan speeds, 3.5 m/s and 4.5 m/s, which have the corresponding cooling airflow rates of 207.1 m^3/h and 268.6 m^3/h, respectively. As the introduced air is drawn directly from the outside of the building, its temperature cannot be controlled. Each test lasted for 60 min, with the inlet temperature of the air fluctuating based on the outdoor air temperature. To facilitate analytical calculations and comparisons, an average temperature was calculated both at the inlet and outlet of the condenser. The fluctuation in average air temperatures at the equipment's inlet are attributed to the tests being carried out on separate days. Table 2 provides an overview of these measurements.

3. Results and Discussion

3.1. Experimental Results

A series of 18 experimental tests were carried out to investigate the performance and efficiency of the equipment under various conditions by manipulating the temperature and air velocity at the inlet of the condenser. The mean air temperature at the outlet of the evaporator was determined by calculating the arithmetic average of the sensor readings taken after the initial 15-min period, during which the temperature reached a stable state. The findings have been summarized and highlighted in Table 2. The temperature measurements presented in the following tables and figures have an associated error of ±0.4% due to the accuracy of the thermometer and ±1.5 °C due to the accuracy of the thermocouple.

To facilitate the visualization of air heating dynamics using the temperature acquired from the heat pipes, we calculated the temperature difference between the average air temperature at the condenser's outlet and inlet. This analysis was conducted for both cases with air velocities of 3.5 m/s and 4.5 m/s, revealing that the difference in temperature between the inlet and outlet increases as the outdoor air temperature drops. These empirical findings have been presented graphically in Figure 3.

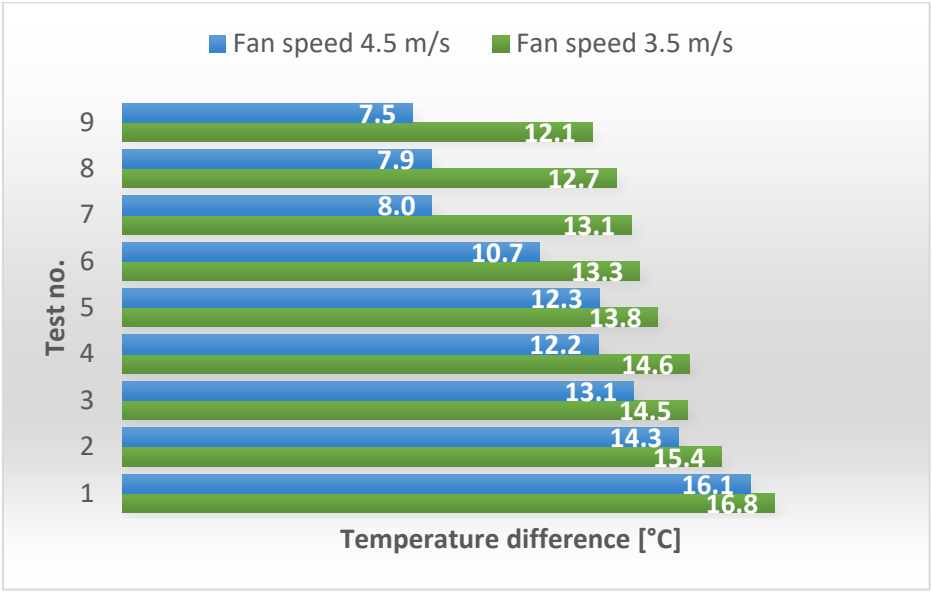

Figure 3. Temperature difference of air between outlet and inlet.

3.2. The Efficiency of the Equipment

In order to quantify the quantity of energy recovered by the heat pipes from the water and subsequently transmitted to the fresh air flow, the thermal heat flow rates were calculated for both the evaporator and condenser in accordance with Equation (1).

$$Q = C_{Ev}(T_{2,air} - T_{1,air}) = C_{Co}(T_{2,water} - T_{1,water}) \quad (1)$$

Equation (2) offers an approach for determining the rate of heat transfer within the heat recovery system. The heat capacity rates for the evaporator (C_{Ev}) and the condenser section (C_{Co}) can be established by multiplying the mass flow rate with the specific heat capacity related to the respective section. The efficiency of the equipment for each test is calculated through the use of Equation (3).

$$C_{Ev} = \dot{m}_{Ev} \times c_{p,Ev} \quad (2)$$

$$\varepsilon = \frac{Q_{Co}}{Q_{Ev}} \quad (3)$$

The findings are presented in Figure 4. The influence of external air temperature on the heat exchanger's efficiency is less pronounced at lower fan speeds compared to scenarios with higher air velocity. Notably, during tests 7, 8, and 9, it was observed that the effectiveness of the equipment drops to 25–27% when the external air temperature is higher, within the range of 13–15 °C.

Nevertheless, its peak efficiency is observed in the higher speed stage during test 1, where, at an external temperature of −3.92 °C, the condenser produced air at 12.23 °C, delivering an equivalent thermal power of 1553 W. Similarly, within the lower speed stage tests, the highest efficiency was also achieved during test 1, with an inlet air temperature of −2.91 °C, resulting in an outlet temperature of 13.86 °C and an equivalent thermal output of 1254 W.

Figure 5 illustrates the performance of the equipment under its most efficient scenario during test 1 when the fans speed is 4.5 m/s. T1,air inlet represents the temperature of the air at the inlet of the condenser while T2,air outlet represents the air temperature at the outlet of the condenser. It is notable that, after approximately 15 min, the air temperature at the outlet of the equipment reaches a state of stability, characterized by a constant value.

Furthermore, the average temperature difference between the outlet and inlet remains at 12.23 °C.

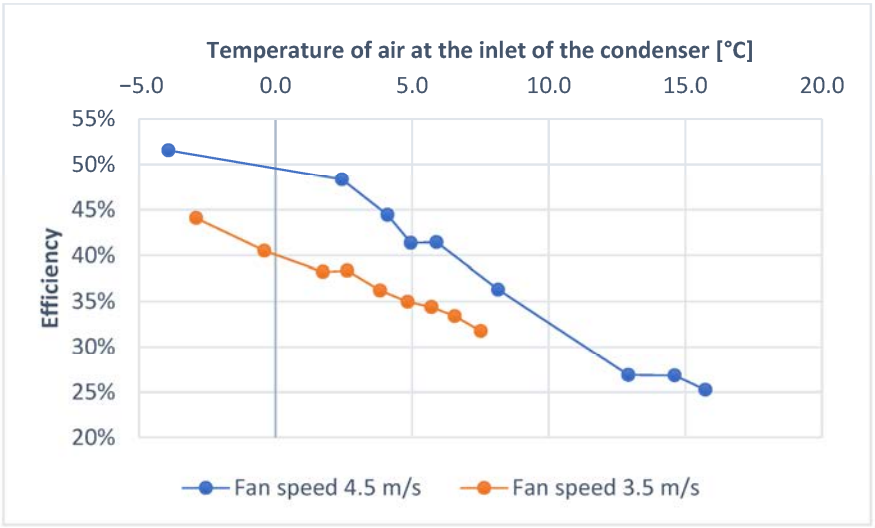

Figure 4. The efficiency of the heat recovery system.

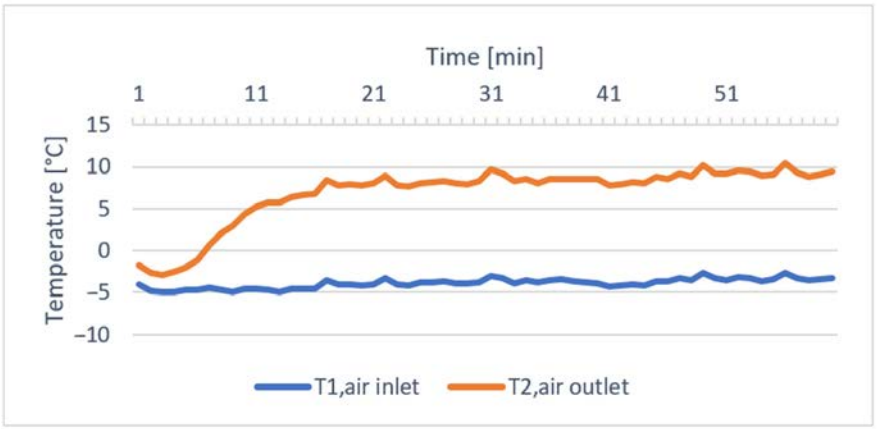

Figure 5. Temperature variation of the air in the most efficient scenario.

In order to compare the results with the performance of other heat exchangers utilizing water as the primary agent and air as the secondary agent, the equipment's overall heat transfer coefficient was calculated using Equation (4).

$$k = \frac{Q_{Co}}{S \times \Delta t_{med}} \quad (4)$$

The average (mean) overall heat transfer coefficient has been determined for each specific scenario, generating values ranging from 39 to 61 W/m^2 K. The average of these measurements was determined to be 49 W/m^2 K, which is within the range of values reported in the existing literature for the overall heat transfer coefficient of water–air exchangers. These reported values typically range from 15 to 70 W/m^2 K [37].

4. Conclusions

This study aimed to design and experimentally investigate a water-to-air heat recovery system utilizing heat pipe technology to harness waste heat from wastewater and transfer it to a fresh air stream. The research addressed the challenge of improving energy efficiency and reducing carbon emissions by leveraging low-grade thermal energy that would otherwise be wasted. Specifically, the research targets the need for efficient heat

recovery solutions across residential, commercial, and industrial settings, focusing on the significant role buildings play in energy consumption and emissions. The heat recovery system developed in this study can be effectively applied in residential settings, where it can be coupled with solar thermal panels to preheat or heat incoming air, reducing the need for conventional heating and enhancing energy efficiency. In industrial settings, such as in steel and aluminum manufacturing, the system can recover waste heat from processes to produce preheated air for ventilation or other uses. This application not only improves energy efficiency but also reduces primary energy consumption and CO_2 emissions.

The experimental setup involved a prototype heat recovery unit, which was rigorously tested under various conditions to evaluate its performance. The system's efficiency varied between 25% and 51.6%, depending on the temperature and speed of the fresh air stream. The global heat transfer coefficient was determined to be 49 W/m^2 K, aligning with values reported in the literature for similar systems.

The results demonstrate that the proposed heat recovery system is a viable solution for enhancing energy efficiency in HVAC systems and other industrial applications. By recovering waste heat and repurposing it for air heating, the system can contribute to significant energy savings and a reduction in CO_2 emissions.

In conclusion, the study highlights the potential of heat pipe-based heat recovery systems in promoting sustainability across various sectors. While this study successfully demonstrates the system's ability to achieve substantial temperature increases in the air, it primarily focused on validating the thermal efficiency of the heat recovery system. However, we acknowledge that other critical factors such as humidity, pressure, and air composition, which are essential for assessing overall air quality and system performance, were not considered in the current study.

Future research should build upon these findings by investigating the impact of the heat recovery system on additional air quality parameters. Exploring how the system affects humidity, pressure, and air composition will provide a more holistic understanding of its performance and suitability for various residential, commercial, and industrial applications. This expanded scope will help optimize the system further and ensure it meets broader environmental and operational standards, enhancing its applicability across different sectors.

Author Contributions: Conceptualization, Ș.E.V., A.B. and C.A.; methodology, Ș.E.V., R.Ș.V. and A.B.; software, M.C.B. and R.Ș.V.; validation, Ș.E.V., A.B., M.C.B. and N.E.K.; formal analysis, C.A. and Ș.E.V.; investigation, Ș.E.V., R.Ș.V., M.C.B. and N.E.K.; resources, M.C.B. and A.B.; data curation, R.Ș.V., C.A. and Ș.E.V.; writing—original draft preparation, Ș.E.V. and R.Ș.V.; writing—review and editing, A.B., C.A. and N.E.K.; visualization, Ș.E.V. and M.C.B.; supervision, C.A., A.B. and R.Ș.V. All authors have read and agreed to the published version of the manuscript.

Funding: This research received no external funding.

Institutional Review Board Statement: Not applicable.

Informed Consent Statement: Not applicable.

Data Availability Statement: The original contributions presented in the study are included in the article, further inquiries can be directed to the corresponding authors.

Conflicts of Interest: The authors declare no conflicts of interest.

Nomenclatures

HPHE	Heat pipe heat exchanger
PCM	Phase change material
$T_{1,air}$	Average temperature of air at the inlet of the condenser [°C]
$T_{2,air}$	Average temperature of air at the outlet of the condenser [°C]
Q	Quantity of heat [W]
C_{Ev}	Heat capacity rate of the evaporator
C_{Co}	Heat capacity rate of the condenser

$T_{1,water}$	Average temperature of water at the inlet of the evaporator [°C]
$T_{2,water}$	Average temperature of water at the outlet of the evaporator [°C]
m_{Ev}	Mass flow rate of water [kg/h]
$C_{p,Ev}$	Specific heat of water [kg/m^3 K]
ε	Efficiency
k	Average (mean) overall heat transfer coefficient [W/m^2 K]
S	Area of heat exchange [m^2]
Δt_{med}	Logarithmic mean temperature difference [°C]

References

1. IEA (International Energy Agency). *Global Energy Review: CO_2 Emissions in 2021*; IEA: Paris, France, 2022.
2. IEA (International Energy Agency). *Net Zero by 2050*; IEA: Paris, France, 2021.
3. Firth, A.; Zhang, B.; Yang, A. Quantification of global waste heat and its environmental effects. *Appl. Energy* **2019**, *235*, 1314–1334. [CrossRef]
4. Miró, L.; Brückner, S.; Cabeza, L.F. Mapping and discussing Industrial Waste Heat (IWH) potentials for different countries. *Renew. Sustain. Energy Rev.* **2015**, *51*, 847–855. [CrossRef]
5. Kuah, C.T.; Koh, Q.Y.; Rajoo, S.; Wong, K.Y. Waste heat recovery research—A systematic bibliometric analysis (1991 to 2020). *Environ. Sci. Pollut. Res.* **2023**, *30*, 72074–72100. [CrossRef] [PubMed]
6. Sreejith, K.; Varghese, B.; Das, D.; Devassy, D.; Harikrishnan, K.; Sharath, G.K. Design and Cost Optimization of Plate Heat Exchanger. *Int. J. Adv. Eng. Res. Sci.* **2014**, *4*, 43–48.
7. Men, Y.; Liu, X.; Zhang, T. A review of boiler waste heat recovery technologies in the medium-low temperature range. *Energy J.* **2021**, *237*, 121560. [CrossRef]
8. Xie, C.-Y.; Tao, H.-Z.; Li, W.; Cheng, J.-J. Numerical simulation and experimental investigation of heat pipe heat exchanger applied in residual heat removal system. *Ann. Nucl. Energy* **2019**, *133*, 568–579. [CrossRef]
9. Jouhara, H.; Khordehgah, N.; Almahmoud, S.; Delpech, B.; Chauhan, A.; Tassou, S.A. Waste heat recovery technologies and applications. *Therm. Sci. Eng. Prog.* **2018**, *6*, 268–289. [CrossRef]
10. Jouhara, H.; Almahmoud, S.; Brough, D.; Guichet, V.; Delpech, B.; Chauhan, A.; Ahmad, L.; Serey, N. Experimental and theoretical investigation of the performance of an air to water multi-pass heat pipe-based heat exchanger. *Energy J.* **2021**, *219*, 119624. [CrossRef]
11. Hakim, I.I.; Sukarno, R.; Putra, N. Utilization of U-shaped finned heat pipe heat exchanger in energy-efficient HVAC systems. *Therm. Sci. Eng. Prog.* **2021**, *25*, 100984. [CrossRef]
12. Mahajan, G.; Thompson, S.M.; Cho, H. Experimental characterization of an n-pentane oscillating heat pipe for waste heat recovery in ventilation systems. *Heliyon* **2018**, *4*, e00922. [CrossRef]
13. Burlacu, A.; Sosoi, G.; Vizitiu, R.Ș.; Bărbuță, M.; Lăzărescu, C.D.; Ciocan, V.; Șerbănoiu, A.A. Energy efficient heat pipe heat exchanger for waste heat recovery in buildings. *Procedia Manuf.* **2018**, *22*, 714–721. [CrossRef]
14. Wang, T.-Y.; Diao, Y.-H.; Zhu, T.-T.; Zhao, Y.-H.; Liu, J.; Wei, X.-Q. Thermal performance of solar air collection-storage system with phase change material based on flat micro-heat pipe arrays. *Energy Convers. Manag.* **2017**, *142*, 230–243. [CrossRef]
15. Maraj, A.; Londo, A.; Gebremedhin, A.; Firat, C. Energy performance analysis of a forced circulation solar water heating system equipped with a heat pipe evacuated tube collector under the Mediterranean climate conditions. *Renew. Energ.* **2019**, *140*, 874–883. [CrossRef]
16. Jouhara, H.; Almahmoud, S.; Chauhan, A.; Delpech, B.; Bianchi, G.; Tassou, S.A.; Llera, R.; Lago, F.; Arribas, J.J. Experimental and theoretical investigation of a flat heat pipe heat exchanger for waste heat recovery in the steel industry. *Energy J.* **2017**, *141*, 1928–1939. [CrossRef]
17. Ma, H.; Yin, L.; Shen, X.; Lu, W.; Sun, Y.; Zhang, Y.; Deng, N. Experimental study on heat pipe assisted heat exchanger used for industrial waste heat recovery. *Appl. Energy* **2017**, *169*, 177–186. [CrossRef]
18. Delpech, B.; Axcell, B.; Jouhara, H. Experimental investigation of a radiative heat pipe for waste heat recovery in a ceramics kiln. *Energy J.* **2019**, *170*, 636–651. [CrossRef]
19. Jouhara, H.; Nieto, N.; Egilegor, B.; Zuazua, J.; González, E.; Yebra, I.; Igesias, A.; Delpech, B.; Almahmoud, S.; Brough, D.; et al. Waste heat recovery solution based on a heat pipe heat exchanger for the aluminium die casting industry. *Energy J.* **2023**, *266*, 126459. [CrossRef]
20. Mathew, A.A.; Thangavel, V. A novel thermal energy storage integrated evacuated tube heat pipe solar dryer for agricultural products: Performance and economic evaluation. *Renew. Energ.* **2021**, *179*, 1674–1693. [CrossRef]
21. Wang, Y.; Chen, Y.; Wang, K.; Li, X. Performance evaluation and thermal analysis of heat pipe flue gas waste heat utilization system. *Energy Rep.* **2022**, *8*, 210–217. [CrossRef]
22. Alizadeh, A.; Ghadamian, H.; Aminy, M.; Hoseinzadeh, S.; Sahebi, H.K.; Sohani, A. An experimental investigation on using heat pipe heat exchanger to improve energy performance in gas city gate station. *Energy J.* **2022**, *252*, 123959. [CrossRef]
23. Xue, L.; Ma, G.; Wang, L. Operation characteristics of air–air heat pipe inserted plate heat exchanger for heat recovery. *Energy Build.* **2019**, *185*, 66–75. [CrossRef]

24. Egilegor, B.; Jouhara, H.; Zuazua, J.; Al-Mansour, F.; Plesnik, K.; Montorsi, L.; Manzini, L. ETEKINA: Analysis of the potential for waste heat recovery in three sectors: Aluminium low pressure die casting, steel sector and ceramic tiles manufacturing sector. *Int. J. Thermofluid Sci. Technol.* **2020**, *1–2*, 100002. [CrossRef]
25. Jouhara, H.; Bertrand, D.; Axcell, B.; Montorsi, L.; Venturelli, M.; Almahmoud, S.; Milani, M.; Ahmad, L.; Chauhan, A. Investigation on a full-scale heat pipe heat exchanger in the ceramics. *Energy J.* **2021**, *223*, 120037. [CrossRef]
26. Shafieian, A.; Khiadani, M.; Nosrati, A. Strategies to improve the thermal performance of heat pipe solar collectors in solar systems: A review. *Energy Convers. Manag.* **2019**, *183*, 307–331. [CrossRef]
27. Ali, H.M. Applications of combined/hybrid use of heat pipe and phase change materials in energy storage and cooling systems: A recent review. *J. Energy Storage* **2019**, *26*, 100986. [CrossRef]
28. Diao, Y.; Qi, N.; Wang, Z.; Zhao, Y.; Chen, C.; Wang, Z. Thermal performance analysis of a solar air collection–cascade storage system integrated with micro-heat pipe arrays. *Sol. Energy* **2021**, *224*, 1271–1290. [CrossRef]
29. Rahim, N.C.; Remeli, M.F.; Singh, B.; Moria, H. Designing a Solar Heat Storage System using Heat Pipe and Phase-Change Material (PCM). *Adv. Res. Fluid Mech.* **2022**, *91*, 102–114. [CrossRef]
30. Spriet, J.; McNabola, A. Decentralized drain water heat recovery: A probabilistic method for prediction of wastewater and heating system interaction. *Energy Build.* **2019**, *183*, 684–696. [CrossRef]
31. Nagpal, H.; Spriet, J.; Murali, M.K.; McNabola, A. Heat Recovery from Wastewater—A Review of Available Resource. *Water* **2021**, *13*, 1274. [CrossRef]
32. Hepbasli, A.; Biyik, E.; Ekren, O.; Gunerhan, H.; Araz, M. A key review of wastewater source heat pump (WWSHP) systems. *Energy Convers. Manag.* **2014**, *88*, 700–722. [CrossRef]
33. Culha, O.; Gunerhan, H.; Biyik, E.; Ekren, O.; Hepbasli, A. Heat exchanger applications in wastewater source heat pumps for buildings: A key review. *Energy Build.* **2015**, *104*, 215–232. [CrossRef]
34. Vizitiu, R.S.; Burlacu, A.; Abid, C.; Balan, M.C.; Vizitiu, S.E.; Branoaea, M.; Kaba, N.E. Investigating the Efficiency of a Heat Recovery–Storage System Using Heat Pipes and Phase Change Materials. *Materials* **2023**, *16*, 2382. [CrossRef] [PubMed]
35. Mazhar, A.R.; Liu, S.; Shukla, A. A key review of non-industrial greywater heat harnessing. *Energies* **2018**, *11*, 386. [CrossRef]
36. Vizitiu, R.S.; Burlacu, A.; Abid, C.; Serban, A.; Verdes, M.; Ciocan, V.; Branoaea, M. Experimental investigation on the optimum filling ratio of heat pipes used for heat recovery systems. In Proceedings of the International Conference Building Services and Energy Efficiency 2020, Iasi, Romania, 22–23 October 2020; pp. 154–161. [CrossRef]
37. Available online: https://www.engineeringtoolbox.com/heat-transfer-coefficients-exchangers-d_450.html (accessed on 23 July 2024).

materials

MDPI

Article

Investigating the Efficiency of a Heat Recovery–Storage System Using Heat Pipes and Phase Change Materials

Robert Stefan Vizitiu [1,*], Andrei Burlacu [1,*], Chérifa Abid [2], Marius Costel Balan [1], Stefanica Eliza Vizitiu [1], Marius Branoaea [1] and Nicoleta Elena Kaba [3]

[1] Faculty of Civil Engineering and Building Services, "Gheorghe Asachi" Technical University of Iasi, 700050 Iasi, Romania
[2] Aix-Marseille Université, CNRS, IUSTI, 13453 Marseille, France
[3] Faculty of Civil Engineering, Politehnica University of Timisoara, 300223 Timișoara, Romania
* Correspondence: robert-stefan.vizitiu@academic.tuiasi.ro (R.S.V.); andrei.burlacu@academic.tuiasi.ro (A.B.)

Abstract: This study presents an experimental and numerical investigation into the efficiency of a two-stage heat recovery–storage system for reducing the thermal energy losses in the industry. The system is designed to recover and store waste thermal energy from residual fluids using heat pipes for recovery and an environmentally friendly phase change material for heat storage. Experimental investigation was conducted using water as the primary agent and varying the temperature between 60 °C, 65 °C, and 70 °C at a constant flow rate of 24 L/min. The secondary agent, also water, was used at an initial temperature of 10 °C and the flow rate was varied between 1 L/min, 2 L/min, and 3 L/min. The results show that the system had a peak efficiency of 78.1% and was able to recover a significant amount of thermal energy. This study demonstrates the potential of this system to reduce the thermal energy losses in the industry and highlight the importance of further research and development in this field, as the industry is responsible for approximately 14% of the total thermal energy losses and finding efficient ways to recover and store waste thermal energy is crucial to achieving sustainable energy consumption.

Keywords: heat recovery; heat storage; heat pipe; PCM

Citation: Vizitiu, R.S.; Burlacu, A.; Abid, C.; Balan, M.C.; Vizitiu, S.E.; Branoaea, M.; Kaba, N.E. Investigating the Efficiency of a Heat Recovery–Storage System Using Heat Pipes and Phase Change Materials. *Materials* **2023**, *16*, 2382. https://doi.org/10.3390/ma16062382

Academic Editors: Corneliu Munteanu and Ioan Doroftei

Received: 24 February 2023
Revised: 10 March 2023
Accepted: 14 March 2023
Published: 16 March 2023

1. Introduction

The negative impact of fossil fuels on the climate is well known and humanity is seeking non-polluting, renewable resources to replace them. The Paris Agreement of 2017 aims to keep the global temperature rise below 2 °C by the end of the century, which would require USD 3.5 trillion in annual investments in renewable and sustainable energy by 2050, according to a study by the International Energy Agency and International Renewable Energy Agency. In 2015, USD 1.8 trillion was invested in energy, with 12% going towards energy efficiency [1].

Heat recovery is a technique that has the potential to contribute to the reduction in greenhouse gas emissions. The process involves the capture and conversion of residual thermal energy into useful forms of energy, such as thermal, electrical, or mechanical energy. The most common forms of residual thermal energy are steam, hot air, or hot water, and the efficiency of the heat recovery process increases with the temperature of the residual heat. There are various heat recovery technologies available, including energy recovery heat exchangers, such as waste heat recovery units. Among these, heat pipe heat exchangers are considered particularly efficient due to the high thermal conductivity of heat pipes, which allows for a minimal temperature drop during heat transfer over long distances.

A number of studies have been conducted to evaluate the various types of heat recovery systems, primarily utilizing residual heat from industrial sources. The sources of energy that can be recovered in this manner include the heat generated from industrial

equipment, heat generated from combustion processes, and the heat lost through radiation, conduction, or convection during industrial processes [2].

Jouhara et al. [3] designed and studied a radiative heat recovery system for recovering waste heat radiated during the steel manufacturing process. Another study, conducted by Delpech et al. [4], examined a heat recovery system that captures waste heat from the cooling of ceramic parts. The results of this study indicate that, at temperatures below 200 °C, the heat transfer is primarily convective, while at higher temperatures, the heat transfer is a combination of radiation and convection. Other studies have also been conducted on heat pipe heat recovery systems utilizing flue gases [5] and hot air [6,7] as primary sources. The waste heat recovery from steam is a well-established method and there have been studies investigating the use of steam generated from nuclear power plants as a primary source of seawater desalination [8].

The heat recovery process can be further optimized by incorporating latent heat storage systems. These systems consist of three main components: a storage medium, typically a phase change material, a heat transfer mechanism, and a containment system [9]. However, one of the main limitations of phase change materials is their low thermal conductivity, which has led to numerous studies aiming to improving their performance [10–13].

There are some experiments combining heat pipe technology with phase change materials [14,15]. A study [16] performed in 2017 by Amini et al. investigated a heat recovery system that uses steam as a primary agent and a salt hydrate PCM which melts at 89 °C as the heat storage medium. The results showed the good efficiency of the systems but it can be improved by increasing the thermal conductivity of the PCM.

Fan et al. [17] investigated a two-stage latent thermal energy storage tank that is integrated with an air purification pilot plant. A test was then carried out under actual operating conditions. The tank has units that are filled with commercial paraffin with a melting point of 70 °C and 48 °C, respectively. For a better heat transfer performance, heat pipes are combined with vertical fins for this research. According to the results, adding a latent thermal energy storage tank to an air separation system allows for a 51,369.5 kJ heat savings during a charging–discharging session. The waste heat requirement of 40 °C allowed for the recovery of 64.7% of the excess heat in the exhaust air and annually, 25,784.3 kg less CO_2 is emitted. In contrast with previous known latent thermal energy storage for industrial purposes, the latent thermal energy storage exhibits great results.

In another study [18] from 2015, a high-temperature latent heat thermal energy storage system assisted by finned heat pipes was subjected to numerical simulations, to check the charging process of PCM with a different configuration of embedded heat pipes. It was found that the bigger the number of heat pipes, the smaller the thermal resistance within the system, resulting a faster charging process.

This previous study is relevant to the recent research, as the use of finned storage units was also explored by [19], as a method to enhance the thermal performance of a vertically configured-cylindrical copper LHTES in combination with nano-enhanced PCM (NEPCM) and both outer and inner longitudinal fins. The study's outcomes demonstrate that the inclusion of six longitudinal fins on the internal and external surfaces of the LHTES wall leads to a notable decrease in the duration needed for discharging and charging by 71% and 62%, correspondingly, compared to the pure PCM reference condition lacking fins.

In their study, Nie et al. [20] also investigated the aspects of successively charging and discharging the phase change material in a thermal energy storage unit with fins. According to the results, it was observed that the heat transmission was enhanced when using a straight fin design, particularly when there are fewer fins used and when the thermal conductivity of the outer tube material is lower. Additionally, it was discovered that, when continuously charging and discharging, heat transfer was improved by using longer fins rather than shorter fins, while the fin volume remained the same.

In-depth experimental and computational investigation by Ruiz et al. [21] resulted in the determination of the optimum design for a water heat recovery and storage unit based on phase change material plates. The phase change material storage unit is designed

to store approximately 75% of the thermal energy during the heat charging phase and some of it is recovered to provide approximately 50% of the thermal energy needed for the subsequent process. The performance of heat transfer for the latent thermal energy storage unit appeared to be strongly linked to the working parameters.

In order to enhance the efficiency of latent heat thermal energy storage (LHTES) with embedded heat pipes, Ladekar et al. [22] experimentally investigated the charging and discharging process in the case of using a heat pipe and a copper pipe. The results show that the capability to store heat for the charging process phase increases when majoring the volume flow rate, and early heat extraction when discharging becomes achievable. The charging and discharging of latent LHTES with integrated heat pipes performed well during testing with a flow rate of 10 L/min. When compared to systems with copper pipes, LHTES with integrated heat pipes has greater and more consistent efficiency and efficacy. It was also concluded that, as the volume flow drops, the overall melting time of the phase-changing material reduces.

The novelty of this research lies in the combination of gravitational heat pipes and phase change materials in a heat recovery–storage system (HRSS) for recovering and storing waste thermal energy from residual fluids. The system utilizes gravitational heat pipes to recover the low-temperature residual heat and store it as latent heat within a phase change material.

Previous research has separately focused on either the use of heat pipes or phase change materials, indicating the lack of experimental studies using both the quick heat transfer ability of heat pipes and the latent heat storage property of phase change materials. Therefore, it is essential to give more attention to the experimental part in order to reveal methods for improving the heat transfer performance of phase change materials and heat pipes [23].

This study proposes a new approach that combines both technologies to increase the efficiency of the heat recovery process and store thermal energy for future use. Heat pipes are used in the device's modular design to increase the efficiency of the heat recovery process, and phase change materials are used to store the thermal energy. The apparatus can recover the waste thermal energy from used water at low and medium temperatures. The thermal energy can then be transformed into additional thermal energy and used to pre-heat or heat water for domestic use or other heating systems.

This research effort seeks to examine the potential of the suggested HRSS in recovering and storing waste thermal energy from low- to medium-temperature residual fluids. The study intends to provide experimental proof of the HRSS' efficiency and highlight the technology's potential benefits in reducing thermal energy losses and achieving sustainable energy management.

In the following sections of this paper, there are descriptions of the design of the equipment and its testing parameters, followed by the presentation of results and conclusions.

2. Materials and Methods

2.1. The Design of the Equipment

The two-stage heat recovery–storage system consists of the connection of a water-to-water heat exchanger (heat exchanger A) to a water-to-water heat exchanger with integrated PCM (heat exchanger B). Heat exchanger A was previously tested as a stand-alone heat recovery system, revealing a high efficiency of up to 76.7% in recovering low- and medium-temperature thermal energy [24].

The design of heat exchanger A is presented in Figure 1. The heat exchanger consists of two main areas called the evaporator and condenser, separated by a sealing flange. Fourteen heat pipes are inserted transversely inside the equipment with the role of extracting thermal energy from the primary agent inside the evaporator and transferring it to the secondary agent inside the condenser. Inside the condenser, there are three rings and two discs, creating a path for the secondary agent. The evaporator, condenser, and separation flange

are made of stainless steel and the rings, discs, and heat pipes are made of copper. The working fluid of the heat pipes is distilled water with a fill ratio of 25%.

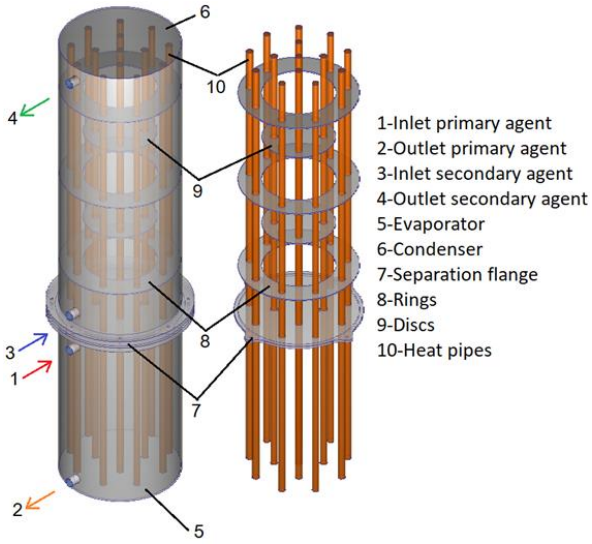

Figure 1. The design of the water–water heat exchanger (heat exchanger A).

The design of heat exchanger B is similar to the design of the heat exchanger, but the major difference is given by the fact that the secondary agent is directed through the condenser by a coil and the volume of the condenser is filled with a phase change material. The coil is made of copper, has a total length of 3.5 m, and has 7 turns with a diameter of 15 cm. The phase change material is coconut oil, and the necessary quantity to fill the condenser is 26.4 kg. The thermophysical properties of these phase change materials are presented in Table 1 [25].

Table 1. Thermophysical properties of coconut oil [24].

Mean specific heat of the solid	3.2 kJ/kg × K
Mean specific heat of the liquid	4.1 kJ/kg × K
Heat of fusion	249 kJ/kg
Melting temperature	35 °C

Figure 2 presents the design of heat exchanger B in 3D.

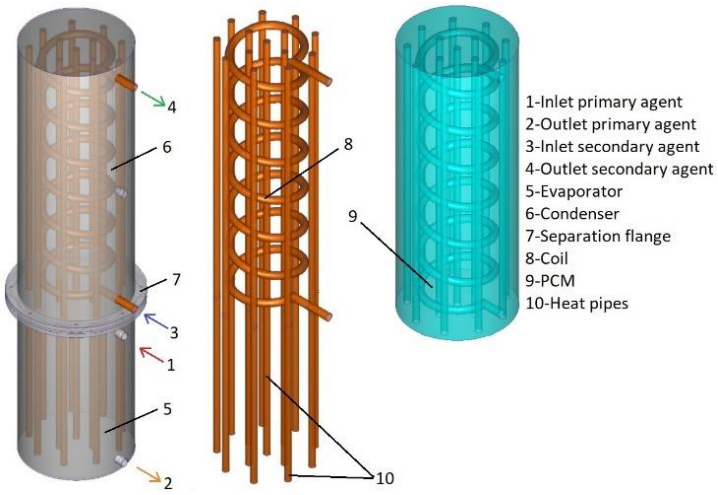

Figure 2. The design of the PCM heat exchanger (heat exchanger B).

The constructive details of the two heat exchangers can be viewed in Table 2.

Table 2. Constructive details of the components.

Component	Height/Length (m)	Diameter (m)
Evaporator	0.395	0.250
Condenser	0.640	0.250
Separation flange	0.005	0.300
Discs	0.005	0.150
Rings	0.005	0.246
Heat pipes	1.000	0.015
Coil	3.500	0.015

2.2. Experimental Setup

The thermal agent from which heat is recovered (primary agent) is water, heated by an 8 kW electric heater. The electric heater is connected to the heat recovery–storage system through flexible stainless-steel pipes. The circuit is equipped with a valve for filling/draining the evaporator and the primary circuit and a probe sheath for measuring the temperature of the primary agent.

The circuit of the secondary agent is directly connected to the water supply network of the laboratory. Two probe sheaths were installed at the inlet of condenser A and at the outlet of condenser B, connected to an electronic thermometer type LT BTM-4208SD which has a precision of ±0.4%. A thermal energy meter of type ELTERM CF 55 is also tracking the volume flow rate and the temperature of the secondary agent at the outlet of condenser B. Figure 3 presents a photo of the experimental stand from the laboratory.

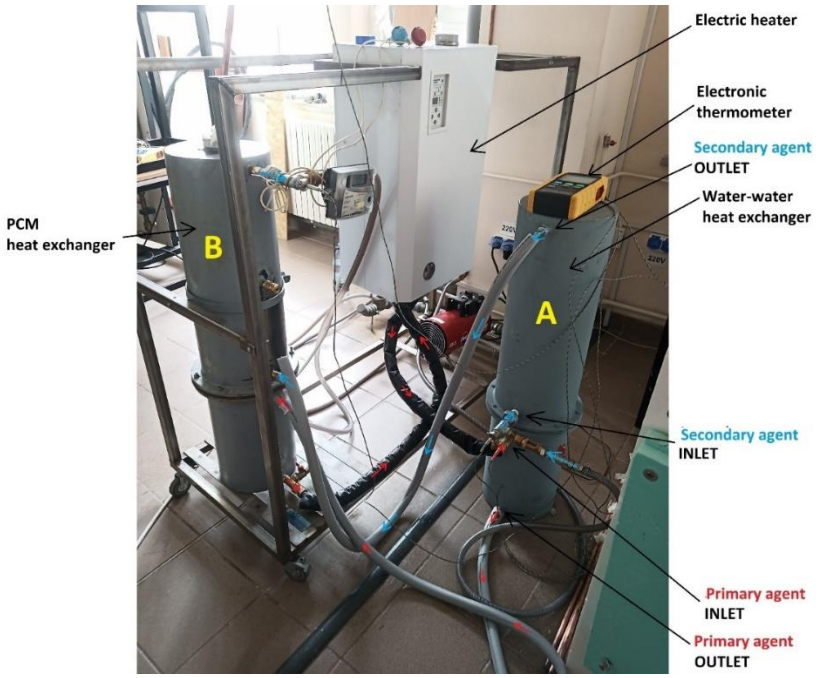

Figure 3. Photo of the experimental stand.

In this study, an electric heater is used to heat the primary agent, which flows through the evaporator of two heat exchangers, A and B. The heat pipes are used to extract thermal energy from the primary agent and transfer it to a secondary agent flowing through heat exchanger A and a phase change material (PCM) volume in heat exchanger B. The heated secondary agent, which exits condenser A, passes through the coil of condenser B, where it extracts additional temperature from the volume of coconut oil. Four sensors are used to measure the temperature of the primary and secondary agents, as well as the PCM. Sensor

CH1 tracks the temperature of the primary agent, while sensors CH2 and CH3 track the temperature of the secondary agent at the inlet and outlet of condenser, respectively. Sensor CH4 tracks the temperature of the PCM.

Figure 4 presents a schematic diagram of the experimental two-stage heat recovery–storage system.

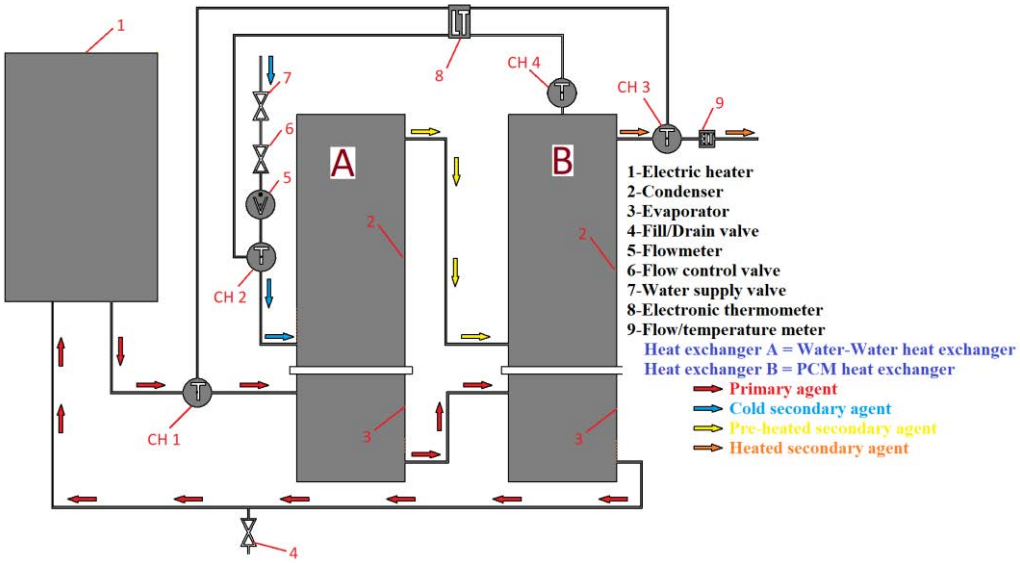

Figure 4. Schematic diagram of the 2-stage heat recovery–storage system.

2.3. Tests Performed

To test the efficiency of the equipment, a series of tests were performed with variations in the temperature of the primary agent and the volume flow rate of the secondary agent. The parameters are presented in Table 3. The volume flow rate of the primary agent was kept constant for all cases by the pump of the electric heater, and the temperature of the secondary agent was kept at 16 °C.

Table 3. Parameters of the experimental tests.

	Primary Agent		Secondary Agent	
	Temperature (°C)	**Volume Flow Rate (L/min)**	**Temperature (°C)**	**Volume Flow Rate (L/min)**
Test 1	60		16	1
Test 2	60		16	2
Test 3	60		16	3
Test 4	65		16	1
Test 5	65	24	16	2
Test 6	65		16	3
Test 7	70		16	1
Test 8	70		16	2
Test 9	70		16	3

Each test lasted 3 h, being staged according to Figure 5. The staging followed the behavior of the heat recovery–storage system and the ability to store the thermal energy of the coconut oil. In the first hour, the electric heater operated constantly to melt the coconut oil and transfer heat to the volume of the secondary agent in unit A. After one hour, the valve of the secondary agent was opened at the volume flow required by the test, thus starting its circulation through the heat exchangers. After the first two hours of operation, the electric heater was turned off, starting the cooling stage where the secondary agent absorbed the heat stored in the volume of phase-changing material.

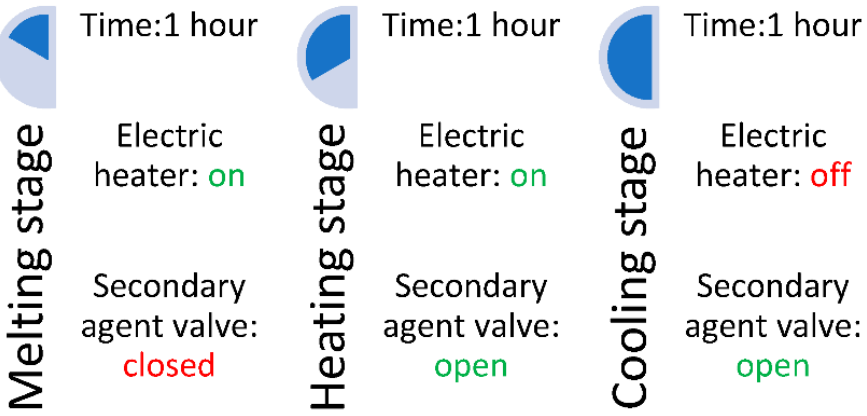

Figure 5. The stages of the tests.

This staging was aimed at the equipment's ability to recover heat in 2 scenarios: if the primary agent has an uninterrupted supply and in the case of an intermittent supply with the primary agent.

2.4. Numerical Simulations

For results with improved accuracy, the heat recovery system was subjected to numerical simulations and the results were compared to the experimental findings. The equipment was created in 3D with the Autodesk Inventor Professional 2018 software, and imported into the Autodesk Simulation CFD 2018 environment.

The first step is to assign a material to each component. The evaporator, the condenser, and the separation flanges are made of stainless steel, while the heat pipes and the coil are made of copper and the primary and secondary agents are water. Coconut oil does not exist in the program database, so a new material with its thermal properties was created.

The boundary conditions used are the same as in the experimental tests. The volume flow rate of the primary agent was set at 24 L/min and the temperature was set specifically for each test. The temperature of the secondary agent was set at 10 °C and the volume flow rates were set according to each scenario (Table 3).

To select the proper flow regime, the Reynolds number was calculated for each case. The results are centralized in Table 4. When the volume flow rate of the secondary agent is 1 L/min or 2 L/min, the Reynolds number is smaller than 2300, resulting in a laminar flow. When the volume flow rate is 3 L/min, the Reynolds number has a value of approximately 2460 which means that there is a transition regime.

Table 4. Reynolds number.

	Secondary Agent			
	Temperature (°C)	**Volume Flow Rate (L/min)**	**Reynolds**	**Regime**
Test 1	16	1	819.8	Laminar
Test 2	16	2	1640.4	Laminar
Test 3	16	3	2461.3	Transition
Test 4	16	1	820.0	Laminar
Test 5	16	2	1640.9	Laminar
Test 6	16	3	2460.1	Transition
Test 7	16	1	820.5	Laminar
Test 8	16	2	1640.6	Laminar
Test 9	16	3	2460.9	Transition

After applying the boundary conditions, the 3D model was discretized into a network of nodes. For the first simulation, the geometry was discretized into a network that consists of 1 million nodes. Then, the number of nodes was increased by 1 million for each simulation until the mesh reached 7 million nodes. After 5 million nodes, the results were

very similar. The higher the number of discretization elements, the greater the processing power and more time was needed, so the number of elements for the calculation of the solution was optimized according to the criteria and the tests performed. The resulting mesh had 5.2 million nodes (Figure 6).

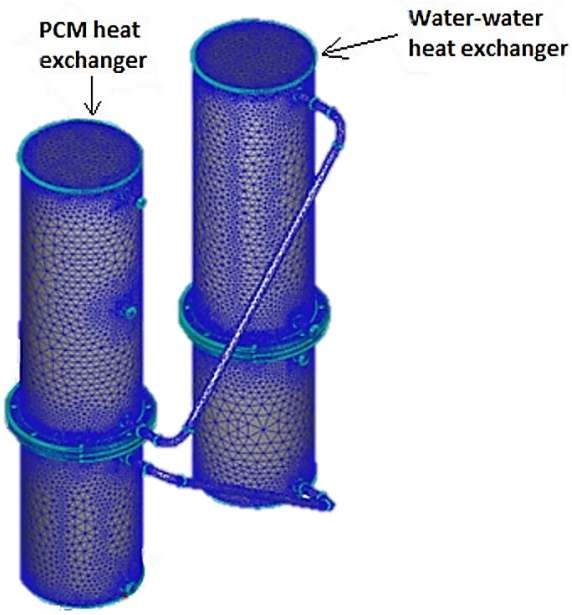

Figure 6. Meshing—2-stage heat recovery–storage system.

Experimental testing was conducted in the laboratory in order to evaluate the performance of the 2-stage heat recovery–storage system. The equipment was tested using several temperatures for the primary agent to check whether the heat pipes are capable of efficiently recovering heat in different scenarios, and different volume flow rates for the primary agent to check the quantity of heat recovered in different instances. Additionally, to check the efficiency of the heat storage, the measurements of temperatures were made in three different stages: a melting stage, a heating stage, and a cooling stage. A detailed description of these stages is given in Section 2.3.

The last step was the calculation of the maximum quantity of heat contained by the primary agent and the quantity of heat recovered by the secondary agent. By comparing these, the efficiency of the equipment can be established for each test.

3. Results and Discussions

The results of the experimental tests are centralized in Figure 7. T max represents the maximum temperature reached by the two-stage recovery system and T med represents the average temperature of the secondary agent at the outlet of the PCM heat exchanger during the heating stage.

In test 1, during the first 27 min of the heating stage, the difference between the temperature of the coconut oil and the temperature of the secondary agent varies between 0 and 2 °C. During this period, this difference increased to 3–5 °C, which is maintained until the end of the test. For test 2, the difference of 1–2 °C was only in the first 10 min of the heating stage, and later, this difference increased to 5–7 °C and remains constant. In test 3, the difference of 1–2 °C was shortened to 8 min but still reached 5–7 °C by the end of the test, as shown in Figure 8.

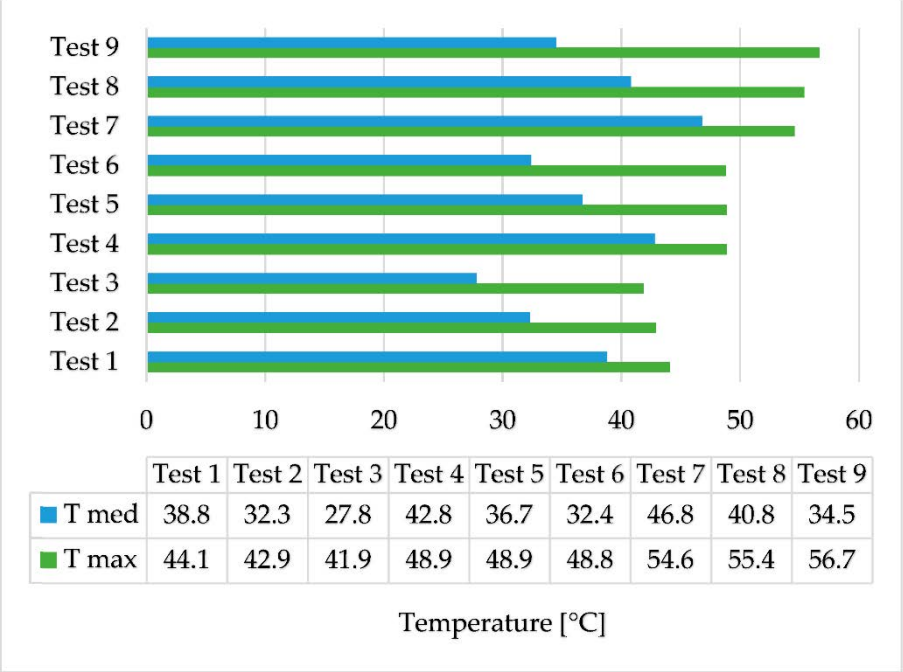

	Test 1	Test 2	Test 3	Test 4	Test 5	Test 6	Test 7	Test 8	Test 9
T med	38.8	32.3	27.8	42.8	36.7	32.4	46.8	40.8	34.5
T max	44.1	42.9	41.9	48.9	48.9	48.8	54.6	55.4	56.7

Figure 7. Average and maximum temperatures obtained.

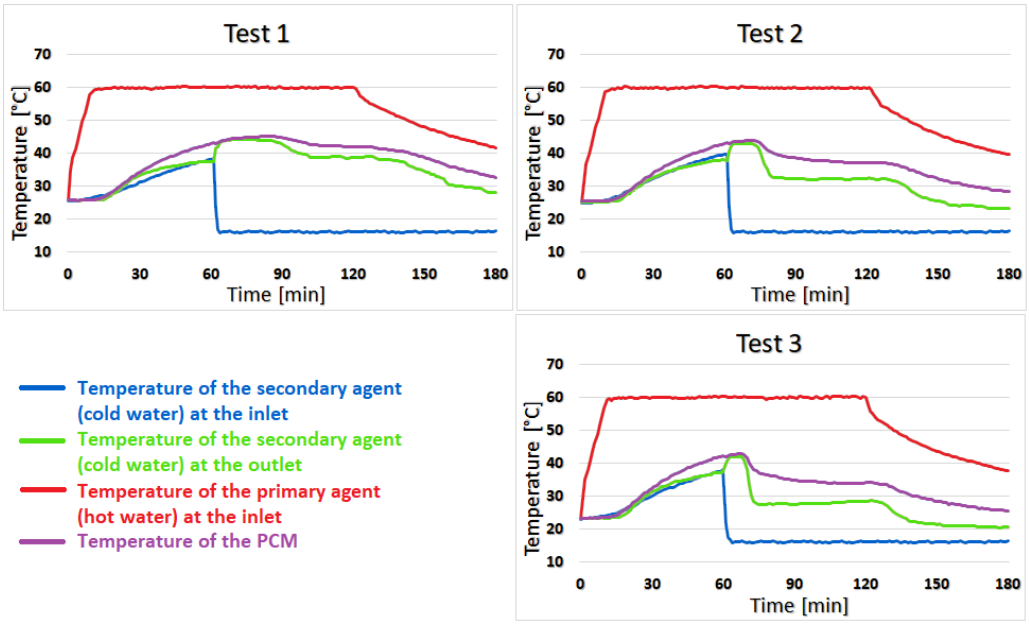

Figure 8. The results for tests 1, 2, and 3.

Test 4 shows almost no temperature difference between coconut oil and the secondary agent for the first 23 min of the heating stage, but the difference increases to 2–3 °C for the next 52 min and towards the second half of the cooling stage, this difference becomes 4–6 °C. The similarity of the temperature of coconut oil to that of the secondary agent lasts 13 min in test 5 with a difference of 0–2 °C. The difference increases quite suddenly at 5–8 °C and is maintained until the end of the test. For test 6, the duration of the 0–2 °C variation is shortened to only 7 min, and the temperature difference between the PCM and the secondary agent sharply increases to 5–9 °C, as can be seen in Figure 9.

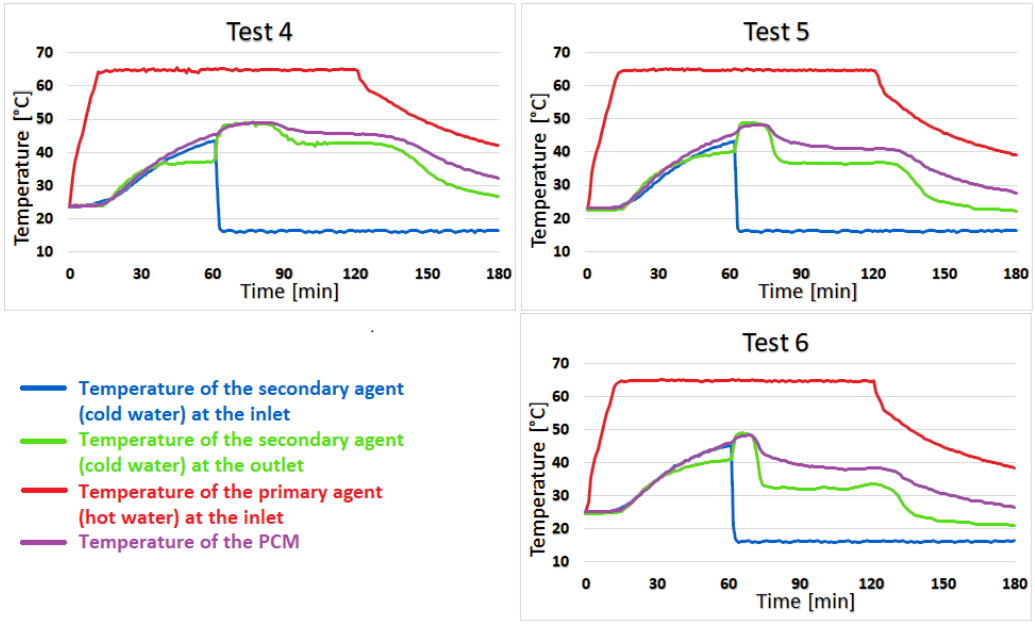

Figure 9. The results for tests 4, 5, and 6.

Test 7 shows the best results of the two-stage recovery system, with an average temperature of the secondary agent during the heating stage of 46.8 °C. The temperature of the secondary agent is higher than the temperature of the coconut oil in the first 20 min of the heating stage. In the last 40 min of this stage, the temperature at the outlet drops below the temperature of the phase change material by 3 °C. The difference then increases to 4–7 °C in the cooling stage and is maintained until the end of the test. Additionally, in tests 8 and 9, the temperature of the secondary agent is higher than that of coconut oil for a short time, but then decreases at the same rate as it, as can be seen in Figure 10.

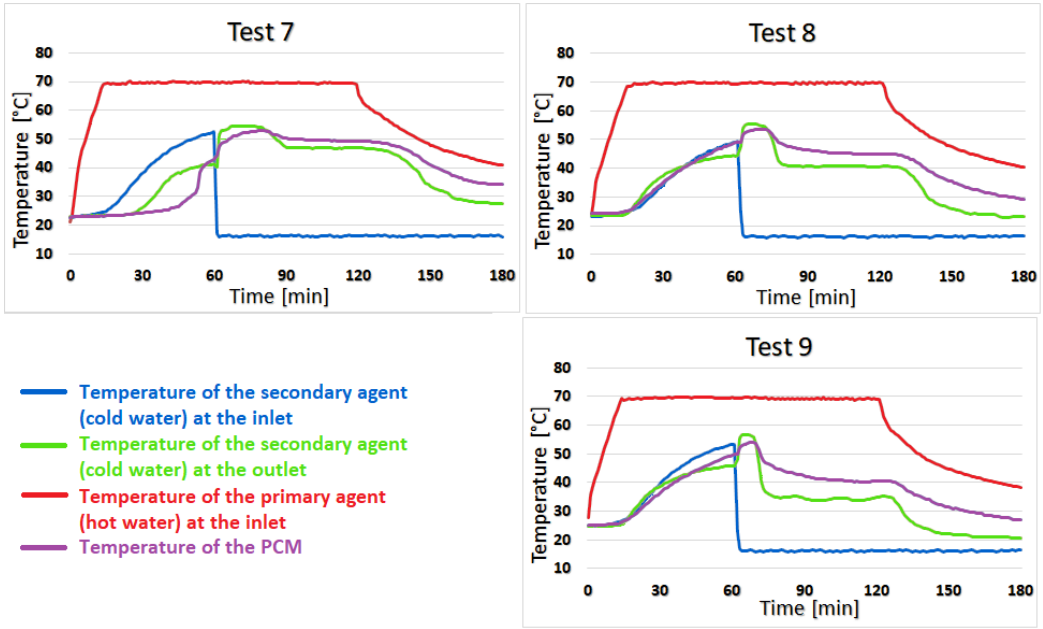

Figure 10. The results for tests 7, 8, and 9.

The temperatures of the secondary agent recorded at the outlet of the system were compared to the average temperatures from the experimental results and they are presented in Figure 11.

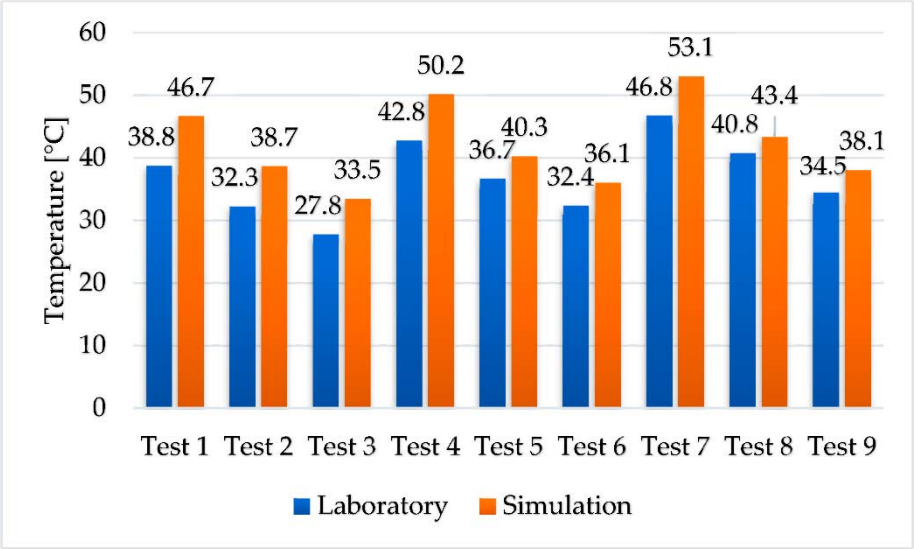

Figure 11. Comparison between the experimental and numerical results.

Since the simulations do not take into account the convective heat losses from the laboratory experiment, the temperature in the experimental results is lower than in the numerical simulations, with values between 3 °C and 8 °C. Since the temperature discrepancies between the experimental results and the simulation results are negligible, it can be concluded that the experimental results are reliable.

In Figure 12, some 3D temperature contours extracted from the results of the numerical simulations are presented for tests 7, 8, and 9 at the end of the cooling stage. The temperature of the secondary agent increases between 3 °C and 6 °C from the outlet of the first condenser to the outlet of the system but the main advantage of the two-stage heat recovery system is the storage of thermal energy, which cannot be tracked in the numerical simulations due to software limitations.

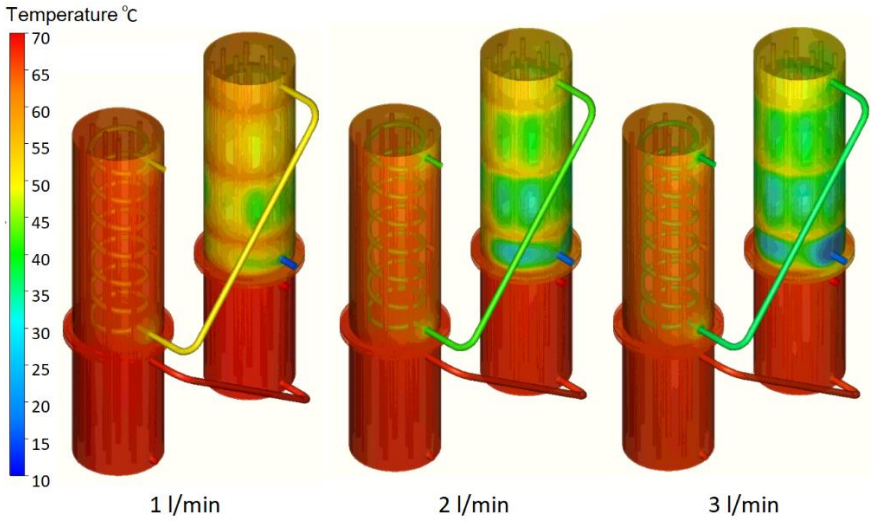

Figure 12. Three-dimensional temperature contours for tests 7, 8, and 9.

The heat quantity in the primary agent was calculated as the product of the mass flow rate, the specific heat capacity of water, and the temperature difference between evaporator A's inlet and evaporator B's outlet. The heat quantity of the secondary agent was determined in a comparable manner, using the secondary agent's mass flow rate, the specific heat capacity of water, and the temperature difference between T med (Figure 7) for each scenario and the cold secondary agent's temperature of 16 °C (Table 4). According

to Equation (1), the efficiency of the two-stage heat recovery–storage system was calculated as a fraction of the heat recovered by the secondary agent and the maximum amount of heat produced by the primary agent. The results are shown in Figure 13.

$$\epsilon = Q_2/Q_1 \quad (1)$$

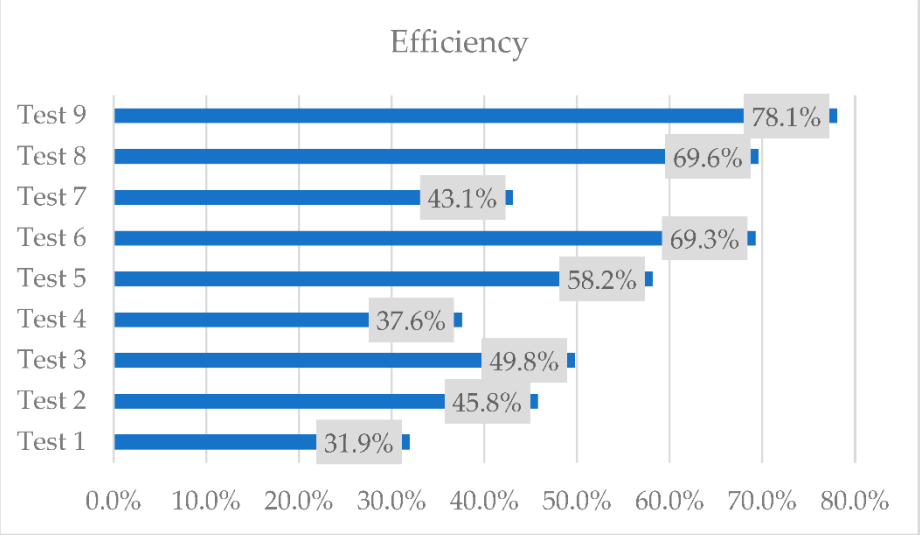

Figure 13. The efficiency of the 2-stage heat recovery–storage system.

The highest efficiency was obtained in test 9 when the volume flow rate of the secondary agent is 3 L/min and the temperature of the primary agent is 70 °C. Although the highest temperatures of the secondary agent were obtained with the smallest volume flow rate, the quantity of heat recovered is smaller.

4. Conclusions

An experimental investigation followed by numerical simulations was carried out on a two-stage heat recovery–storage system. From the experimental results, the highest temperature recorded was when the volume flow rate of the secondary agent was the lowest and the temperature of the primary agent was the highest, at 70 °C, with an average temperature of the secondary agent of 46.8 °C. However, the highest efficiency of the equipment regarding the quantity of the recovered heat was in test 9, with an efficiency of 78.1%.

The ability of the equipment to store heat was observed in all nine tests conducted. During the cooling stage, when the heat source is shut down, the secondary agent still keeps a higher temperature at the outlet of the equipment compared to the one at the inlet by 11.5 °C–4.1 °C, depending on its volume flow rate.

Compared to a common heat recovery system, the two-stage heat recovery–storage system comes with a heat storage capability, which makes the heat recovery process more efficient, especially when the heat source is intermittent. The organic phase change material used for heat storage is a plant-based product, which makes it environmentally friendly.

Another important advantage is the ability to recover heat passively through the gravitational heat pipes, which means that there is no additional pumping system required. The two-stage heat recovery–storage system also has a low cost of production and maintenance compared to common heat exchangers. The two thermal agents are completely separated since the mean of transporting the heat are the heat pipes, which means there are very small chances of accidental mixing. Additionally, if one of the heat pipes malfunctions, the equipment can still function at a slower pace until the heat pipe is replaced, and thus, the maintenance is simple.

Author Contributions: Conceptualization, R.S.V. and A.B.; Methodology, R.S.V., A.B., C.A., M.C.B. and S.E.V.; Software, R.S.V., S.E.V., M.B. and N.E.K.; Validation, A.B., C.A. and M.C.B.; Formal analysis, C.A. and M.B.; Investigation, R.S.V., A.B., M.C.B., S.E.V. and M.B.; Resources, A.B., M.C.B. and N.E.K.; Data curation, R.S.V., A.B., C.A., S.E.V. and M.B.; Writing—original draft, R.S.V., S.E.V. and M.B.; Writing—review & editing, A.B., C.A. and M.C.B.; Visualization, R.S.V., M.C.B. and S.E.V.; Supervision, A.B., C.A. and N.E.K.; Project administration, R.S.V., A.B., C.A., M.C.B. and N.E.K.; Funding acquisition, A.B. and N.E.K.. All authors have read and agreed to the published version of the manuscript.

Funding: This work was supported by a grant from the Romanian Ministry of Education and Research, CCCDI-UEFISCDI, project number PN-III-P2-2.1-CI-2017-0774, within PNCDI III.

Institutional Review Board Statement: Not applicable.

Informed Consent Statement: Not applicable.

Data Availability Statement: Not applicable.

Conflicts of Interest: The authors declare no conflict of interest.

Nomenclature

PCM	Phase change material
NEPCM	Nano-enhanced phase change material
HRSS	Heat recovery–storage system
LHTES	Latent heat thermal energy storage
T max	Maximum temperature
T med	Average temperature
ϵ	Efficiency of the equipment
Q_1	Quantity of heat of the primary agent
Q_2	Quantity of heat of the secondary agent

References

1. IEA (International Energy Agency). *Perspectives on the Energy Transition*; IEA: Paris, France, 2017.
2. Jouhara, H.; Khordehgah, N.; Almahmoud, S.; Delpech, B. Waste heat recovery technologies and applications. *Therm. Sci. Eng. Prog.* **2018**, *6*, 268–289. [CrossRef]
3. Jouhara, H.; Almahmoud, S.; Chauhan, A.; Delpech, B.; Bianchi, G.; Tassou, S.; Llera, R.; Lago, F.; Arribas, J.J. Experimental and theoretical investigation of a flat heat pipe heat exchanger for waste heat recovery in the steel industry. *Energy* **2017**, *141*, 1928–1939. [CrossRef]
4. Delpech, B.; Axcell, B.; Jouhara, H. Experimental investigation of a radiative heat pipe for waste heat recovery in a ceramics kiln. *Energy* **2019**, *170*, 636–651. [CrossRef]
5. Tian, E.; He, Y.-L.; Tao, W.-Q. Research on a new type waste heat recovery gravity heat pipe exchanger. *Appl. Energy* **2017**, *188*, 586–594. [CrossRef]
6. Mahajan, G.; Thompson, S.M.; Cho, H. Experimental characterization of an n-pentane oscillating heat pipe for waste heat recovery in ventilation systems. *Heliyon* **2018**, *4*, e00922. [CrossRef]
7. Mahajan, G.; Thompson, S.M.; Cho, H. Energy and cost savings potential of oscillating heat pipes for waste heat recovery ventilation. *Energy Rep.* **2017**, *3*, 46–53. [CrossRef]
8. Jouhara, H.; Anastasov, V.; Khamis, I. Potential of heat pipe technology in nuclear seawater desalination. *Desalination* **2009**, *249*, 1055–1061. [CrossRef]
9. Kuravi, S.; Trahan, J.; Goswami, D.Y.; Rahman, M.M.; Stefanakos, E.K. Thermal energy storage technologies and systems for concentrating solar power plants. *Prog. Energy Combust. Sci.* **2013**, *39*, 285–319. [CrossRef]
10. Mostafavi, A.; Parhizi, M.; Jain, A. Semi-analytical thermal modeling of transverse and longitudinal fins in a cylindrical phase change energy storage system. *Int. J. Therm. Sci.* **2020**, *153*, 106352. [CrossRef]
11. Ahmed, N.; Elfeky, K.E.; Lu, L.; Wang, Q.W. Thermal performance analysis of thermocline combined sensible-latent heat storage system using cascaded-layered PCM designs for medium temperature applications. *Renew. Energ.* **2020**, *152*, 684–697. [CrossRef]
12. Zhang, C.; Meng, Y.; Fan, Y.; Zhang, X.; Zhao, Y.; Qiu, L. Numerical study on heat transfer enhancement of PCM using three combined methods based on heat pipe. *Energy* **2020**, *195*, 116809. [CrossRef]
13. Yazdani, M.R.; Laitinen, A.; Helaakoski, V.; Farnas, L.K.; Kukko, K.; Saari, K.; Vuorinen, V. Efficient storage and recovery of waste heat by phase change material embedded within additively manufactured grid heat exchangers. *Int. J. Heat Mass Transf.* **2021**, *181*, 121846. [CrossRef]
14. Song, H.; Zhang, W.; Li, Y.; Yang, Z.; Ming, A. Exergy analysis and parameter optimization of heat pipe receiver with integrated latent heat thermal energy storage for space station in charging process. *Appl. Therm. Eng.* **2017**, *119*, 304–311. [CrossRef]

15. Hu, B.; Wang, Q.; Liu, Z. Fundamental research on the gravity assisted heat pipe thermal storage unit (GAHP-TSU) with porous phase change materials (PCMs) for medium temperature applications. *Energy Convers. Manag.* **2015**, *89*, 376–386. [CrossRef]
16. Amini, A.; Miller, J.; Jouhara, H. An investigation into the use of heat pipe technology in thermal energy storage heat exchangers. *Energy* **2017**, *136*, 163–172. [CrossRef]
17. Fan, Y.; Zhang, C.; Jiang, L.; Zhang, X.; Qiu, L. Exploration on two-stage latent thermal energy storage for heat recovery in cryogenic air separation purification system. *Energy* **2022**, *239*, 122111. [CrossRef]
18. Tiari, S.; Qiu, S. Three-dimensional simulation of high temperature latent heat thermal energy storage system assisted by finned heat pipes. *Energy Convers. Manag.* **2015**, *105*, 260–271. [CrossRef]
19. Khedher, N.B.; Rashad, A.B.; Kolsi, L.; Omri, M. Performance investigation of a vertically configured LHTES via the combination of nano-enhanced PCM and fins: Experimental and numerical approaches. *Int. J. Heat Mass Transf.* **2022**, *137*, 106246. [CrossRef]
20. Nie, C.; Deng, S.; Liu, J. Numerical investigation of PCM in a thermal energy storage unit with fins: Consecutive charging and discharging. *J. Energy Storage* **2020**, *29*, 101319. [CrossRef]
21. Morales-Ruiz, S.; Rigola, J.; Oliet, C.; Oliva, A. Analysis and design of a drain water heat recovery storage unit based on PCM plates. *Appl. Energy* **2016**, *179*, 1006–1019. [CrossRef]
22. Ladekar, C.L.; Chaudhary, S.K.; Khandare, S.S. Experimental Investigate for Optimization of Heat Pipe Performance in Latent Heat Thermal Energy Storage. *Mater. Today Proc.* **2017**, *4*, 8149–8157. [CrossRef]
23. Li, Z.; Lu, Y.; Huang, R.; Chang, J.; Yu, X.; Jiang, R.; Yu, X.; Roskilly, A.P. Applications and technological challenges for heat recovery, storage and utilisation with latent thermal energy storage. *Appl. Energy* **2021**, *283*, 116277. [CrossRef]
24. Vizitiu, R.S.; Burlacu, A.; Abid, C.; Verdes, M.; Balan, M.C.; Branoaea, M. Experimental and Numerical Study of Thermal Performance of an Innovative Waste Heat Recovery System. *Appl. Sci.* **2021**, *11*, 11542. [CrossRef]
25. Putri, W.A.; Fahmi, Z.; Sutjahja, I.M.; Kurnia, D.; Wonorahardjo, S. Thermophysical parameters of coconut oil and its potential application as the thermal energy storage system in Indonesia. *J. Phys. Conf. Ser.* **2016**, *739*, 012065. [CrossRef]

materials

MDPI

Article

Experimental Investigation on Mechanical and Thermal Properties of Concrete Using Waste Materials as an Aggregate Substitution

Gavril Sosoi [1,2], Cherifa Abid [2], Marinela Barbuta [1], Andrei Burlacu [1,*], Marius Costel Balan [1,*], Marius Branoaea [1], Robert Stefan Vizitiu [1] and Fabrice Rigollet [2]

[1] Faculty of Civil Engineering and Building Services, "Gheorghe Asachi" Technical University of Iasi, 700050 Iasi, Romania; gavrilsosoi@gmail.com (G.S.); marinela.barbuta@academic.tuiasi.ro (M.B.); marius.branoaea@tuiasi.ro (M.B.); robert.vizitiu@tuiasi.ro (R.S.V.)

[2] IUSTI UMR 7343, Aix-Marseille Université, 13453 Marseille, France; cherifa.abid@univ-amu.fr (C.A.); fabrice.rigollet@univ-amu.fr (F.R.)

* Correspondence: andrei.burlacu@tuiasi.ro (A.B.); marius-costel.balan@academic.tuiasi.ro (M.C.B.)

Abstract: The continuous growth of the concrete industry requires an increased quantity of cement and natural aggregates year after year, and it is responsible for a major part of the global CO_2 emissions. These aspects led to rigorous research for suitable raw materials. Taking into account that these raw materials must have a sustainable character and also a low impact on environmental pollution, the replacement of the conventional components of concrete by residual waste can lead to these targets. This paper's aim is to analyze the density, compressive strength and the thermal conductivity of nine concrete compositions with various rates of waste: four mixes with 10%, 20%, 40% and 60% chopped PET bottles aggregates and 10% fly ash as cement partial substitution; a mix with 60% waste polystyrene of 4–8 mm and 10% fly ash; a mix with 20% waste polystyrene of 4-8 mm, 10% waste polystyrene of 0–4 mm and 10% fly ash; a mix with 50% waste polystyrene of 4–8 mm, 20% waste polystyrene of 0–4 mm and 20% fly ash two mixes with 10% fly ash and 10% and 40% waste sawdust, respectively. Using 60% PET aggregates, 60% polystyrene granules of 4–8 mm, or 20% polystyrene of 0–4 mm together with 50% polystyrene of 4–8 mm led to the obtainment of lightweight concrete, with a density lower than 2000 kg/m^3. These mixes also registered the best results from a thermal conductivity point of view, after the concrete mix with 40% saw dust. Regarding compressive strength, the mix with 10% PET obtained a result very close to the reference mix, while those with 20% PET, 40% PET, 30% polystyrene, and 10% saw dust, respectively, registered values between 22 MPa and 25 MPa, values appropriate for structural uses.

Keywords: cement based concrete; ecological concrete; waste aggregates; compressive strength; thermal conductivity

Citation: Sosoi, G.; Abid, C.; Barbuta, M.; Burlacu, A.; Balan, M.C.; Branoaea, M.; Vizitiu, R.S.; Rigollet, F. Experimental Investigation on Mechanical and Thermal Properties of Concrete Using Waste Materials as an Aggregate Substitution. *Materials* **2022**, *15*, 1728. https://doi.org/10.3390/ma15051728

Academic Editor: Luigi Coppola

Received: 17 January 2022
Accepted: 18 February 2022
Published: 25 February 2022

1. Introduction

Energy consumption in the world is increasing and, therefore, a need for taking into consideration the ongoing energy crisis and the impact it has on the environment is present. In terms of energy demand, the built environment is a net consumer of energy, demanding over 36% of the global energy, and upwards to 50% of raw materials worldwide. In terms of the environmental impact, buildings are responsible for over 39% of the global greenhouse gas emissions [1].

It is estimated that: 1 ton of Portland cement produces 0.96 tons of CO_2 and 1 ton of concrete produces 0.108 tons CO_2. According to experts, the concrete industry is responsible for 7 to 9% of the global greenhouse gas emissions [2,3].

The use of wastes as an aggregate substitution in construction materials represents a great alternative, especially in cement based concretes, due to large scale use in the

construction industry. By using waste materials, such as chopped PET bottles, granular polystyrene, and waste wood, as aggregates in the concrete mixture, an ecological and performant concrete can be obtained, such as lightweight concrete, that can be used to reduce the weight of buildings. Another significant advantage of this type of concrete mixture is the valorification of waste materials that can produce a negative impact on the environment.

The purpose of this paper is to investigate the density, compressive strength and thermal conductivity of various concrete mixes using waste as aggregates and cement substitutions. The study implied the development of ten concrete mixes, which included a reference concrete mix made with conventional components only (river aggregates and cement), and nine concrete compositions with waste materials as aggregates and cement partial replacements, as follows: four mixes with 10%, 20%, 40% and 60% chopped PET bottles aggregates and 10% fly ash as cement partial substitution; a mix with 60% waste polystyrene of 4–8 mm and 10% fly ash; a mix with 20% waste polystyrene of 4–8 mm, 10% waste polystyrene of 0–4 mm and 10% fly ash; a mix with 50% waste polystyrene of 4–8 mm, 20% waste polystyrene of 0–4 mm and 20% fly ash two mixes with 10% fly ash and 10% and 40% waste sawdust, respectively. Using the waste materials mentioned can contribute significantly to reducing waste quantity and CO_2 emissions, by decreasing the produced quantity of cement, and by natural aggregates' use in a concrete mix.

If waste, such as chopped PET, granular polystyrene, and waste sawdust, are to be used as aggregates in the composition of concrete, then the pollution and impact of the construction sector on the environment will decrease, these facts represent a great advantage both in terms of recycling and reducing the consumption of natural ingredients, such as sand.

2. State of the Art

There are various recent studies on the use of waste chopped polyethylene terephthalate, granular polystyrene, and waste wood (sawdust) in the composition of the concrete mixture by replacing natural aggregates [4–11].

Furthermore, by investigating the mechanical properties of the concrete with waste chopped PET bottles, granular polystyrene, and waste wood as a substitution in the concrete mix, researchers obtained results that highlight the fact that the mechanical properties of fresh and hardened concrete are being influenced by the ratio of the replaced material in the concrete mix [12–21].

In terms of research trends, scientist have analyzed the incorporation of various materials into concrete in order to reduce the required raw materials, ranging from crushed recovered concrete and ceramics, vegetal byproducts and even plastics. Some examples of such studies are presented in Table 1.

2.1. Concrete with PET and Polystyrene

The use of PET and polystyrene in concrete mixtures, both in structural or lightweight concrete, was analyzed in a number of studies with the aim to reduce the waste in the world and reduce the quantity of required raw materials. The analyzed properties of these concretes include—but are not limited to—compressive strength, density, tensile strength, elasticity modulus, flexural strength, durability, thermal properties and fire resistance.

In their study on concrete with polystyrene with a ratio ranging from 20% to 80% of the total volume and a resin mixture of 0.5%, 1%, and 1.5% of the total weight, Kaya and Kar concluded that, as the added components percentage increase, the porosity of the concrete increases and the mechanical properties, such as density, tensile strength, compressive strength, and thermal conductivity, decrease [11].

Table 1. Summary of research papers on concrete with waste materials.

NR.	Contents of the Paper	Year	Ref.
1	The study analyzed the substitution of raw materials with fine—fMRA (25% and 50%) and coarse—cMRA (0%, 25% and 50%) mixed recycled aggregates. The study determined that the optimal percentage of an fMRA replacement is 25%.	2021	[22]
2	The paper highlighted a correlation and regression analysis of lightweight concretes with presoakedred ceramic waste aggregate, expanded clay coarse aggregate as waste aggregate and varying degrees of copper coated steel fibre used as reinforcement.	2022	[23]
3	This study analyzed the mechanical properties and durability of medium quality concrete with a replacement of the natural coarse aggregate (NCA) with various percentages of recycled coarse aggregate, RCA, (25%, 50%, 75% and 100%). The results reveal few differences between the concrete with RCA and the reference concrete in terms of the mechanical properties and durability related measurements.	2021	[24]
4	This research involved the experimental investigation of using fly ash admixture collected by a wet process as a replacement of the fine part of the aggregates in concrete. The experimental results show a favourable behaviour of the concretes based on fly ash to sulphate aggressive actions in the first part of life.	2020	[25]
5	The purpose of this paper was analyzing the performance of concrete with granules of corn cob and sunflower with a sodium silicate solution treatement (0%, 20% and 40%). The experimental analysis highlighted that the concrete with vegetal raw materials had a reduced density but, at the same time, a reduced compressive strength as vegetal aggregates have higher water absorption capacity. Sunflower concrete presents superior mechanical strengths in comparison to corn cob concrete.	2020	[26]
6	This study, through a statistical experimental analysis, evaluates the performance of concrete reinforced with recycled PET fibres with various fibre doses and aspect ratios. The results highlighted that the introduction of recycled PET fibres into concrete provides residual strength capacity to the concrete, with a reduced effect on the volumetric weight, ultimate flexural and compressive strength.	2021	[27]
7	The experimental research involved analysing the properties of concrete with sawdust as a replacement of sand containing 0%, 5%, 10% and 15% of sawdust. Through adding sawdust the results showed that the biological oxygen demand increased as the replacement percentage increased, but the compressive strength decreased.	2019	[28]
8	The study researched the properties of fly ash as a basic raw material used in the production of concrete. The inclusion of fly ash in concrete, referenced through multiple studies, provide increased mechanical and microstructure properties in comparison to the use of cement alone.	2020	[29]
9	The paper analyzed the incorporation of waste materials, such as sugarcane bagasse ash (SCBA), metakaolin (MK), and millet husk ash (MHA), and determines their effect on the fresh, hardened properties and embodied carbon of concrete. The study revealed that the use of SCBA, MK, and MHA up to 10–15% separate and combined as ternary cementitious material (TCM) in concrete provides ideal results for structural applications.	2022	[30]
10	The researchers reviewed the impact natural seawater has on the properties of concrete. The study points out that, in the long term, seawater is harmful to the concrete structures built in marine environments and that, through the use of supplementary cementitious materials (SCMs) such as rice husk ash, coal bottom ash and blast furnace slag in the concrete mix, the degradation is reduced. Another interesting fact is that, through adding seawater during the curing and mixing of concrete, the tensile properties of the concrete are increased.	2021	[31]

In their research, Saikia and Brito performed an experimental investigation on specimens for compressive strength, split tensile strength, and flexural strength, observing that an increase in the concentration of the PET ratio as aggregate in the mixture leads to a decrease in the compressive strength, split tensile strength and flexural strength of the concrete [12].

The study published by Rahmani et al. investigated the mechanical properties of cubic and cylindrical concrete specimens with 5% to 15% substitution of sand with particles of PET and different water to cement ratios. The experimental study revealed that the

compressive and flexural strength initially tend to increase, however, they tend to decrease after a period of time. Moreover, the experiments highlighted that the samples containing PET particles have a lower density, splitting tensile strength, modulus of elasticity, and workability [13].

Jahidul et al. carried out an experimental investigation on the properties of PET aggregate concrete by replacing between 0 and 50% of the volume of coarse aggregates, observing that this type of concrete provided better workability than regular concrete while using a similar w/c ratio, the density of the PET concrete was reduced by 4 to 10%, thus reducing the self-weight of the structural element. The optimal substitution ratio was 20%, this percentage ensuring comparable compressive strength with natural aggregate concrete [15].

Maldonado-Bandala et al. observed similar results regarding mechanical parameters such as density and compressive strength—that these parameters decrease as the ratio of polystyrene increases—but the experiment revealed that the corrosion protection of the concrete with polystyrene is greatly superior to conventional concrete [16].

Studies performed by Sayadi et al. revealed that adding expanded polystyrene into the concrete mixture translates to a decrease in thermal parameters such as thermal conductivity and fire resistance [17].

2.2. Concrete with Sawdust

Sawdust, as a byproduct of the wood industry, has been researched and implemented in various forms since the 20th century in regions such as the United State of America, Asia (Malaysia and Singapore) and Europe (Germany and the UK). The possible applications of this material are significant, as highlighted by the fact that this material, in various forms and adaptations, has been used for building elements such as walls and floors [32].

Sales et al. analyzed the incorporation of untreated wood shavings into concrete to obtain lightweight concrete. The study highlighted that, through the introduction of sawdust into the concrete mixture, some key parameters were improved: the thermal conductivity of the concrete was improved and the mass density was reduced. At the same time, the sawdust presented a good adherence to the concrete matrix and the structure of the mixture was homogeneous [33].

Sofi et al. investigated the compressive strength of concrete samples with a volume of added sawdust ranging from 0% to 15% in the concrete mix at two curing periods, at 7 and 28 days. The results obtained after the curing periods show that the compressive strength is higher for concrete samples with a lower substitution percentage of sawdust [18].

The implementation of sawdust in concrete has not reached the level of widespread adoption due to the limitations of sawdust, which has low compressive strength. At the same time, the advantages of concrete with sawdust (reduction in structural weight and, as a consequence, reduced loads on the foundation, reduced damage phenomena and increased the lifespan of the structure, along with easier handling and reduced consumption of raw materials) justify the increasing interest in this type of material.

2.3. Concrete with Fly Ash

Fly ash is a byproduct of burning coal in power plants in the form of ultrafine solid residue. In numerous developed and developing countries, such as US, China and India, where coal is used, it is one of the largest solid wastes. Fly ash has been implemented as an additive in concrete since the mid-20th century as a replacement for some raw materials such as cement or as a mixture with a clinker [34].

The analysis performed by multiple researchers highlights the increase in interest towards ecological concrete and its potential to reduce the carbon footprint buildings impose on the environment. Even though some mechanical parameters are not as high with the substitution of natural aggregates, these types of walls can be applied in nonstructural elements.

3. Experimental Works

3.1. Materials

3.1.1. Cement and Fly Ash

The cement used in the concrete mixture is Portland cement type CEM II 45.2 R produced in Romania following the EN 197-1 standard, this fact is evidenced both from the producer's multiple declarations of conformity, performance certificates and through independent tests conducted on a cement sample. The cement has the following components: Portland clinker maximum dosage 94%, limestone 6–20%, and auxiliary components 0–5% [35,36].

The fly ash used as a replacement for the cement, which is released with the exhaust fuel gases, presented in Figure 1 is a byproduct from the Holboca Electric Power Plant in Iasi, with a bulk density ranging from 2400 to 2550 kg/m^3, specific surface area of 520 m^2/kg, particle size ranging from 0.01 to 400 μm and, as main chemical components, O_2 (43.3%), Si (30.8%), Al (19.2%) and Fe (3.05%) [37,38].

Figure 1. Fly ash from Holboca Electric Power Plant.

3.1.2. Aggregates

The aggregates used in the composition of the concrete can be classified into:

Natural aggregates such as sand with a specific gravity of 2.68, bulk density 1700 kg/m^3, and absorption of 1%, and two sorts of river stone (sort I 4–8 mm and sort II 8-16 mm) with a specific gravity of 2.62, bulk density 1400 kg/m^3, and absorption of 0.9%, presented in Figure 2.

Figure 2. Natural aggregates used in concrete mix.

Waste aggregates, evidenced by Figure 3, such as:

- Chopped PET from bottles (having dimensions between 0–4 mm), resulting from cutting discarded polyethylene terephthalate (PET) bottles. After the cutting of the material it was sieved in order to obtain the desired particle dimensions. This waste

material presents high stability and nonreactivity with substances. The unit weight of the chopped PET was determined experimentally and has a value of 433 kg/m^3 [39];

- Granular polystyrene (with dimensions 0–4 mm and 4–8 mm), which can be reused in the shape of granules, resulting from shredding, cutting or thermal treatment;
- Waste wood/sawdust (with dimensions 0–4 mm), is a byproduct resulting from the wood industry. The collected sawdust was air dried and afterwards sieved, in order to imitate the size of the natural aggregates. Sawdust in terms of chemical composition is comprised of carbon (60.8%), hydrogen (5.2%), oxygen (33.8%), and nitrogen (0.9%). The primary components of dry wood are cellulose, lignin, hemicelluloses, and small amounts (5–10%) of extraneous materials. The unit weight of the sawdust was determined experimentally and has a value of 168 kg/m^3 [39,40].

(**a**) (**b**) (**c**)

Figure 3. Waste aggregates used in the concrete mixture: (**a**) chopped PET bottle; (**b**) granular polystyrene; (**c**) sawdust/waste wood.

3.2. Concrete Mixture

The concrete mixture without any substitutions was made according to the following recipe: sand 803 kg/m^3, river gravel with 4–8 mm in diameter 384 kg/m^3, river gravel with 8–16 mm in diameter 559 kg/m^3, cement 360 kg/m^3, water 180 l/m^3 and a 1% superplasticizer additive of the cement mass.

In order to conduct the experiments and determine the mechanical parameters and the advantages and disadvantages of the partial substitution of the natural aggregate with either chopped PET, granular polystyrene, or waste wood (sawdust), nine types of different concrete mixtures were considered, with the mixing proportions and the quantities of the used materials presented in Table 2. The concrete was casted into 10 cubic shape specimens and 6 plate shape specimens for each concrete mixture.

The concrete mixture realization process involved adding the materials and water in the two-blade mixer, the mixing process was finished after 30–40 min.

Samples S1 to S4 also contain fly ash, which replaced 10% of the cement, and from 10% to 60% chopped PET replacing the same mass volume of cement.

In the concrete mix using waste granular polystyrene, three samples in which 10% of cement was replaced with fly ash, and the substitution of natural aggregates used were replaced by 60% of the sort I aggregate mass 4–8 mm were replaced with granular polystyrene 4–8 mm, resulting the concrete sample notated S5.

Following this, the concrete mixture was changed once again by replacing two natural aggregates in order to create sample S6, as follows: 90% of the sand was used, the remaining 10% being substituted by 10% of the sand mass with granular polystyrene 0-4 mm in volume, and, as a secondary substitution, only 80% of the original sort I, with a size of the granules of 4–8 mm, 20% from the sort I mass was replaced with granular polystyrene 4–8 mm in volume and a further substitution of 10% of the cement was made with fly ash.

Table 2. Concrete mixture with waste substitution.

Concrete Sample		Materials							
		Sand		Rocks (4–8 mm)		Rocks (8–16 mm)		Cement	
		Percent	Volumic Mass	Percent	Volumic Mass	Percent	Volumic Mass	Percent	Volumic Mass
S0	natural aggregate waste substitution	100%	803.16 0% PET	100%	384.12 0% PET	100%	558.72 0% PET	100%	360 0% fly ash
S1	natural aggregate waste substitution	90%	722.84 10% PET	100%	384.12 0% PET	100%	558.72 0% PET	90%	324 10% fly ash
S2	natural aggregate waste substitution	80%	642.52 20% PET	100%	384.12 0% PET	100%	558.72 0% PET	90%	324 10% fly ash
S3	natural aggregate waste substitution	60%	481.9 40% PET	100%	384.12 0% PET	100%	558.72 0% PET	90%	324 10% fly ash
S4	natural aggregate waste substitution	40%	321.26 60% PET	100%	384.12 0% PET	100%	558.72 0% PET	90%	324 10% fly ash
S5	natural aggregate waste substitution	100%	803.16 0% polystyrene	40%	153.64 60% polystyrene 4–8 mm	100%	558.72 0% polystyrene 8–16 mm	90%	324 10% fly ash
S6	natural aggregate waste substitution	90%	722.84 10% polystyrene 0–4 mm	80%	307.29 20% polystyrene 4–8 mm	100%	558.72 0% polystyrene 8–16 mm	90%	324 10% fly ash
S7	natural aggregate waste substitution	80%	642.52 20% polystyrene 0–4 mm	50%	192.06 50% polystyrene 4–8 mm	100%	558.72 0% polystyrene 8–16 mm	80%	288 20% fly ash
S8	natural aggregate waste substitution	90%	722.84 10% saw dust	100%	384.12 0% saw dust	100%	558.72 0% saw dust	90%	324 10% fly ash
S9	natural aggregate waste substitution	60%	481.9 40% saw dust	100%	384.12 0% saw dust	100%	558.72 0% saw dust	90%	324 10% fly ash

For the concrete sample S7, another modification in the concrete mixture was made, in which 20% of the cement was replaced with fly ash and two more natural aggregates were partially replaced with granular polystyrene, replacing 20% of the sand mass with granular polystyrene 0–4 mm in volume and 50% of the sort I mass 4–8 mm was replaced by 50% granular polystyrene 4–8 mm in volume.

The last two samples, S8 and S9, were realized by further modifying the mixture: 10% of the cement was replaced with fly ash in both concrete samples and a percentage of the sand was replaced with its corresponding volume of sawdust. In the case of sample S8 only 10% of the sand was replaced and in the case of sample S9, 40% of the sand mass was replaced with the same volume of sawdust.

3.3. Preparation of Concrete Samples

Following the mixing process, the concrete mixtures were poured into cubic shapes with the side length of 150 mm, Figure 4a, and rectangular prismatic shapes with the following dimensions 150 mm in length, 120 m width, and 20 mm depth, Figure 4b, in order to perform the experimental measurements.

The concrete samples in cubic shapes were made for the experiment of the compressive strength and density investigation; the rectangular prismatic concrete samples (plate concrete samples) were made for the experiment of the heat transfer coefficient investigation.

After the preparation, the concrete samples were left for curing for 28 days in laboratory conditions at a controlled temperature.

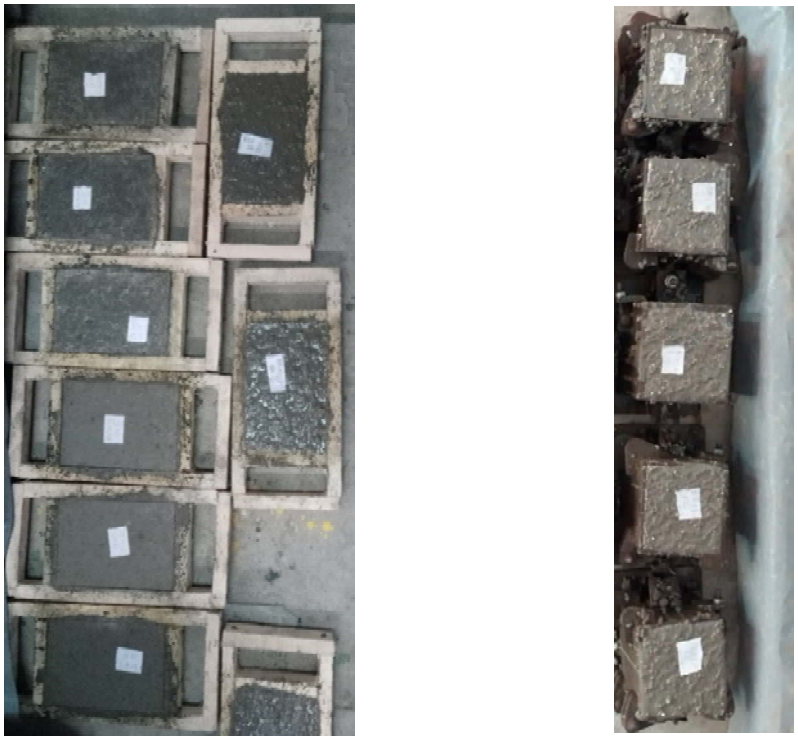

(**a**) (**b**)

Figure 4. View of concrete samples: (**a**) cubic shape concrete samples, (**b**) plate shape concrete samples.

4. Characterization of Concrete Properties

4.1. Density

Experimental investigation on the density of the concrete samples was carried out according to the EN12390-7 standard [35] on tree specimens for every type of concrete mix with waste substitution by determining the mass and the volume of the specimens. The volume was determined with the reference method by water displacement after ensuring that the specimens were in saturated conditions. The mass in water was measured by raising the water level from a tank until the stirrup without the specimens was touching the bottom of the tank. After this procedure, the water surface surplus was removed by wiping the specimens and the mass of the specimens in air conditions was measured. With the values obtained we calculated the volume of the specimens with the Formula (1):

$$V = \frac{m_a - [(m_{st} + m_w) - m_{st}]}{\rho_w} \quad (1)$$

The mass of the specimens was measured after the curing period, according to the EN12390-7 standard 35.

The density can be calculated with the formula:

$$\rho = \frac{m}{V} \quad (2)$$

4.2. Compressive Strength

The preparing and keeping of the concrete samples were performed respecting the indications of EN 12390-2 standard [41]. Following the standard instructions the concrete samples were cured for a period of 28 days. During the curing period the samples were kept in water for 7 days after that in dry conditions at constant temperature of 20 °C with the maximum tolerance ±2 °C.

The compressive strength was determined according to EN 12390-3 standard [42] on tree specimens for every type of concrete mix with waste substitution on the hardened cubic concrete samples with the edge of 150 mm. The samples were tested after the curing period with a press having a maximum load force of 2000 kN. The preparation of the specimen for the experimental investigation on compressive strength was realized by centering the specimen on the lower platen.

In the testing procedure presented in Figure 5, a first initial rate load force of 0.6 N/mm^2·s constant at the beginning is applied on the area of the concrete sample without shock, after applying the first load force to the specimen, the load was increased continuously at a constant rate ±10% until the specimen reached the maximum load failure.

Figure 5. Experimental test of the compressive strength.

4.3. Discussion and Analysis

The experimental determination of the concrete density is presented in Figure 6. From the measurements, the fact that an increase in the concentration of added waste aggregates leads to a decrease in the concrete density. For the obtained values for the densities of the concrete samples with waste as aggregate substitution, the uncertainty on the results calculated for the density is from 3.6% to 36.88%.

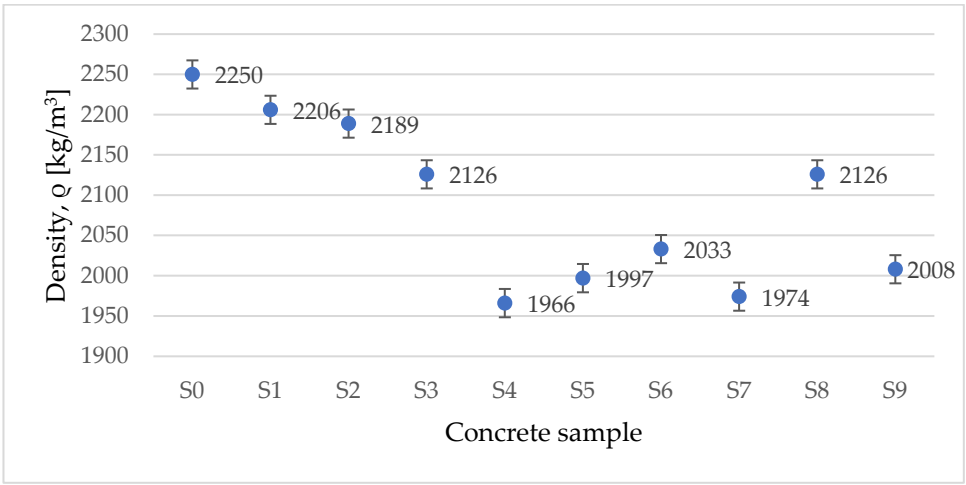

Figure 6. Variation of density for tested concrete samples.

In the testing procedure presented in Figure 6, an initial load force of 0.6 N/mm^2·s constant force is applied at the beginning on the surface area of the concrete sample without shock. After applying the first load force to the specimen, the load was increased continuously at a constant rate of ±10% until the specimen reached the maximum load failure.

The uncertainty of the obtained results was calculated for the compressive strength on the studied specimens and it resulted in a minimum of 0.3% and a maximum value of 1.35%.

The variation of compressive strength presented in Figure 7 represents the average of the measured results on tree concrete specimens. As we expected, the compressive strength is decreasing by using even a small percentage of waste as a substitution.

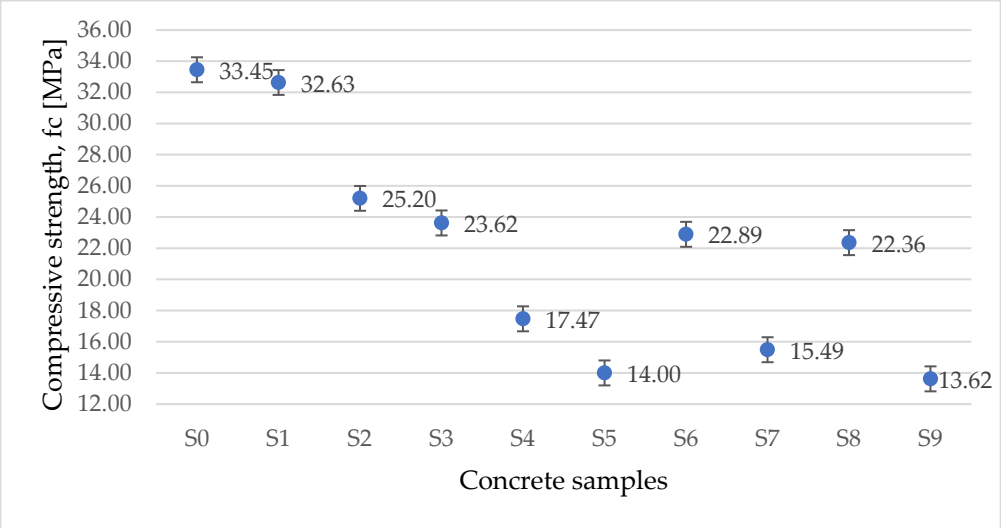

Figure 7. Variation of compressive strength for tested concrete samples.

In Figure 8a–d the variation of the density versus compressive strength of the concrete samples with waste substitution compared with the concrete sample with no waste replacement was analyzed.

A first analysis was performed by comparing the density versus compressive strength of concretes in which one natural aggregate was replaced with the same waste used in the concrete mixture, in this case, the natural aggregate sand was substituted with waste chopped PET.

By comparing the obtained results Figure 8a, in which only one natural aggregate was replaced, we observed that, up to a ratio of 20% substitution of natural aggregate with waste chopped PET, the results of the compressive strength show that the concrete can be used as a structural element and, due to it having a relatively high density, the concrete can be used as a heat-accumulating wall. Meanwhile, by increasing the waste substitution up to 60%, we observed that the compressive strength and density decrease, with the result that the concrete structure can be used as a self-sustained material or even as a heat-accumulating wall.

The second analysis was carried out on the concrete samples, substituting the natural aggregates with granular polystyrene. The results presented in Figure 8b highlight the fact that, in the case where a high percentage of aggregate sand, the compressive strength is greatly reduced and the density is slightly lower in comparison to the results of concrete samples with two natural aggregates as a substitution. The types of concrete with a high percentage of aggregates substitution can be used as a self-sustained structure and thermal insulating material, while replacing a small percentage of the natural aggregates with waste. Continuing the analyses of the mechanical properties for the concrete samples with waste wood substitution, Figure 8c, the results show that a higher percentage of substitution has the same effect as in the case of using waste chopped PET and granular polystyrene.

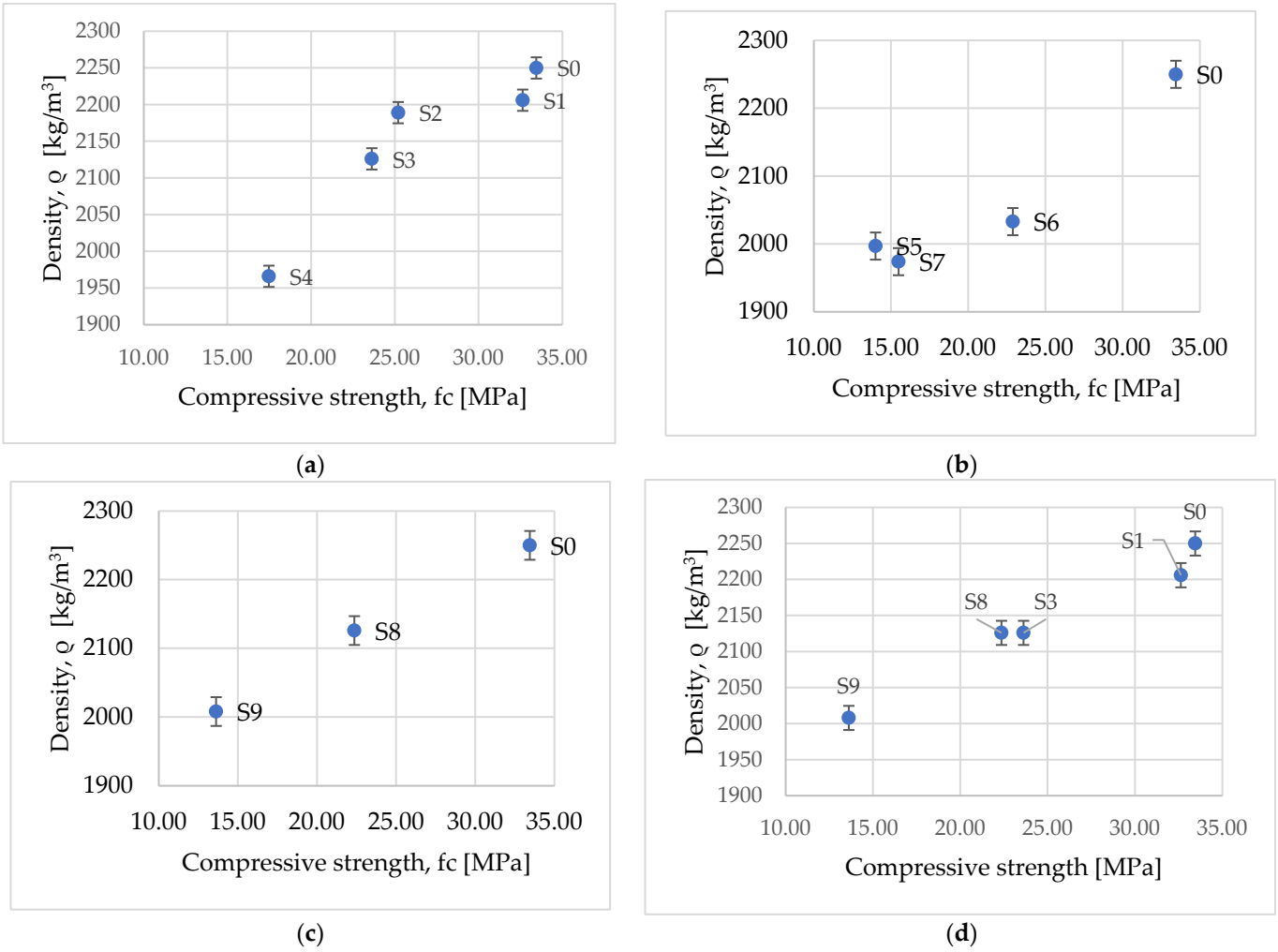

Figure 8. Variation of density versus compressive strength for concrete with waste: (**a**) concrete with waste chopped PET; (**b**) concrete with granular polystyrene; (**c**) concrete with sawdust; (**d**) concrete with waste chopped PET and sawdust.

A final analysis on the mechanical properties for the concrete with different waste substitution at the same percentage as the waste replacement is presented in Figure 8d, which highlights that the concrete has the same density at 40% substitution with waste chopped PET as at 10% of the substitution with sawdust, resulting that the waste wood is negatively affecting the mechanical properties even at a reduced percentage of substitution, the concrete could be used as self-sustained material or as heat accumulator wall.

Results from Figure 8 were obtained after testing three specimens for the same concrete mix with waste aggregates. The values presented in Figure 8 were obtained by calculating the average of the measured values obtained at the end of the test.

5. Characterization of Concrete Thermal Properties

5.1. Experimental Set Up and Process

The thermal properties were determined using an experimental device, developed at IUSTI Laboratory, which is based on the hot plane method with temperature measurements on both sides of the sample. The characterization is carried out at room temperature. A scheme of the experimental device is shown in Figure 9.

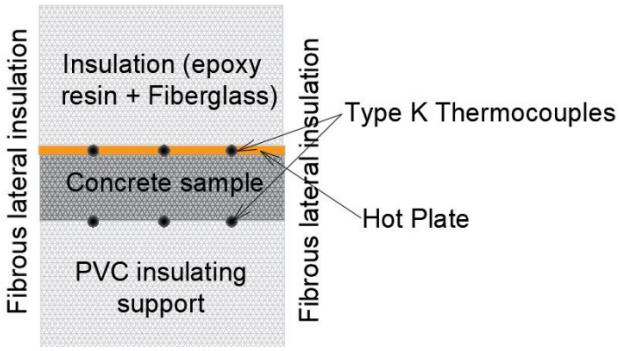

Figure 9. Experimental device.

The concrete sample is heated in the front face by a heating sole (hot plane) (Figure 9) consisting of a flat electrical resistance pasted to a copper plate. This part of the sample is grooved in order to allow the placement of three K thermocouples in contact with the sample. Three other thermocouples are placed in grooves of the sample holder that will be in contact with the 'rear face' of the sample (Figure 9). A thermal paste provides good contact between the faces of the sample, the hot plate, and the sample holder. Thanks to the uniformity of the supplied heat flux and the limitation of the lateral thermal losses, the heat transfer in the sample are assumed to be 1D. For each test, the experimental parameters to adjust are the heat flux supplied to the hot plane, the heating duration, and the test duration. Thus, for these various samples, the duration of the heating is 6 min for a heat flux of 16 W.

To achieve these measurements, the concrete sample was first positioned in the thermal device (Figure 9), and then heated for 6 min; then the heating was stopped and the cooling of the sample was awaited until it reached its steady state. The temperature signals were recorded; the signals corresponding to the 3 K thermocouples in the front face of the sample (Figure 9) were averaged to provide the thermogram of the front face; the same process was performed for the signals given by the 3 K thermocouples at the rear face of the sample (Figure 9).

A transient thermal model (thermal quadrupoles) was used to calculate the theoretical thermogram of the rear face, by convolution of the thermogram of the front face of the sample. This theoretical thermogram is a function of the following parameters:

- $t_d = e^2/a$
- $a = k/\rho Cp$
- $x = b/b_{PVC}$, corresponding to the ratio of the samples upon the sample's holder (PVC) effusivities.

The effusivity is given by:

- $b = \sqrt{k\rho c_p} = k/\sqrt{a} = \rho c_p \sqrt{a}$

These parameters were then identified by a least squares method, minimizing the gap between the theoretical and experimental thermograms, over range duration around the diffusive time.

The appropriate following parameters are then extracted.

- The thermal diffusivity a;
- The thermal effusivity b;
- The thermal conductivity $k = b\sqrt{a}$;
- The thermal capacity $c_p = b/\rho\sqrt{a}$.

The uncertainties calculation were carried out taking into account:

- The error of the thermocouples measurements (standard deviation: 0.005°C);
- The error due to the considered known parameters for determining a, b, k, ρ, and C_p, i.e.,: error on the thickness e: 1%; error on the PVC effusivity b_{PVC}: 10% and density error ρ: 4%.

First, a calibration was achieved to determine the sample holder (PVC) thermal diffusivity and effusivity. It was found that b_{PVC} is around (518 ± 10%) $Jm^{-2}K^{-1}s^{-0.5}$, which corresponds to values given by the manufacturer.

5.2. Results and Discussion

For each sample, the same process was applied in order to determine the various thermal parameters. In Figure 10, the thermal conductivity is plotted for the various considered concrete samples.

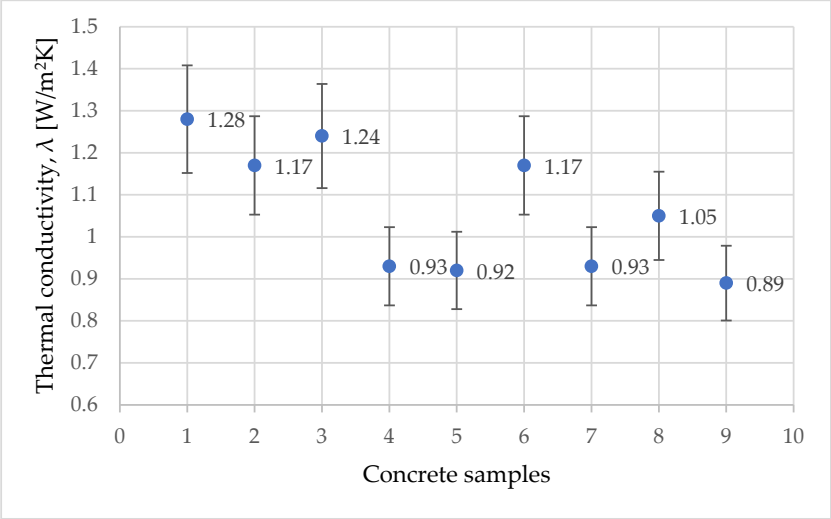

Figure 10. Variation of thermal conductivity.

From the thermal conductivity measurements, one can observe that the values of thermal conductivity are lower than the thermal conductivity of the standard concrete (S0). This result is consistent with the results found in the literature, since the thermal conductivity of the added waste is below the concrete one. Furthermore, reducing the thermal conductivity of concrete would provide better insulation for the building.

Following the measurements, Figure 11 was created highlighting the variation of thermal conductivity of the samples versus their density. As for compressive strength, the same behavior is highlighted; indeed, low density leads to low thermal conductivity.

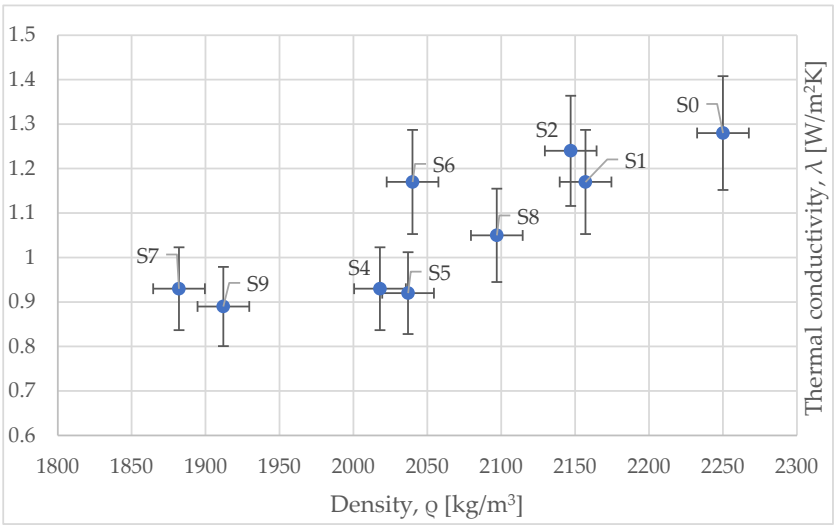

Figure 11. Variation of thermal conductivity versus density.

In order to illustrate the effect of the addition of waste on the global behavior of the concrete, another figure was created, Figure 12, which shows the compressive strength ratio versus the thermal conductivity.

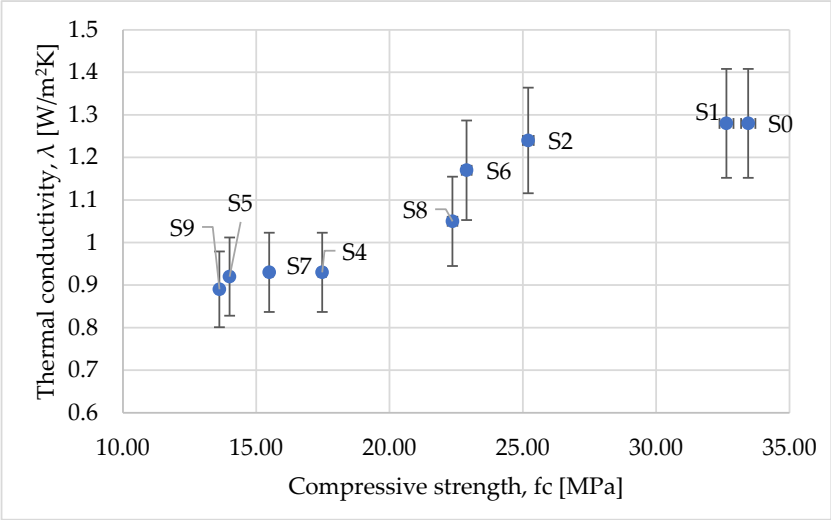

Figure 12. Variation of compressive strength versus density.

From Figure 12, one can notice the existence of three zones:

- The first one corresponds to concrete formed by the addition of a high concentration of waste, typically higher or equal to 50% (S4, S5, S7, and S9); the thermal conductivity was approximately reduced by almost 25%, while the compressive strength was reduced by 45–60%. One can consider that this zone is rather characterized by a constant thermal conductivity.
- The second zone gathers a moderate concentration of waste (S2, S3, S6, and S8), showing that the compressive strength is rather constant (a reduction of around 25%) whereas the thermal conductivity ratio is reduced by between approximately 5 and 20%. This zone will be considered as a zone with a constant compressive strength.
- Finally, the third zone, corresponding to the low concentration of waste, behaves mechanically as the standard concrete, the only noticeable difference being the lower thermal conductivity.

These results fall into accordance with the results found in the literature and infer the fact that, depending on the type of application, the appropriate concentration of waste aggregate can provide significant advantages in comparison to regular concrete. For example, through adding a low concentration of waste materials, the mechanical properties of the newly formed concrete are similar to those of the regular concrete, being good for the structural elements of buildings or, through adding an increased quantity of waste materials, the mixture provides a lower material conductivity, helping insulate the building and preventing heat loss [22–25,27–29].

6. Conclusions

The experimental study investigated the use of waste materials as a partial substitution of aggregates and cement in manufacturing concrete, and analyzed the mechanical properties via the compressive strength, density variations, and the thermal properties via the thermal conductivity parameter.

Three zones of behaviors were highlighted, the first one, corresponding to high waste concentration, leads approximately to a constant reduction in the thermal conductivity. The second, characterized by moderate waste concentration, behaves as a constant compressive strength. In addition, finally, the third one, defined by very low waste concentration,

induces only a very small reduction of the thermal conductivity with the compressive strength approximately the same as standard concrete.

By analyzing the compressive strength of the concrete with waste aggregates substitution, the study highlighted that the concrete can be used as a structural material such as self-sustained walls for low waste concentration, the differences in mechanical properties being negligible. On the other hand, high concentrations of waste aggregate in the concrete lead to a decrease in thermal conductivity, providing good solution for nonstructural walls with an increased insulation capacity in comparison to regular concrete walls, preventing heat loss.

One of the most important key factors is that, through reusing the waste and not using conventional aggregates, the carbon footprint of the building is reduced, this being a significant factor in the development of the construction sector in the future.

The studies revealed that a 10% replacement of the cement with fly ash and a 10% replacement of the sand with chopped PET had minimal impact on the properties of concrete, but on an environmental scale, if concrete were to have a portion of the natural aggregates replaced, this would have a significant impact both in terms of the reduction in necessary materials and in terms of pollution, as the waste materials would be given a new purpose.

Author Contributions: Conceptualization, C.A., M.B. (Marinela Barbuta), A.B., M.B. (Marius Branoaea) and R.S.V.; data curation, F.R.; formal analysis, G.S.; funding acquisition, M.C.B.; investigation, G.S.; methodology, G.S.; project administration, C.A., M.B. (Marinela Barbuta) and A.B.; resources, M.C.B.; supervision, C.A., M.B. (Marinela Barbuta) and A.B.; visualization, G.S.; writing—original draft. All authors have read and agreed to the published version of the manuscript.

Funding: This work was supported by a publications grant of the "Gheorghe Asachi" Technical University from Iasi, Romania (TUIASI), project number GI/P28/2021.

Institutional Review Board Statement: Not applicable.

Informed Consent Statement: Not applicable.

Data Availability Statement: All data are contained within the article.

Acknowledgments: The authors are thankful to Nathalie EHRET and Fabrice RIGOLLET from IUSTI Laboratory, Aix-Marseille Université, CNRS, Marseille, France for the support provided to realize the experimental investigation for determining the thermal properties of the concrete samples.

Conflicts of Interest: The authors declare no conflict of interest.

Nomenclature

PET	Polyethylene terephthalate
V	The volume of the specimen [m^3]
m_a	The mass of the specimen in air [kg]
m_{st}	The apparent mass of the immersed stirrup [kg]
m_w	The apparent mass of the immersed specimen [kg]
ρ_w	The density of water, at 20 °C [kg/m^3]
ρ_c	The density of the specimen [kg/m^3]
m	The mass of the specimen [kg]
t_d	The diffusive time of the sample
e	The sample thickness [m]
a	Thermal diffusivity [m^2/s]
b	Thermal effusivity [$Jm^{-2}K^{-1}s^{-0.5}$]
k	Thermal conductivity [W/mK]
C_p	Thermal capacity [J/kgK]
x	The ratio of the sample

References

1. Santamouris, M.; Vasilakopoulou, K. Present and future energy consumption of buildings: Challenges and opportunities towards decarbonisation. *E-Prime Adv. Electr. Eng. Electron. Energy* **2021**, *1*, 100002. [CrossRef]
2. Andrew, M. Global CO_2 emissions from cement production, 1928–2018. *Earth Syst. Sci. Data* **2019**, *11*, 1675–1710. [CrossRef]
3. Guo, R.; Wang, J.; Bing, L.; Tong, D.; Ciais, P.; Davis, S.J.; Andrew, R.M.; Xi, F.; Liu, Z. Global CO2 uptake of cement in 1930–2019. *Earth Syst. Data* **2020**, *13*, 1791–1805. [CrossRef]
4. Mohammed, A.A. Modelling the mechanical properties of concrete containing PET waste aggregate. *Constr. Build. Mater.* **2017**, *150*, 595–605. [CrossRef]
5. Nursyamsi, W.S.B.Z. The Influence of Pet Plastic Waste Gradations as Coarse Aggregate Towards Compressive Strength of Light Concrete. *Procedia Eng.* **2017**, *171*, 614–619. [CrossRef]
6. Pereira, E.L.; de Oliveira Junior, A.L.; Fineza, A.G. Optimization of mechanical properties in concrete reinforced with fibers from solid urban wastes (PET bottles) for the production of ecological concrete. *Constr. Build. Mater.* **2017**, *149*, 837–848. [CrossRef]
7. Cadere, C.A.; Barbuta, M.; Rosca, B.; Serbanoiu, A.A.; Burlacu, A.; Oancea, I. Engineering properties of concrete with polystyrene granules. *Procedia Manuf.* **2018**, *22*, 288–293. [CrossRef]
8. Gregorova, V.; Ledererova, M.; Stefunkova, Z. Investigation of Influence of Recycled Plastics from Cable, Ethylene Vinyl Acetate and Polystyrene Waste on Lightweight Concrete Properties. *Procedia Eng.* **2017**, *195*, 127–133. [CrossRef]
9. Xu, Y.; Jiang, L.; Xu, J.; Li, Y. Mechanical properties of expanded polystyrene lightweight aggregate concrete and brick. *Constr. Build. Mater.* **2012**, *27*, 32–38. [CrossRef]
10. Duan, P.; Yan, C.; Zhou, W.; Luo, W. Fresh properties, mechanical strength and microstructure of fly ash geopolymer paste reinforced with sawdust. *Constr. Build. Mater.* **2016**, *111*, 600–610. [CrossRef]
11. Kaya, A.; Kar, F. Properties of concrete containing waste expanded polystyrene and natural resin. *Constr. Build. Mater.* **2016**, *105*, 572–578. [CrossRef]
12. Saikia, N.; de Brito, J. Mechanical properties and abrasion behaviour of concrete containing shredded PET bottle waste as a partial substitution of natural aggregate. *Constr. Build. Mater.* **2014**, *52*, 236–244. [CrossRef]
13. Rahmani, E.; Dehestani, M.; Beygi, M.H.A.; Allahyari, H.; Nikbin, I.M. On the mechanical properties of concrete containing waste PET particles. *Constr. Build. Mater.* **2013**, *47*, 1302–1308. [CrossRef]
14. Gesoglu, M.; Güneyisi, E.; Hansu, O.; Etli, S.; Alhassan, M. Mechanical and fracture characteristics of self-compacting concretes containing different percentage of plastic waste powder. *Constr. Build. Mater.* **2017**, *140*, 562–569. [CrossRef]
15. Islam, M.J.; Meherier, M.S.; Islam, A.K.M.R. Effects of waste PET as coarse aggregate on the fresh and harden properties of concrete. *Constr. Build. Mater.* **2016**, *125*, 946–951. [CrossRef]
16. Maldonado-Bandala, E.E.; Nieves-Mendoza, D.; Romero-López, R.; Tobias-Jaramillo, R.; Almeraya-Calderón, F.; Barrios-Durstewitz, C.P.; Núñez Jaquez, R.E. Electrochemical and Mechanical Properties of Lightweight Concrete Blocks with Expanded Polystyrene Foam. *Int. J. Electrochem. Sci* **2015**, *10*, 472–485.
17. Sayadi, A.A.; Tapia, V.; Neitzert, R.; Clifton, G. Effects of expanded polystyrene (EPS) particles on fire resistance, thermal conductivity and compressive strength of foamed concrete. *Constr. Build. Mater.* **2016**, *112*, 716–724. [CrossRef]
18. Sofi, A.; Saxena, A.; Agrawal, P.; Sharma, A.; Sharma, K. Strength Predictions of Saw Dust and Steel Fibres in Concrete. *Int. J. Innov. Res. Sci. Eng. Technol.* **2015**, *4*, 12473–12477.
19. Bajpai, P.; Brar, A.; Nara, A.; Dudeja, N. Effect on strength properties of concrete by using waste wood ash as partial replacement of cement. *Int. J. Adv. Technol. Eng. Sci.* **2017**, *5*, 545–549.
20. Zeggar, M.L.; Azline, N.; Safiee, N.A. Fly ash as supplementry material in concrete: A review. *IOP Conf. Ser. Earth Environ. Sci.* **2019**, *357*, 012025. [CrossRef]
21. Susanti, E.; Istiono, H.; Komara, I.; Pertiwi, D.; Septiarsilia, Y.; Syahputra, F.K. Effect of fly ash to water-cement ratio on the characterization of the concrete strength. *IOP Conf. Ser. Mater. Sci. Eng.* **2021**, *1010*, 012035. [CrossRef]
22. González, D.; Caballero, P.P.; Fernández, D.B.; Vidal, M.M.J.; Sáez del Bosque, I.F.; Martínez, C.M. The Design and Development of Recycled Concretes in a Circular Economy Using Mixed Construction and Demolition Waste. *Materials* **2021**, *14*, 4762. [CrossRef] [PubMed]
23. Horňáková, M.; Lehner, P. Analysis of Measured Parameters in Relation to the Amount of Fibre in Lightweight Red Ceramic Waste Aggregate Concrete. *Mathematics* **2022**, *10*, 229. [CrossRef]
24. Tran, D.V.P.; Allawi, A.; Albayati, A.; Cao, T.N.; El-Zohairy, A.; Nguyen, Y.T.H. Recycled Concrete Aggregate for Medium-Quality Structural Concrete. *Materials* **2021**, *14*, 4612. [CrossRef] [PubMed]
25. Diaconu, L.I.; Rujanu, M.; Diaconu, A.C.; Serbanoiu, A.A.; Babor, D.; Plian, D. Improvement of the concrete behaviour to sulphate corrosion using fly ash admixture collected by wet process. *IOP Conf. Ser. Mater. Sci. Eng.* **2020**, *789*, 012018. [CrossRef]
26. Grădinaru, C.M.; Muntean, R.; Serbanoiu, A.A.; Ciocan, V.; Burlacu, A. Sustainable Development of Human Society in Terms of Natural Depleting Resources Preservation Using Natural Renewable Raw Materials in a Novel Ecological Material Production. *Sustainability* **2020**, *12*, 2651. [CrossRef]
27. Meza, A.; Pujadas, P.; Meza, L.M.; Pardo-Bosch, F.; López-Carreño, R.D. Mechanical Optimization of Concrete with Recycled PET Fibres Based on a Statistical-Experimental Study. *Materials* **2021**, *14*, 240. [CrossRef] [PubMed]
28. Suliman, N.H.; Razak, A.A.A.; Mansor, H.; Alisibramulisi, A.; Amin, N.M. Concrete using sawdust as partial replacement of sand: Is it strong and does not endanger health? *MATEC Web Conf.* **2019**, *258*, 01015. [CrossRef]

29. Bouaissi, A.; Li, L.Y.; Abdullah, M.M.A.B.; Ahmad, R.; Razak, R.A.; Yahya, Z. Fly Ash as a Cementitious Material for Concrete. In *Zero-Energy Buildings—New Approaches and Technologies*; IntechOpen: London, UK, 2020.
30. Bheel, N.; Ali, M.O.; Khahro, S.H.; Keerio, M.A. Experimental study on fresh, mechanical properties and embodied carbon of concrete blended with sugarcane bagasse ash, metakaolin, and millet husk ash as ternary cementitious material. *Environ. Sci. Pollut. Res.* **2022**, *29*, 5224–5239. [CrossRef] [PubMed]
31. Mangi, S.A.; Makhija, A.; Raza, M.S.; Khahro, S.H.; Jhatial, A.A. Comprehensive Review on Effects of Seawater on Engineering Properties of Concrete. *Silicon* **2021**, *13*, 4519–4526. [CrossRef]
32. Paramasivam, P.; Loke, Y.O. Study of sawdust concrete. *Int. J. Cem. Compos. Lightweight Concr.* **1980**, *2*, 57–61. [CrossRef]
33. Sales, A.; Rodrigues de Souza, F.; Nunes dos Santos, W.; Zimer, A.M.; Almeida, F.d.C.R. Lightweight composite concrete produced with water treatment sludge and sawdust: Thermal properties and potential application. *Constr. Build. Mater.* **2010**, *24*, 2446–2453. [CrossRef]
34. Joshi, C.; Lohita, R.P. *Fly Ash in Concrete: Production, Properties and Uses*; Gordon & Breach Science Publishers: London, UK, 1997.
35. EN12390-7. *Testing Hardened Concrete—Part 7: Density of Hardened Concrete*; British Standards Institution: London, UK, 2019.
36. Holcim. Available online: https://www.holcim.ro/en/business/products/cement/cem-iia-ll-425r (accessed on 9 November 2021).
37. Buema, G.; Lisa, G.; Kotova, O.; Ciobanu, G.; Ivaniciuc, L.; Favier, L.; Harja, M. Application of thermal analysis to improve the preparation conditions of zeolitic materials from flying ash. *Environ. Eng. Manag. J.* **2021**, *20*, 377–388.
38. Bhatt, A.; Priyadarshini, S.; Mohanakrishnan, A.A.; Abri, A.; Sattler, M.; Techapaphawit, S. Physical, chemical, and geotechnical properties of coal fly ash: A global review. *Case Stud. Constr. Mater.* **2019**, *11*, e00263. [CrossRef]
39. Bărbuţă, M.; Ţăranu, N.; Harja, M. Wastes Used in Obtaining Polymer Composite. *Environ. Eng. Manag. J.* **2009**, *8*, 1145–1150.
40. Horisawa, S.; Sunagawa, M.; Tamai, Y.; Matsuoka, Y.; Miura, T.; Terazawa, M. Biodegradation of nonlignocellulosic substances II: Physical and chemical properties of sawdust before and after use as artificial soil. *J. Wood Sci.* **1999**, *45*, 492–497. [CrossRef]
41. EN 12390-2. *Testing Hardened Concrete—Making and Curing Specimens for Strength Tests*; British Standards Institution: London, UK, 2019.
42. EN 12390-3. *Testing Hardened Concrete—Part 3: Compressive Strength of Test Specimens; British Standards Institution: London, UK, 2019.*

applied sciences

MDPI

Article

Experimental and Numerical Study of Thermal Performance of an Innovative Waste Heat Recovery System

Robert Stefan Vizitiu [1], Andrei Burlacu [1,*], Cherifa Abid [2], Marina Verdes [1], Marius Costel Balan [1,*] and Marius Branoaea [1]

[1] Faculty of Civil Engineering and Building Services, "Gheorghe Asachi" Technical University of Iasi, 700050 Iasi, Romania; robert.vizitiu@tuiasi.ro (R.S.V.); marina.verdes@academic.tuiasi.ro (M.V.); marius.branoaea@tuiasi.ro (M.B.)

[2] IUSTI Laboratory, Aix-Marseille University, 13453 Marseille, France; cherifa.abid@univ-amu.fr

* Correspondence: andrei.burlacu@tuiasi.ro (A.B.); marius-costel.balan@academic.tuiasi.ro (M.C.B.)

Abstract: One of the biggest challenges the world is facing these days is to reduce the greenhouse gases emissions in order to prevent the global warming. Since a significant quantity of CO_2 emissions is the result of the energy producing process required in industry or buildings, the waste heat recovery is an important aspect in the fight for preserving the planet. In this study, an innovative waste heat recovery system which can recover waste heat energy from cooling liquids used in industry or in different processes, was designed and subjected to experimental investigations. The equipment uses heat pipes to capture thermal energy from the residual fluids transiting the evaporator zone and transfer it to the cold water transiting the condenser zone. The efficiency of the heat exchanger was tested in 9 scenarios, by varying the temperature of the primary agent to 60, 65 and 70 °C and the volume flow rate of the secondary agent to 1, 2 and 3 L/min. The temperature of the secondary agent and the volume flow rate of the primary agent were kept constant at 10 °C, respectively 24 L/min. The results were later validated through numerical simulations, and confirmed that the equipment can easily recover waste thermal energy from used water with low and medium temperatures at very low costs compared to the traditional heat exchangers. The results were promising, revealing an efficiency of the equipment up to 76.7%.

Keywords: waste heat recovery; heat pipe; energy efficiency

Citation: Vizitiu, R.S.; Burlacu, A.; Abid, C.; Verdes, M.; Balan, M.C.; Branoaea, M. Experimental and Numerical Study of Thermal Performance of an Innovative Waste Heat Recovery System. *Appl. Sci.* **2021**, *11*, 11542. https://doi.org/10.3390/app112311542

Academic Editor: Alberto Benato

Received: 16 November 2021
Accepted: 1 December 2021
Published: 6 December 2021

1. Introduction

According to a study [1] made in 2019, the building sector is responsible for about 16% of the wasted heat energy. The waste heat energy with a value lower than 100 °C is considered low-temperature, the one with a temperature between 100 °C and 300 °C is medium-temperature, while the waste heat energy with a temperature higher than 300 °C is considered high-temperature. The highest losses of thermal energy are in the low-temperature sector, with a percentage of 64%. Waste heat recovery can have a significant impact on the energy efficiency of buildings by reducing the heat losses. There are various heat recovery technologies such as waste heat boilers [2], economisers [3], plate heat exchangers [4], heat pipe heat exchangers [5] and others, which all have the purpose to capture the waste thermal energy and convert it to active thermal or electrical energy [6].

The waste heat utilization is very diverse and it has been developed in the last few years. There are numerous works in the literature which concentrate on waste heat recovery using heat pipes. The original contribution of this work consists in designing and testing a compact equipment which can recover thermal energy from low-temperature residual fluids at low costs of production and maintenance using termosyphons. Since the gravitational heat pipes is a passive technology and do not require any moving parts, the costs of recovering thermal energy are reduced.

Asl et al. [7] made a theoretical and practical research on three different approaches to implement a geothermal waste heat recovery system which is supplying the necessary heat to the pools of a fish farm. The results showed that when the most efficient method is used, the minimum costs of establishing a heat recovery system decrease by 60.65%. Liang et al. [8] tried to improve the performance of the exhaust heat recovery from diesel engines by using a regenerative super-critical carbon dioxide Brayton cycle/organic Rankine cycle dual loop system. The results showed an improvement of the engine power output by 6.78%, which can be translated as a lower fuel consumption.

A team of researchers made a numerical study on a waste heat recovery steam generator for hydrogen production. The research was aimed to improve the heat transfer mechanism of semi-coke and steam. The 7.5 kg/h proved to be the best steam flow for an efficient heat recovery rate [9].

Scientist have studied the possibility of introducing heat pipes in process of heat recovery for an improved efficiency of these type of systems. A heat pipe consists of a sealed enclosure, made from a heat conductive material and a working fluid. When heat is applied to the evaporator zone, the working fluid turns into vapor and transfers the heat to the condenser zone at a high rate. The vapors turn into liquid droplets and returns to the evaporator zone either with the help of gravity or through wick (Figure 1). Because the pressure inside the heat pipe is very low, the working fluid evaporates at a lower temperature than usual, making the heat pipe a super-conductor even at low temperatures.

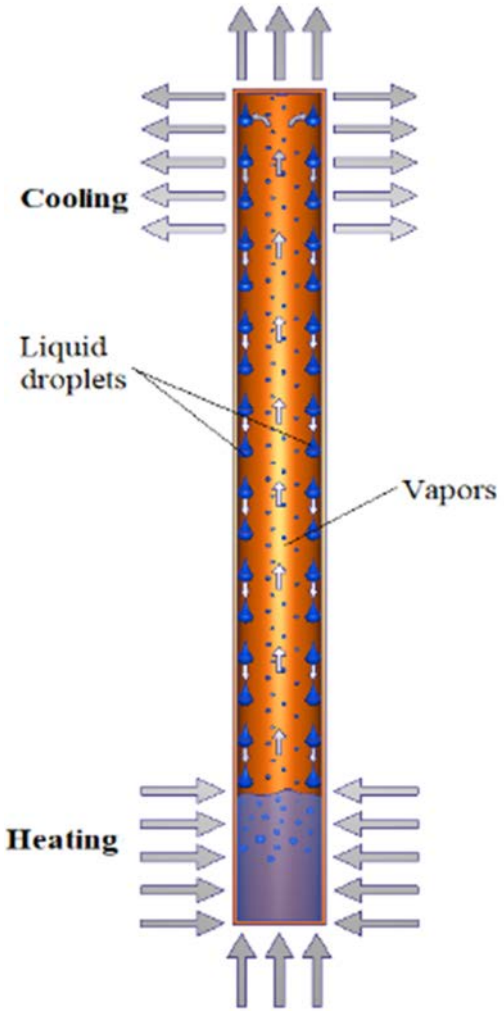

Figure 1. The operating principle of heat pipes.

The most important benefit of heat pipes is that it is a passive way to recover thermal energy, which makes the process of waste heat recovery cheaper. Another advantage is

their high conductance potential compared to common heat recovery technologies. Since each heat pipe functions individually, a heat pipe heat exchanger can operate properly even if one of them fails. Also, the fluids involved in the heat recovery process will not be mixed or contaminated in case of a heat pipe failure.

The most common use of heat pipes is for solar applications. Studies have tried to improve the efficiency of heat pipes in solar collectors by testing different working fluids [10], by using thermal oil [11] or by adding fins to the condenser region of the heat pipes [12]. The optimum fill ratio is also an important factor on the efficiency heat pipes [13]. A study by Yang [14] investigated a novel high-temperature two-phase closed flat heat pipe which uses sodium as a working fluid. Burlacu [15] performed numerical simulations on a system which proposes the introduction of heat pipes in glazed facades.

There are also many applications of heat pipes in the waste heat recovery field. Mahajan proved in his study [16] that by using oscillating heat pipes in waste heat recovery ventilation can save more than 2500 $ annually in cities with continental climatic conditions. Jouhara [17] presented a nuclear seawater desalination system based on heat pipe technology, while Tian [18] recovered waste heat from exhaust gases using a heat recovery gravity heat pipe heat exchanger. A study [19] made in 2018 presented a heat pipe heat exchanger with concentric tube heat pipes and acetone as working fluid used for low-temperature heat sources. Heat pipes were also used in designing a dual heat recovery system which recovers waste heat from residual fluids and produces simultaneously hot water and warm air [20]. A study [21] presented in 2019 analyzed the possibility of combining heat pipes with phase change materials in order to recover and store thermal energy more efficiently.

Delpech et al. [22] designed a heat pipe heat exchanger which has the purpose to recover the heat resulted during the cooling of a ceramic kiln. The recovered heat is used to heat up an air stream which will be used in the ceramic process to dry the ceramic parts. The heat pipe-based heat exchanger was able to recover more than 863 MWh of thermal energy and also reduce the fuel consumption of the ceramic process by 110,600 Sm^3/year which is the equivalent of 164 tons/year of CO_2. In another experiment, Delpech et al. [23] improved the process of heat recovery in the ceramics industry using a radiative heat pipe system which was able to recover heat through radiation and natural convection in an enclosed kiln. Depending on the heater's temperature, the heat pipe can recover between 400 W and 3100 W.

Jouhara et al. [24] developed a heat recovery system based on a flat heat pipe heat exchanger which was tested in the laboratory and on an industrial plant. The equipment is meant to recover the radiative heat resulted during the cooling process of steel wires. The rate of heat recovery for the laboratory tests was 5 kW, while for tests made on the industrial plant the efficiency was doubled.

This research presents a numerical and experimental study of thermal performance on an innovative prototype of a waste heat recovery system designed and manufactured in the laboratory of the Faculty of Civil Engineering and Building Services of Technical University "Gheorghe Asachi" of Iasi, Romania. The device has a modular design, with two main components, the evaporator and the condenser, and is using heat pipes for improving the heat transfer inside the device. The novelty and the originality brought by this research consists in using the axial flow for the primary and the secondary agent around the heat pipes for increasing the heat exchange surface and consequently the energy performance of the waste heat recovery system. Thus, the equipment can easily recover waste thermal energy from used water with low and medium temperatures at very low costs compared to the traditional heat exchangers, which represents an important goal in the research domain of modern heat exchangers. The recovered energy can be used for preheating or heating water for domestic use or for other heating systems without any additional pumping system or any other forms or additional energy resulting a high energy efficient innovative waste heat recovery system. The results of the experimental investigations were validated through numerical simulations.

2. Materials and Methods

2.1. The Design of the Heat Pipe Heat Recovery System

The heat pipe heat recovery system (HPHE) is used to recover waste heat from used water through the heat pipes and use it for heating up a volume of cold water. The equipment has a circular design, with a diameter of 0.25 m and a height of 1.04 m. The material used for building the evaporator and condenser is steel, while the heat pipes are made of cooper. The heat pipes do not have a wick structure inside, they use gravity to return the condensate and they were specially designed for this equipment. The working fluid of the heat pipes is water and the pressure inside was set close to 4300 Pa, in order for the fluid to evaporate when it will reach a temperature of 30 °C, thus making the heat pipe efficient in low-temperature applications.

Inside the HPHE there are 14 heat pipes inserted vertically through the separation flange, which are transporting the heat recovered from the primary agent inside the evaporator to the secondary agent inside the condenser. Inside the condenser there are three steel rings and two steel discs for a better circulation of the secondary agent and a more uniform heating. The condenser, the evaporator and the separation flange are connected using 9 screws and nuts. The constructive details of the components can be viewed in Table 1. The design of the heat pipe heat recovery system was made using the Autodesk Inventor 2018 software. The model and its components can be seen in Figure 2.

Table 1. Constructive details of the components.

Component	Height [m]	Diameter [m]
Evaporator	0.395	0.25
Condenser	0.64	0.25
Separation flange	0.005	0.246
Discs	0.005	0.15
Rings	0.005	0.246
Heat pipes	1	0.015

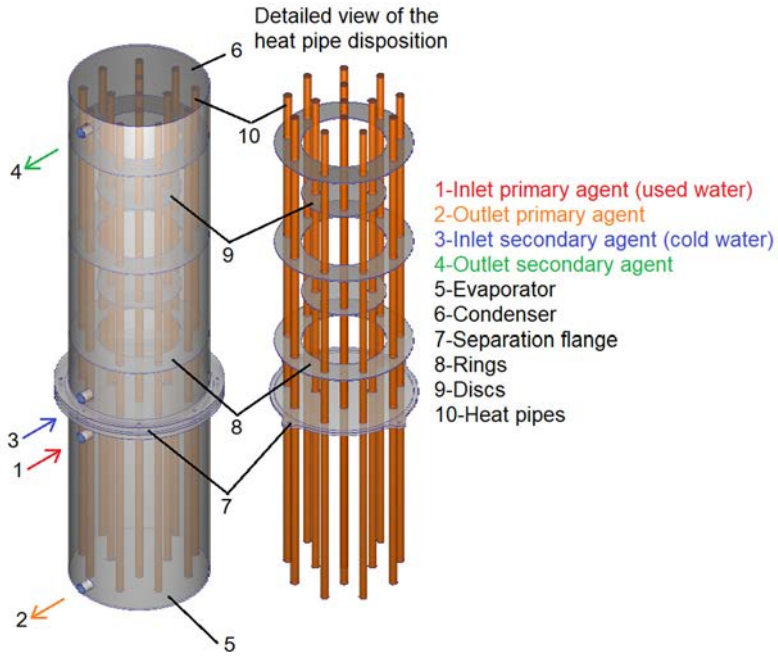

Figure 2. The 3D design of the HPHE.

2.2. Experimental Setup

Using the 3D model we built a prototype of the equipment and tested it in the laboratory. Also, a stand has been designed and manufactured as shown in Figure 3.

The primary agent was hot water heated by an electric heater with a power of 8 kW and the temperature could be adjusted as needed.

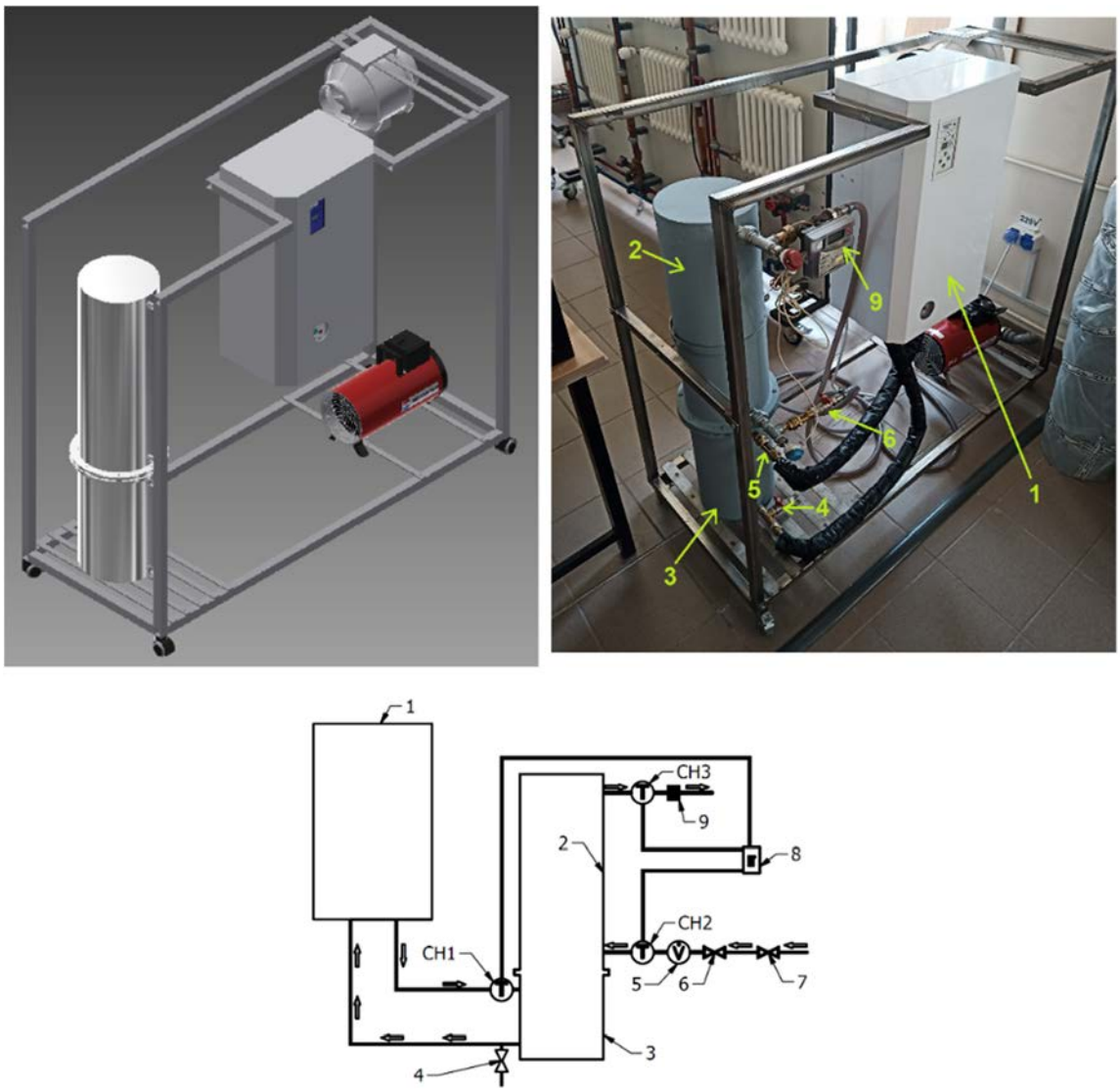

Figure 3. The experimental stand: 1—Electric heater, 2—Condenser, 3—Evaporator, 4—Faucet for filling/emptying the primary circuit, 5—Flowmeter, 6—Faucet for controlling the volume flow rate, 7—Water supply faucet, 8—LT BTM-420SD electronic thermometer, 9—Elterm CF 55 flow temperature meter.

The electric heater is connected to the heat recovery system through flexible stainless-steel pipes with a diameter of 16 mm. The pipe circuit was equipped with a faucet for filling/emptying the evaporator and the primary circuit, and a probe sheath for measuring the temperature of the primary agent. The circuit of the secondary agent is connected directly to the water supply network of the laboratory. Two probe sheaths were installed at the inlet and outlet of the condenser to track temperature variations and also an ELTERM CF 55 thermal energy meter which is tracking the volume flow rate and the temperature of the secondary agent. The thermal sensors inserted in the probe sheaths are connected to an LT BTM-4208SD electronic thermometer which has a precision of $\pm 0.4\%$.

The equipment was tested with different temperatures of the primary agent and different volume flow rates, using the parameters presented in Table 2. For each test, the valve on the circuit of the secondary agent was opened at maximum to keep the secondary agent as cold as possible during the process of heating up the secondary agent.

When the temperature of the secondary agent reached the value required for testing, the valve was set for the proper volume flow rate required for the test.

Table 2. Testing parameters.

	$T_{Ev,1}$ [°C]	$T_{Co,1}$ [°C]	q_1 [L/min]	q_2 [L/min]
Test no. 1	60	10	1	24
Test no. 2	60	10	2	24
Test no. 3	60	10	3	24
Test no. 4	65	10	1	24
Test no. 5	65	10	2	24
Test no. 6	65	10	3	24
Test no. 7	70	10	1	24
Test no. 8	70	10	2	24
Test no. 9	70	10	3	24

2.3. Numerical Simulations

The 3D model designed in the Autodesk Inventor environment was imported in Autodesk CFD Simulation software. The geometry was discretized in a network consisting 500,000 nodes and the first simulation was run. In order to find a proper mesh that presents the most accurate results, the number of meshing elements was increased gradually until the differences between two consecutive simulations were insignificant.

Another criteria for choosing the proper number of mesh elements was the computational power. The higher the number of elements, the longer time required for calculation. According to these criteria, the optimum mesh network was chosen the one consisting in 1.2 M nodes.

The boundary conditions can be observed in Table 2. There were carried out 9 simulations with various parameters.

The temperature of the secondary agent, $T_{Co,1}$, and the volume flow rate of the primary agent, q_2, were kept constant at 10 °C respectively 24 L/min, while the temperature of the primary agent, $T_{Ev,1}$, was varied to 60 °C, 65 °C and 70 °C and the volume flow rate of the secondary agent, q_1, was varied to 1 L/min, 2 L/min and 3 L/min.

The simulations were run in steady state and the results obtained are defining the moment when the temperature at the outlet of the secondary agent reaches a quasi-constant temperature.

The governing equations for fluid flow and heat transfer are the Navier-Stokes or momentum equations and the First Law of Thermodynamics or energy equation. These equations are used by the Autodesk CFD Simulation software to calculate and describe the heat transfer process.

3. Results

3.1. Experimental Results

The temperature of the primary agent was kept constant for one hour. Since the temperature of the secondary agents is rising very slowly after about 50 min, and the variations are small, we considered that after 1 h of constant temperature in the condenser the temperature of the evaporator reaches a quasi-constant state.

The sensors CH1, CH2, and CH3 are responsible for tracking the temperature variation in time. CH1 is placed at the inlet of the condenser, CH2 at the outlet of the condenser and CH3 at the inlet of the evaporator. The electronic thermometer was set to record the temperature every 60 s.

The temperature recorded after 60 min for the test no. 1 was 40.7 °C, for the test no. 2 the results showed 35.7 °C, while for the test no. 3 the temperature was 32.1 °C. As we can observe in Figure 4, the most significant temperature variation takes place in the first 10 min. After this period of time, the rising of temperature is slower.

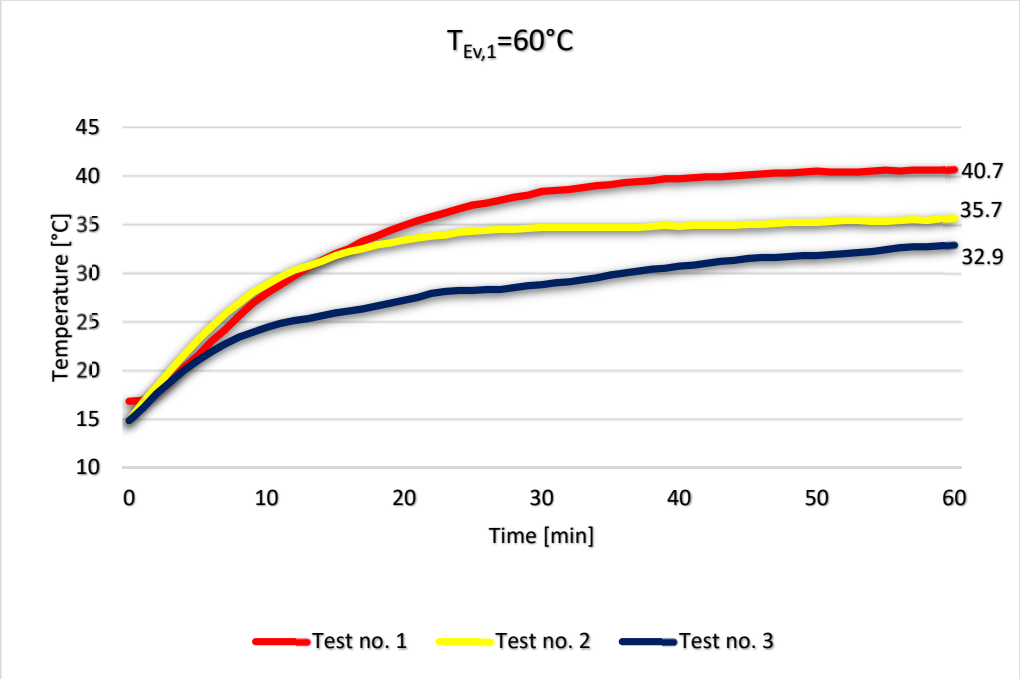

Figure 4. The variation of temperature at the outlet of the condenser for tests no. 1, 2, 3.

To visualize the external temperature of the heat recovery system, we took some photos with a FLIR thermal vision camera during test no. 1. In Figure 5 we can observe that most of the heat recovered is first absorbed by the water in the middle of the condenser during the first 15 min of the test, but after that, the temperature tends to become uniform inside the condenser.

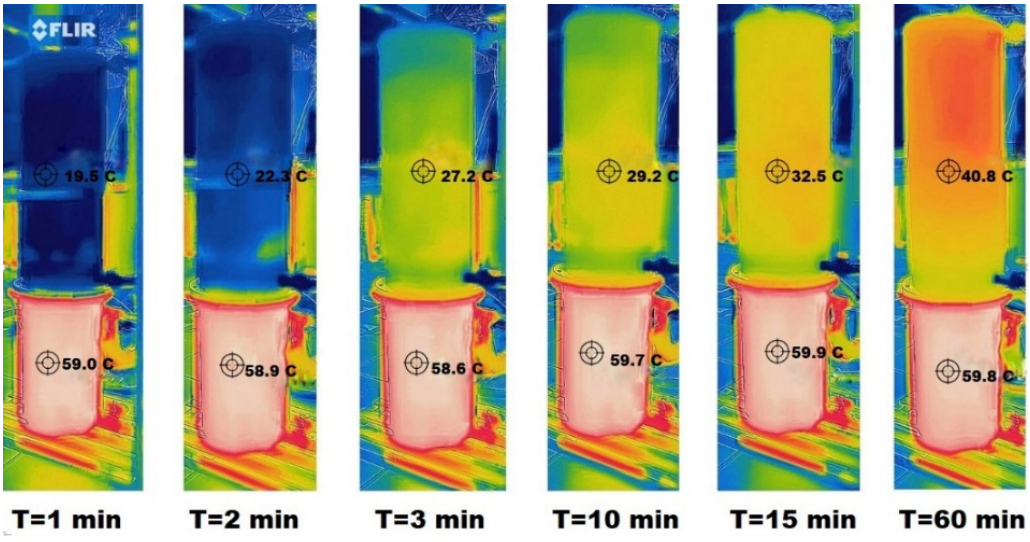

Figure 5. Photos with FLIR thermal camera during test no. 1.

For the next 3 tests we used a temperature of 65 °C at the inlet of the evaporator and the sensors revealed a temperature of 47.4 °C for test no. 4, 41.8 °C for test no. 5 and 36.3 °C for test no. 6. In the first 10 min, the volume flow rate of the secondary agent does not have a significant impact on the heat recovery rate. After about 20 min, the temperature rise in the condenser is slow, with about 0.1 °C/min for all of the three cases (Figure 6).

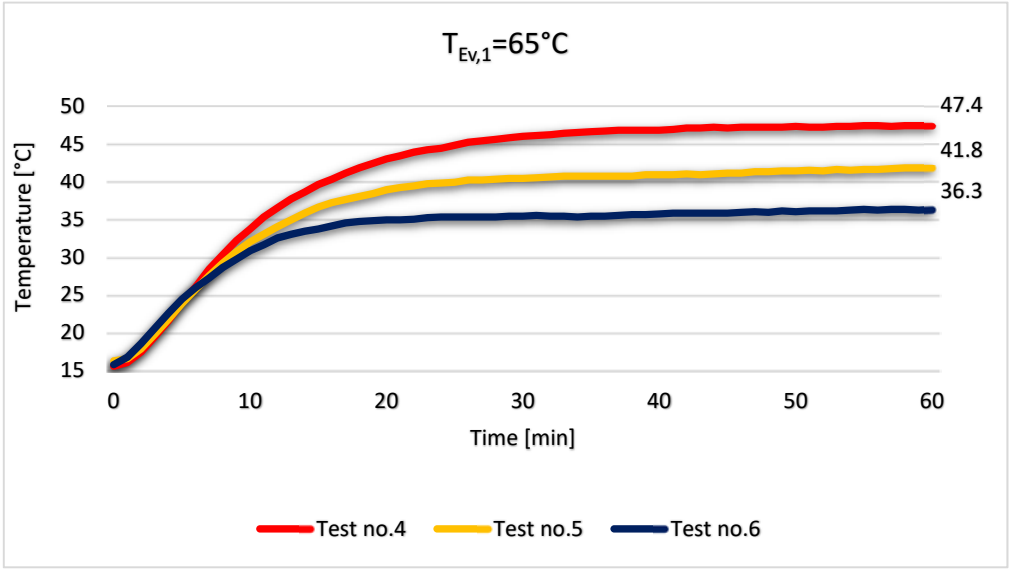

Figure 6. The variation of temperature at the outlet of the condenser for tests no. 4, 5, 6.

The tests were repeated for the same volume flow rates but this time with the temperature of the primary agent of 70 °C. As we can observe in Figure 7, the temperature of the secondary agent after 60 min was 56.1 °C for case no. 7, 46.7 °C for case no. 8 and 41.1 °C for case no. 9. Again, the amount of heat recovered in the first 10 min does not depend on the volume flow rate of the secondary agent. After 10 min, the ΔT between the inlet and the outlet of the condenser is about 18.5 °C for all three cases (Figure 7).

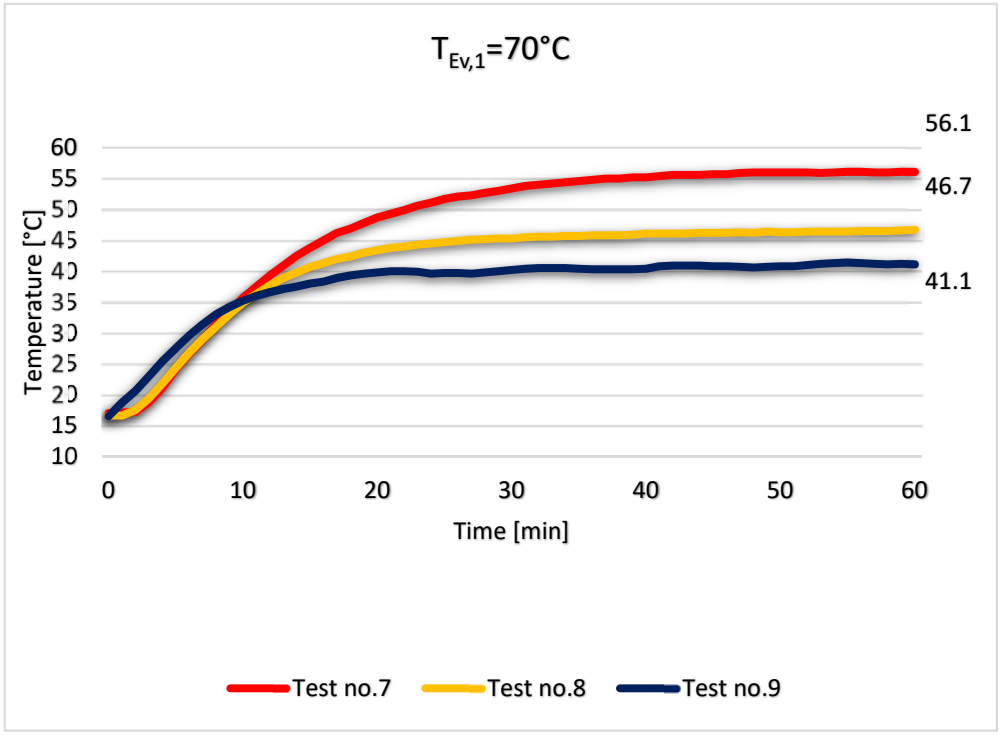

Figure 7. The variation of temperature at the outlet of the condenser for tests no. 7, 8, 9.

3.2. Numerical Simulations Results

For the numerical simulations we used as boundary conditions the same parameters as in the experimental setup, presented in Table 2. The temperature of the primary agent to 60, 65 and 70 °C and the volume flow rate of the secondary agent to 1, 2 and 3 L/min.

The temperature of the secondary agent and the volume flow rate of the primary agent were kept constant at 10 °C, respectively 24 L/min.

The mesh consisted in 1.2 million of elements and the simulations were run in steady state. By using the surface refinement tool, the mesh was refined at the interfaces between fluids and solids and on the smaller areas of the equipment, for an improved capture of the heat transfer. The results were centralized in a graph in Figure 8.

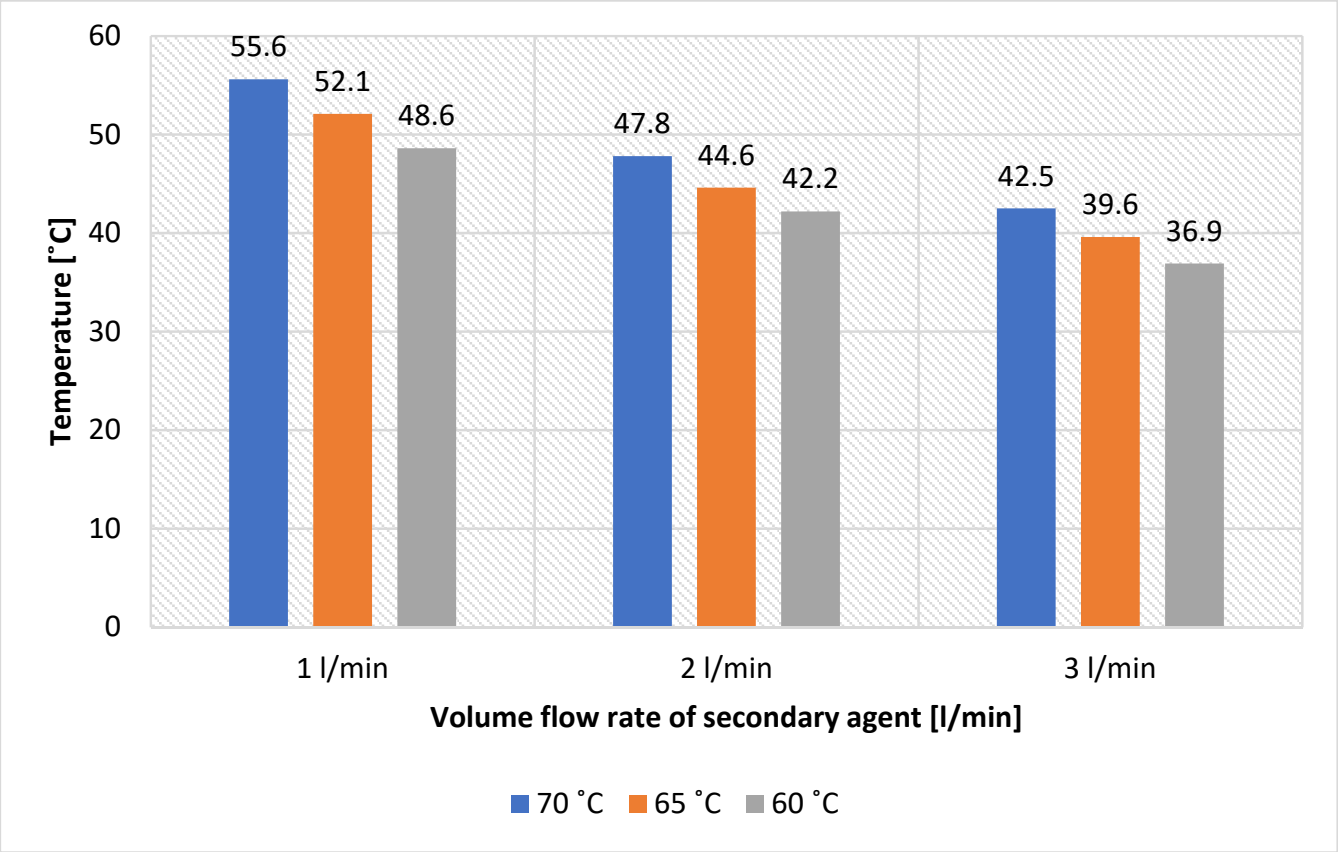

Figure 8. Results of the numerical simulations.

The experimental results were validated by the numerical simulations. The temperatures obtained in the numerical simulations were slightly higher than the experimental ones, with values between 2 and 5 °C. This can be explained due to heat losses from the experimental test, which the simulation does not take into account.

The simulation environment is also a useful tool for observing the heat process that happens inside the heat recovery system. Figure 9 presents a 2D section through the middle of the equipment for the 9 tests.

From Figure 9 it can be concluded that the heat transfer inside the condenser can be further improved by creating a path for the secondary agent.

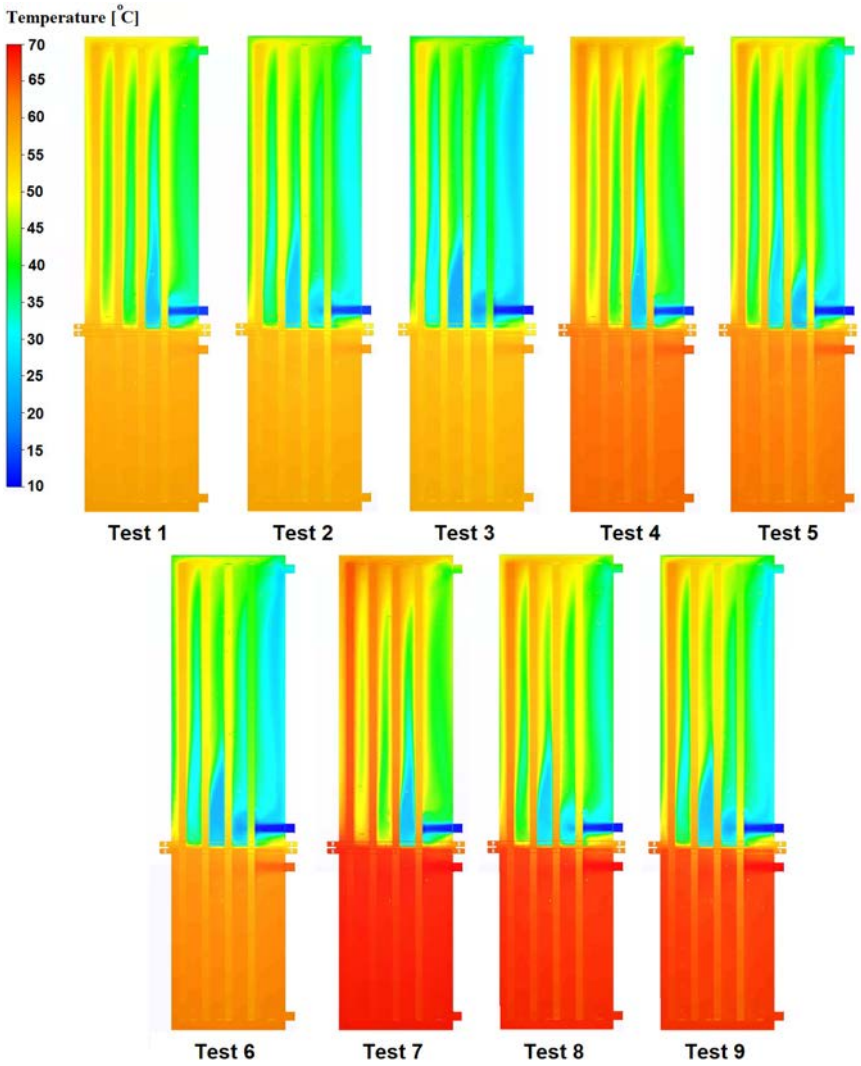

Figure 9. 2D section plane.

3.3. The Efficiency of the Equipment

The efficiency of the heat pipe heat exchanger can be evaluated as its thermal effectiveness which is the ratio between the heat transfer rate, Q, and the maximum heat transfer rate of the equipment, Q_{max}. The equation can be expressed as:

$$\varepsilon = \frac{Q}{Q_{max}} \tag{1}$$

$$Q = C_{Ev}(T_{Ev,\,1} - T_{Ev,\,2}) = C_{Co}(T_{Co,\,2} - T_{Co,\,1}) \tag{2}$$

By using the Equation (2) we can determine the heat transfer rate for the heat recovery system. C_{Ev} and C_{Co} represent the heat capacity rate for the evaporator and the condenser section and can be determined as the product of the mass flow rate and the specific heat capacity for the referred section.

$$C_{Ev} = \dot{m}_{Ev} \times c_{p,Ev} \tag{3}$$

$$Q_{max} = C_{min}(T_{Ev,\,1} - T_{Co,\,1}) \tag{4}$$

$$Q_{max} = \dot{m}_{Co} \times C_{p,Co}(T_{Ev,\,1} - T_{Co,\,1}) \tag{5}$$

For the expression of Q_{max} we have used C_{min} instead of C_{max} because Q_{max} represents the maximum heat transfer rate for the heat exchanger but for this case, we have a limiting factor represented by the minimum heat capacity rate between the two fluids.

By applying the Equations (2) and (5), the Equation (1) can be written as follows:

$$\varepsilon = \frac{Q}{Q_{max}} = \frac{\dot{m}_{Ev} \times C_{p,Ev} \times (T_{Ev,1} - T_{Ev,2})}{\dot{m}_{Co} \times C_{p,Co} \times (T_{Ev,1} - T_{Co,1})} \quad (6)$$

The highest efficiency of the heat recovery system was in test no. 7, when the temperature of the secondary agent after 1 h was 56.1 °C compared to 70 °C, the temperature of the primary agent, which means an efficiency of 76.7% (Figure 10).

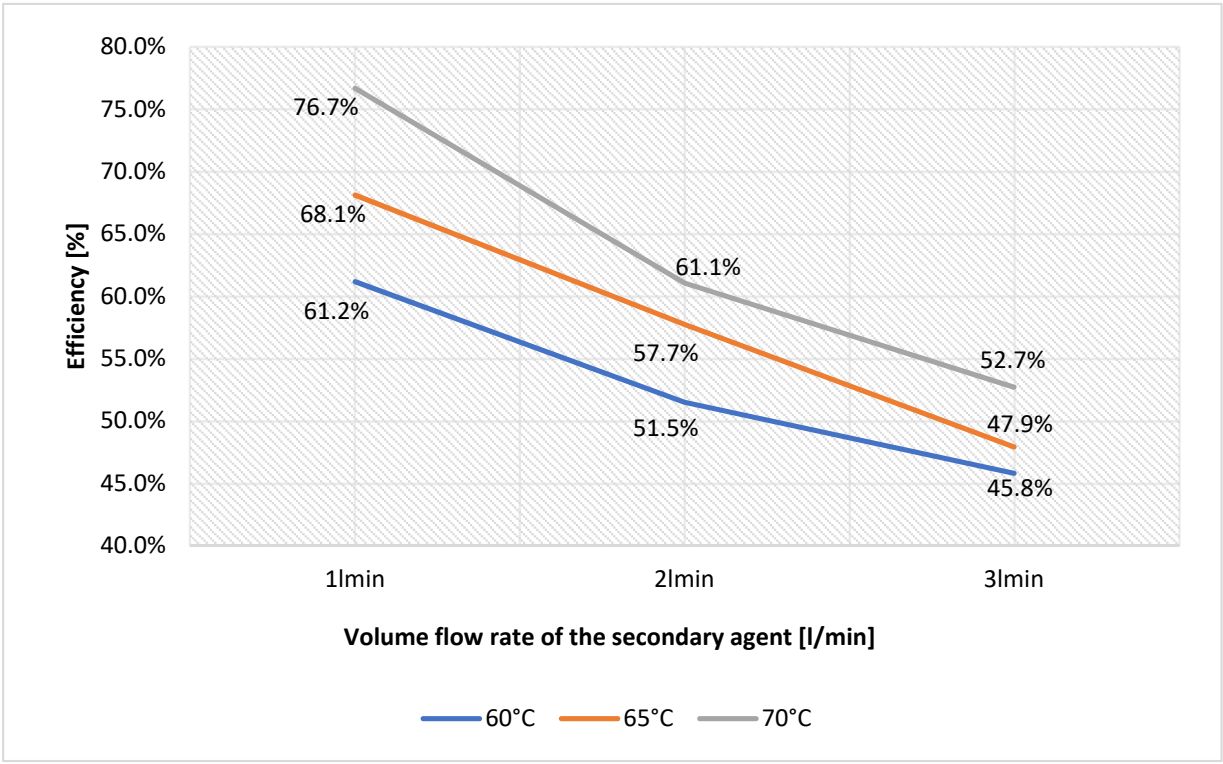

Figure 10. The efficiency of the heat recovery system.

4. Conclusions

A heat pipe heat recovery system was designed, manufactured and tested. The thermal performance of the equipment was investigated through experimental tests and confirmed by numerical simulations. Also, an efficiency calculation was made based on the experimental data obtained.

Compared with classic heat recovery system, this equipment produces hot water at lower costs, given the fact that the heat pipes are a passive technology and do not require any moving parts. The results showed that it needs about 10–15 min until it is able to produce hot water at almost constant temperature. The efficiency of the heat pipes is increasing directly proportional to the temperature of the primary agent. An efficiency of 76.7% was obtained with a temperature of 70 °C of the primary heat source, but the results showed that this percentage can be further improved.

It can be concluded that the heat pipe heat recovery system can be a feasible solution for recovering thermal energy from used waters. As further researches, the equipment can be tested at even higher volume flow rates for the secondary agents and the number of heat pipes could be varied. Also, industrial tests may be carried out to check the efficiency of the heat pipe heat recovery system in factories.

Author Contributions: Conceptualization, R.S.V., A.B. and M.C.B.; methodology, A.B.; software, R.S.V.; validation, R.S.V., A.B., C.A. and M.V.; formal analysis, R.S.V., C.A. and M.B.; investigation, R.S.V., A.B., C.A. and M.B.; resources, M.V.; data curation, R.S.V. and M.B.; writing—original draft preparation, R.S.V. and M.B.; writing—review and editing, A.B., C.A., M.V. and M.C.B.; visualization, R.S.V. and A.B.; supervision, A.B., C.A. and M.C.B.; project administration, A.B., C.A., M.V. and M.C.B.; funding acquisition, M.V. and M.C.B. All authors have read and agreed to the published version of the manuscript.

Funding: This work was supported by a publications grant of the TUIASI, project number GI/P28/2021.

Institutional Review Board Statement: Not applicable.

Informed Consent Statement: Not applicable.

Data Availability Statement: Not applicable.

Acknowledgments: This work was supported by a publications grant of the TUIASI, project number GI/P28/2021.

Conflicts of Interest: The authors declare no conflict of interest.

Nomenclatures

HPHE	Heat pipe heat recovery system
$T_{Ev,1}$	Temperature of the primary agent at the inlet of the evaporator [°C]
$T_{Co,1}$	Temperature of the secondary agent at the inlet of the condenser [°C]
q_1	Volume flow rate of the primary agent [L/min]
q_2	Volume flow rate of the secondary agent [L/min]
CH1	Thermal sensor at the inlet of the evaporator
CH2	Thermal sensor at the inlet of the condenser
CH3	Thermal sensor at the outlet of the condenser
T	Time [min]
λ	Thermal conductivity [W/m*K]
ε	Thermal effectiveness of the HPHE [%]
Q	Heat transfer rate of the HPHE [W]
Q_{max}	Maximum theoretical heat transfer rate of the HPHE [W]
C_{ev}	Heat capacity rate of the evaporator [W/K]
$T_{Ev,2}$	Temperature of the primary agent at the outlet of the evaporator [°C]
C_{co}	Heat capacity rate of the condenser [W/K]
$T_{Co,2}$	Temperature of the secondary agent at the outlet of the condenser [°C]
$\dot{m}_{Ev}$	Mass flow rate of the primary agent [kg/m^3]
$\dot{m}_{Co}$	Mass flow rate of the secondary agent [kg/m^3]
$C_{p,Ev}$	Specific heat of the primary agent [J/kg*K]
$C_{p,Co}$	Specific heat of the secondary agent [J/kg*K]
C_{min}	Minimum heat capacity rate between the two fluids [W/K]

References

1. Firth, A.; Zhang, B.; Yang, A. Quantification of global waste heat and its environmental effects. *Appl. Energy* **2019**, *235*, 1314–1334. [CrossRef]
2. Men, Y.; Liu, X.; Zhang, T. A review of boiler waste heat recovery technologies in the medium-low temperature range. *Energy* **2021**, *237*, 121560. [CrossRef]
3. Termtech. Reducing Energy Costs with Economisers. Available online: https://thermtech.co.uk/reducing-energy-costs-with-economisers/ (accessed on 25 November 2021).
4. Arsenyeva, O.; Klemes, J.J.; Kapustenko, P.; Fedorenko, O.; Kusakov, S.; Kobylnik, D. Plate heat exchanger design for the utilisation of waste heat from exhaust gases of drying process. *Energy* **2021**, *233*, 121186. [CrossRef]
5. Xie, C.Y.; Tao, H.Z.; Li, W.; Cheng, J.J. Numerical simulation and experimental investigation of heat pipe heat exchanger applied in residual heat removal system. *Ann. Nucl. Energy* **2019**, *133*, 568–579. [CrossRef]
6. Jouhara, H.; Khordehgah, N.; Almahmoud, S.; Delpech, B. Waste heat recovery technologies and applications. *Therm. Sci. Eng. Prog.* **2018**, *6*, 268–289. [CrossRef]
7. Asl, S.G.; Gilandeh-Abbaspour, Y. Theoretical and practical analysis of waste heat recovery system in off-season rainbow trout production. *Aquac. Eng.* **2019**, *85*, 65–73. [CrossRef]

8. Liang, Y.; Bian, X.; Qian, W.; Pan, M.; Ban, Z.; Yu, Z. Theoretical analysis of a regenerative supercritical carbon dioxide Brayton cycle/organic Rankine cycle dual loop for waste heat recovery of a diesel/natural gas dual-fuel engine. *Energy Convers. Manag.* **2019**, *197*, 111845. [CrossRef]
9. Gao, H.; Liu, Y.; Song, X.; Zheng, B.; Sun, P.; Lu, M.; Ma, Y.; Gao, Z. Numerical study of heat transfer characteristics of semi-coke and steam in waste heat recovery steam generator for hydrogen production. *Int. J. Hydrogen Energy* **2019**, *44*, 25160–25168. [CrossRef]
10. Jayanthi, N.; Suresh Kumar, R.; Karunakaran, G.; Venkatesh, M. Experimental investigation on the thermal performance of heat pipe solar collector (HPSC). *Mater. Today Proc.* **2020**, *26*, 3569–3575. [CrossRef]
11. Abd-Elhady, M.S.; Nasreldin, M.A.; El-Sheikh, M.N. Improving the performance of evacuated tube heat pipe collectors using oil and foamed metals. *Ain Shams Eng. J.* **2018**, *9*, 2683–2689. [CrossRef]
12. Brahim, T.; Dhaou, M.H.; Jemni, A. Theoretical and experimental investigation of plate screen mesh heat pipe solar collector. *Energy Convers. Manag.* **2014**, *87*, 428–438. [CrossRef]
13. Dehaj, M.S.; Mohiabadi, M.Z. Experimental investigation of heat pipe solar collector using MgO nanofluids. *Sol. Energy Mater. Sol. Cells* **2019**, *191*, 91–99. [CrossRef]
14. Yang, L.; Ling, X.; Peng, H.; Duan, L.; Chen, X. Starting characteristics of a novel high temperature flat heat pipe receiver in solar power tower plant based of "Flat-front" Startup model. *Energy* **2019**, *183*, 936–945. [CrossRef]
15. Burlacu, A.; Lăzărescu, C.D.; Ciocan, V.; Verdes, M.; Balan, M.C.; Serbanoiu, A.A. CFD Heat transfer analysis for heat pipes integration into buildings with glazed facades. *Procedia Eng.* **2017**, *181*, 658–665. [CrossRef]
16. Mahajan, G.; Thompson, S.M.; Cho, H. Energy and cost savings potential of oscillating heat pipes for waste heat recovery ventilation. *Energy Rep.* **2017**, *3*, 46–53. [CrossRef]
17. Jouhara, H.; Anastasov, V.; Khamis, I. Potential of heat pipe technology in nuclear seawater desalination. *Desalination* **2019**, *249*, 1055–1061. [CrossRef]
18. Tian, E.; He, Y.L.; Tao, W.Q. Research on a new type waste heat recovery gravity heat pipe exchanger. *Appl. Energy* **2017**, *188*, 586–594. [CrossRef]
19. Xiaoxing, H.; Yaxiong, W. Experimental investigation of the thermal performance of a novel concentric tube heat pipe heat exchanger. *Int. J. Heat Mass Transf.* **2018**, *127*, 1338–1342.
20. Vizitiu, R.S.; Sosoi, G.; Burlacu, A.; Turcanu, F.E. CFD Analysis of a Dual Heat Recovery System. *E3S Web Conf.* **2019**, *85*, 02007. [CrossRef]
21. Vizitiu, R.S.; Burlacu, A.; Isopescu, D.N.; Verdes, M.; Sosoi, G.; Lazarescu, C.D. CFD analysis of an innovative heat recovery system. *Procedia Manuf.* **2019**, *32*, 488–495. [CrossRef]
22. Delpech, B.; Milani, M.; Montorsi, L.; Boscardin, D.; Chauhan, A.; Almahmoud, S.; Axcell, B.; Jouhara, H. Energy efficiency enhancement and waste heat recovery in industrial processes by means of the heat pipe technology: Case of the ceramic industry. *Energy* **2018**, *158*, 656–665. [CrossRef]
23. Delpech, B.; Axcell, B.; Jouhara, H. Experimental investigation of a radiative heat pipe for waste heat recovery in a ceramics kiln. *Energy* **2019**, *170*, 636–651. [CrossRef]
24. Jouhara, H.; Almahmoud, S.; Chauhan, A.; Delpech, B.; Bianchi, G.; Tassou, S.A.; Llera, R.; Lago, F.; Arribas, J.J. Experimental and theoretical investigation of a flat heat pipe heat exchanger for waste heat recovery in the steel industry. *Energy* **2017**, *141*, 1928–1939. [CrossRef]

JOURNAL OF APPLIED ENGINEERING SCIENCES
ISSN: 2247-3769 / e-ISSN: 2284-7197

sciendo

VOL. 9(22), ISSUE 1/2019
ART.NO. 249 pp. 25-28

INDOOR CLIMATE SIMULATION IN A CHURCH DURING WINTER SEASON

ANCAS Ana Diana [a, *], TURCANU Florin-Emilian [a], PROFIRE Mihai [a], VERDES Marina[a], BALAN Marius Costel [a]

[a] Technical University "Ghe. Asachi" of Iasi, Faculty of Civil Engineering and Building Servicies, Department Building Sevicies, D. Mangeron 67 str., 700050, Romania, e-mail: ancas05@yahoo.com

Received: 21.02.2019 / Accepted: 23.03.2019/ Revised: 25.04.2019 / Available online: 31.05.2019

DOI: 10.2478/jaes-2019-0003

KEY WORDS: hydronic heating systems, indoor climate modelling, thermal comfort.

ABSTRACT:

In the paper is presented a heating system installed in church and the interior climate generated. Thermal Comfort is the purpose of each designer, since the design stage and has to be ensure for the churchgoers, but even for the interior finishes. The heating system that uses hydronic radiators is evaluated trough the CFD modelling, in order to evaluate pro and contra arguments. The simulation has been made in a 3d simulation software environment, in Autodesk CFD with good results.

1. INTRODUCTION

The indoor microclimate that's has been analysed is found in the church of Saint Cross Rising, in the village of Săbăoani, country of Neamț (Figure 1a). The church has been built in the years of 2000, on a mixt structure of masonry and columns and girders of reinforced concrete. At the top the church has a dome made from reinforced concrete. The heating system is formed by a hydronic radiator systems and a boiler with the power of 40 kW, that burn wood. The heating systems is mounted on the exterior walls under the windows (Figure 1b).

Church is formed by a single shape nave, with the opening of 13,5 meters and a total height of 14 meters. Also the total length is of 23 meters, this numbers gives a total heating volume for the church of 3000 m^3 (Figure 2 a, b).

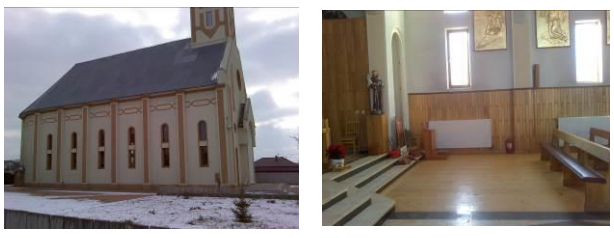

a b

Figure 1. a) Exterior view of the studied church b) Existing heating system inside the church

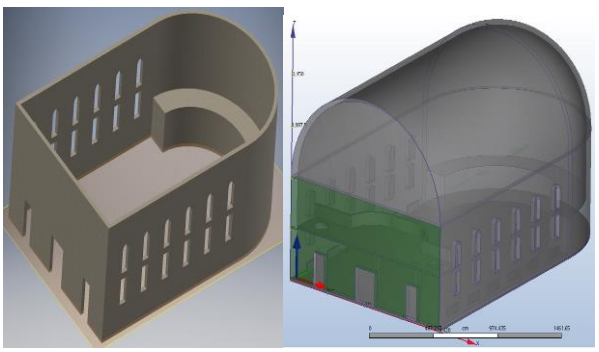

a b

Figure 2. a) ,b) View of the church from the modelling process

Exterior walls have the weight of 0.4 meters, covered with a layer of 0.05 meters of polystyrene insulation and the exterior windows are made from insulated glass with woodwork made from PVC.

To create an indoor climate, distinct from the outside one, is the main purpose for almost all buildings and in our case for worship buildings. Also the climate created in the churches provides the thermal comfort for the churchgoers. By controlling the parameters that generate the indoor climate leads to an appropriate and sustainable use of the energy resources with a high cost-efficiency management. (Schellen and Lambertus, 2002, Sen, 2008).

In the current practice of heating systems that lead to the creation of the indoor climate in churches, the technical solution are

* Corresponding author: ANCAS Ana Diana, e-mail: ancas05@yahoo.com

always a reference, meanwhile the real difficulties are choosing the criteria that form a suitable climate. That is why the literature refers to the following parameters when it comes to the indoor thermal climate of the places of worship: 1. Air temperature; 2. Surface Temperature; 3. Relative humidity; 4. Displacement of Air Currents (Sen, 2008, Vuerich, 2008).

In order to understand how we can control the indoor microclimate in the places of worship, there is a need for a physical and also quantitative understanding of the complex interaction that exists between the above mentioned parameters (Varas Muriel et al., 2014).

2. MODELLING INDOOR MICROCLIMATE

CFD modelling based on FVM (Finite Volume Methods) has opened the way for solving moment, mass and energy equations. Also, the k-e turbulence model and a standard model to define the wall flow, created the premises for dynamics simulations with a high degree of trust for thermal modelling of the interior climate, air movements etc (Martinez Garrido et al., 2016).

This paper analyses the hydronic heating of the air volume inside the church. The modelling allowed to identify the airflows patterns that are generated and theirs effect on the interior finishes as well as the thermal comfort of the churchgoers. The interior temperature that the heating system generate inside the interior volume has been evaluate as well (Liu J.et al., 2012 Napp, 2015).

The church has been evaluated in a 3d environment in Autodesk Inventor, as faithfully as possible based on the construction plans. From Autodesk CFD the building has been exported in Autodesk CFD 2018 for further analysis (Figure 3.a, 3.b). In this stage has been define the materials for all the surfaces that form the indoor heating volume. For all the surface have been imposed the limit condition. The exterior walls have a thermal resistance of R = 1.8 W/m^{2}K and the outside temperature is taken for measurements made outside during winter that has a maximum of T= - 18^{0}C (Figure 3.c). Also the discretization have been made at a step of 0.5 meters resulting 4 million of elements (Figure 3.d).

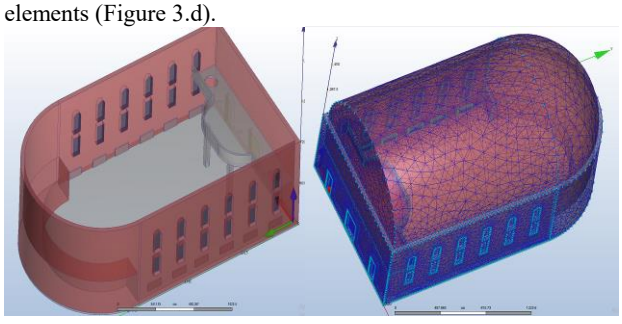

a b

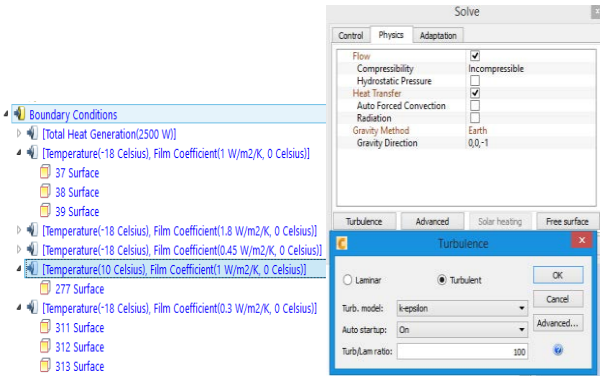

c d

Figure 3. a) Defining the materials for the surface that form the interior volume b) Discretization of the interior volume c) Imposing the boundary conditions d) Defining the turbulence model along others parameters for running the analysis

For numerical simulation of the indoor climate as well as for all simulations it is important to reduce numerical errors. Therefore, for volume simulations, meshing refinements were made by minimizing the size of the elements to achieve constant meshing (Baratasz et al., 2007, Torres and Freitas, 2007).

The transfer equations between the wall and the volume of air is solved by the k-e model equation at the wall, being the scalar equation type (Camuffo et.al. 2014, Camuffo et al. 2010).

3. CONCLUSIONS

Hydronic heating system works on the basis of natural convection in large proportion (90%). The air enters the bottom, is heated due to the buoyancy phenomenon and it comes out at the top (Figure 4a, b).

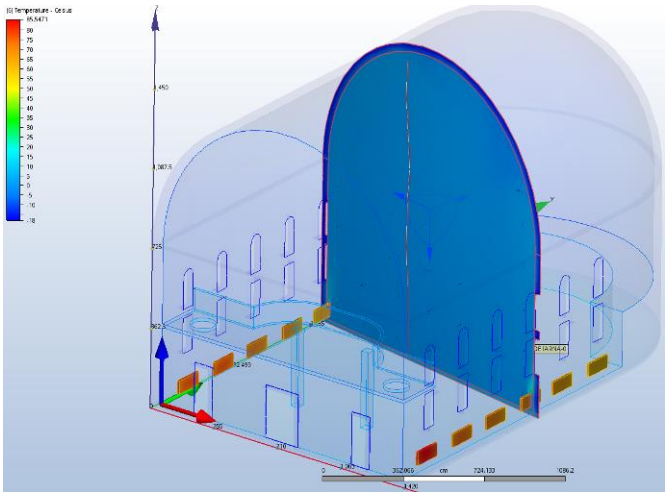

a

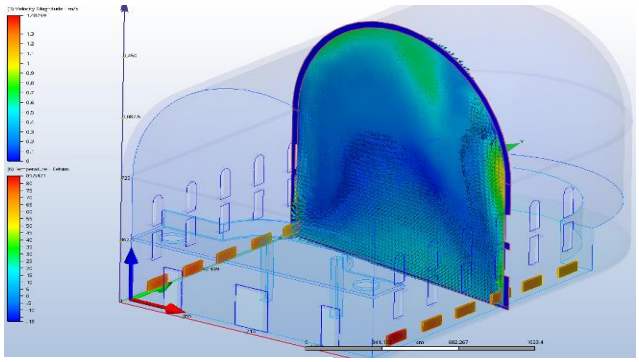

b.

Figure 4. a) Temperature in a transversal section plane b) Air velocity and temperature along a transversal plane

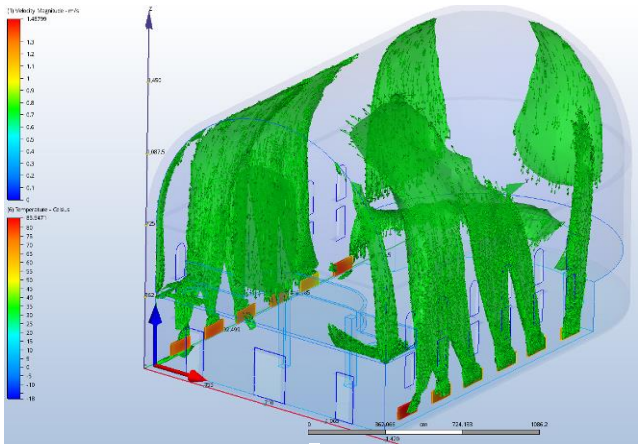

a

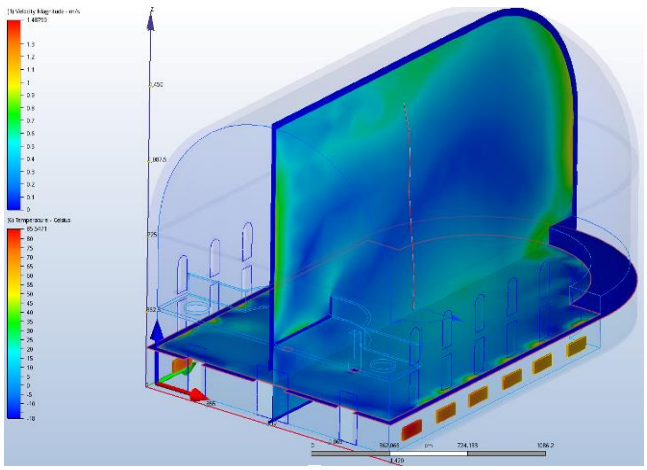

b

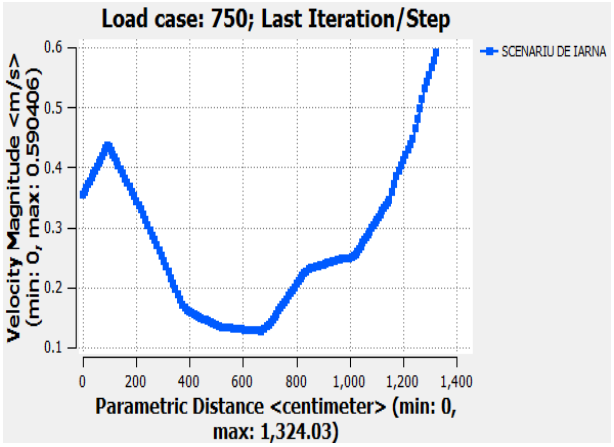

c

From the point of view of the internal thermal comfort, the system is efficient when is used without interruption (Figure 5 a, b, c), but also when the number of radiators is enough and the temperature of the heated volume is homogeneous, especially for small volumes of air.

From visual point of view the hydronic heating system brings discomfort both through the heating bodies and the pipes that are connected to each other and with the boiler.

References

Bratasz L., Kozlowski, R., Camuffo D., Pagan E., 2007: *Impact of indoor heating on painted wood: Monitoring the altarpiece in the church of Santa Maria Magdalena in Rocca Pietore*, Italy. Stud. Conserv., 52, pp.199–210.

Camuffo, D., Pagan, E., Schellen, H. & Limpens-Neilen, D., 2014. *A practical guide to the pros and cons of the various heating systems with a view to the conservation of the Cultural Heritage in Churches*. Results of the European Project Friendly Heating EVK4-CT-2001-00067, s.l.: s.n.

Camuffo, D., Pagan, E., Rissanen S, Bratasz L.,2010, *An advancedchurch heating system favourable to artworks,* Journal of Cultural Heritage 11 (2), pp.2015-219.

Jung-Yoon K., Chao-Hsien C., Sang-Moon S., 2014, *ISSAQ an integrated sensing systems for real-time indoor air quality monitoring,* IEEE Sensors Journal, 14(12), pp.4230-4244.

Liu, J., Yao, R. & McCloy, R., 2012. *A method to weight three categories of adaptive thermal comfort*. Energy and Buildings, 47, pp. 312–320.

Martinez Garrido, M. I., Fort, R. & Varas Muriel, M. J., 2016. *Sensor-based monitoring of heating system effectiveness and efficiency in Spanish churches*. Indoor and Built Environment, 21(1), pp. 156-165.

Napp M.,Kalamees T., 2015, *Energy use and indoor climate of conservation heating, dehumidification and adaptive ventilation for the climate control of mediaeval church in a cold climate,* Energy and Buildings, 108, pp.61-71.

Schellen, H.; Lambertus H. 2002: *Heating Monumental Churches - Indoor Climate and Preservation of Cultural Heritage*. Eindhoven (NL): Technische Universiteit Eindhoven.

Șen, Z., 2008. *Solar energy fundamentals and modelling techniques: atmosphere, environment, climate change and renewable energy*. London: Springer-Verlag Limited.

Silva H., Henriques F., 2014, *Microclimatic analysis of istoric Buildings – a new methodology for temperate climates,* Building and Environment, 82, pp.381-387.

Torres M.I., Freitas V.P, 2007. *Treatment of rising damp in historical buildings: wall base ventilation*. Build. Environ. 42(1), pp.424–435.

Varas Muriel, M., Martinez Garrido, M. & Fort, R., 2014. *Monitoring the thermal–hygrometric conditions induced by traditional heating systems in a historic Spanish church (12th–16th C)*. Energy and Buildings, 75(3), pp. 119-132.

Vuerich E., Malaspina F., Barazutti M., Georgiadis M., 2008, *Indoor measurements of microclimate variables and ozone in the church of San Vicenzo, Italy,* Microchemical Journal, 88 (2), pp.218-223.

Available online at www.sciencedirect.com

ScienceDirect

Procedia Technology 12 (2014) 591 – 597

Procedia Technology

The 7th International Conference Interdisciplinarity in Engineering (INTER-ENG 2013)

Technical-economic analysis of ensuring the heat independence for residential building in Romania

Marius-Costel Balan[a,]*, Marina Verdes[a], Ion Serbanoiu[a], Vasilica Ciocan[a], Gabriel Teodoriu[a]

[a]"Gheorghe Asachi" Technical University of Iasi- Romania, Faculty of Civil Engineering and Building Services, 43, D.Mangeron, IASI-700050, ROMANIA

Abstract

This paper presents a comparative study between two systems for production of thermal energy for heating and hot water for a residential building. The first system using non-conventional energy sources (proposed and analyzed) and the second system using current sources of energy. To accurately assess the performance of a hybrid system providing heat and hot water requires some assumptions about the consumption of heat and domestic hot water, taking into account the climate zones of the target location, intensity of solar radiation for these areas and energy price.

Keywords: non-conventional energy; system; biomass; indicators; simulation

1. Introduction

Renewable energy sources offer the potential of unlimited, which exploited through performance equipment, paves the way to the future of the energy sector.

* Corresponding author. Tel.: +40766588168; fax: +4 0232233368.
*E-mail address:*balanmariuscostel@gmail.com

doi:10.1016/j.protcy.2013.12.534

It is becoming increasingly predictable that future development of the energy sector will consider the production of renewable energy, partial energy from gas utility vessels and less more energy from conventional reserves of oil and coal.

Thermal conversion of solar energy is the oldest and widespread technology of solar energy. Over many centuries, engineers and architects have perfected buildings projects to use as rationally natural source of light and heat - the sun. From this point of view, the closure of buildings inertial elements can be considered - heat accumulator and windows and rooms - solar heat collectors, allowing penetration of solar radiation in the visible band (shortwave) inside and not allow infrared radiation (long wave) to leave the room [1,7].

This technology, and the systems used for this, they later were called passive systems or methods of using solar energy.

Technologies or active systems for conversion the solar energy, are equipped with special solar collectors, through which solar radiation is converted into heat, and then through a fluid (usually water or air) is transported to the site or remains stored in the tank.

Further we present an active system of non-conventional energy consumption.

2. Systems description

The reference system taken into account is a gas central heater. This equipment is very used in Romanian individual heating systems. The gas central heater is composed mainly of a casing fixed to the wall, in which there are: a burner, a combustion chamber, a flue gas outlet, a main heat exchanger, a circulation pump, a three way valve, an expansion tank, valves for filling, emptying and venting, sensors and control electronics [1].

The proposed system is composed of a storage tank with double coil. The role of this tank is to increase system efficiency, reduce costs and to reduce installation space. Fig. 1 shows a schematic diagram of such a system.

The system which includes the dual coil storage tank is fed - as in the case of solar domestic hot water consumption - through a solar circuit, using a simple automation based on temperature difference [3,6,10].

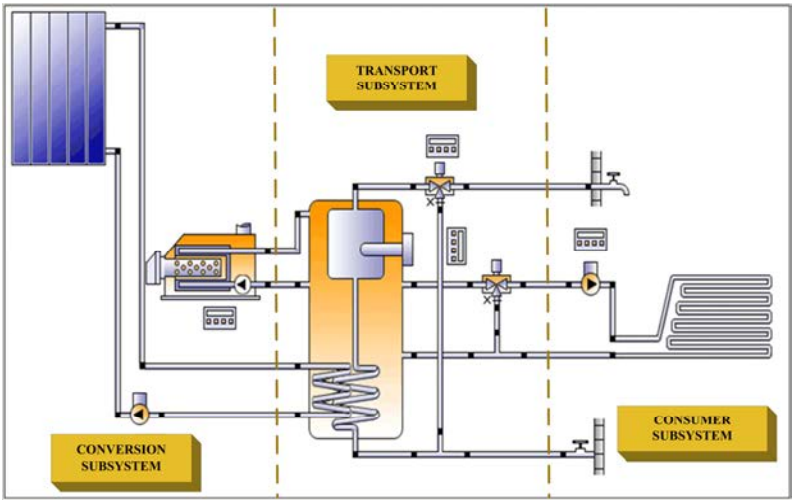

Fig. 1. Hybrid system scheme with biomass central and solar thermal panels (Polysun)

The active system is composed of three subsystems:

- The conversion subsystem includes solar panels for capture the thermal energy and auxiliary non-conventional heat source;
- The transport subsystem includes dual coil tank battery and control elements of the quality parameters of the water that goes to the consumers;
- The consumer subsystem includes heating facilities and hot water consumers.

3. Calculation assumptions

Simulating the operation of technically, economically and financially integrated systems of thermal power generation was achieved using computer program RETScreen [1,4,8,9].

Analysis program for renewable energy projects,RETScreen International, is a modern technology in facilitating analyzes of pre-feasibility and feasibility of clean energy technologies.

The program is made up of integrated and standardized analysis models that can be used worldwide to evaluate the energy production, life-cycle facility costs and reducing emissions of greenhouse gases for various systems using renewable forms of energy. For all models of energy conversion technologies found in this software is used similar structure to facilitate decision making [2].

For this calculation we have considered the following assumptions [1]:

- A single-family house with an average area (proposed) - 100 mp ;
- The family consists of 4 people;
- In the application, the systems were placed successively in the four climatic zones (according to the Romanian standard STAS 1907-91) from Romania:
  1. Zone IV – Miercurea – Ciuc;
  2. Zone III – Iași;
  3. Zone II – Timisoara ;
  4. Zone I – Constanta;
- Hot water necessary, according to the Romanian standard, STAS 1478-90 is:
  1. 60 l/person/day - running time seven days per week for residential buildings;
- Medium necessary of thermal energy is :
  1. 63 W/mp for buildings located in the IV zone;
  2. 58 W/mp for buildings located in the III zone;
  3. 53 W/mp for buildings located in the II zone;
  4. 48 W/mp for buildings located in the I zone.
- The cost of natural gas (in the year 2012 in Romania) is 0.035 euro/ kWh. In the Fig. 2 we see the trend of price increase of natural gas which reinforces the use of system how use non-conventional energy sources.

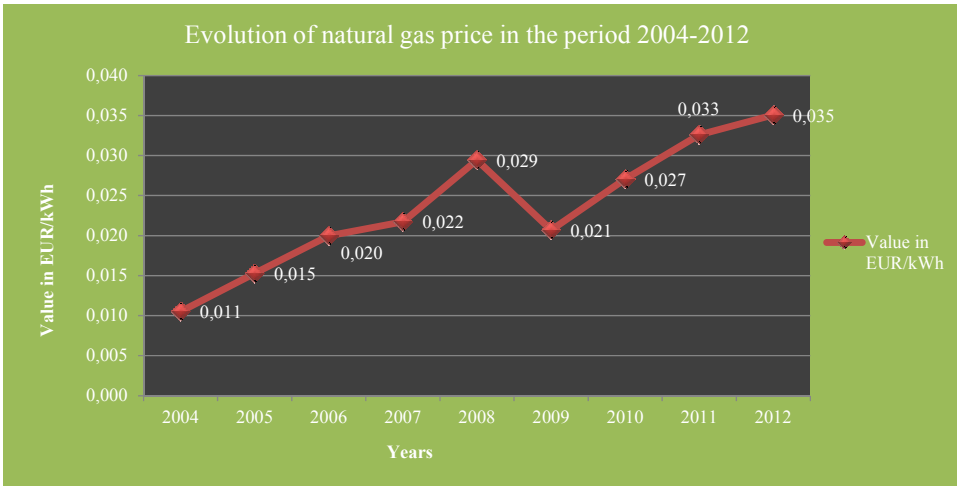

Fig. 2. Evolution of natural gas price in the period 2004-2012

- The price of a tone of wood fuel (pellets) is about 130 euro / tone;
- Inflation rate is about 4%;

- Central heating biomass (pellets) was used with an efficiency of 98% and the heat capacity differs from one climate zone to another ;
- The average price of the system considered :
  1. Central heating biomass system with and thermal solar collectors is 400 euro / kW ;
- For the system maintenance was take into account the value of 25 euro / year ;
- For the reference case the efficiency of the central gas heating was 80%

4. Simulation results

Simulation of technical-economic and financial performance of systems that use non-conventional energy sources was achieved through the performance indicators [1,4,9]:

- Thermal energy necessary-T_{EN}, Fig. 3a, calculated as working hypotheses and resulting different values for the four climate zones

- Annual fuel consumption for references system-A_{FCR}, Fig. 3b, the figure shows the annual fuel consumption (natural gas) by gas central heater in the four climate zones.

- Annual fuel consumption for proposed system- A_{FCP}, Fig. 4a, the figure shows the annual fuel (biomass) consumption by central biomass heater in the four climate zones.

- Fuel price consumption for references an proposed system- F_{PCR}/ F_{PCP}, Fig. 4b, the figure shows that the proposed case consuming less more energy than the references case and this is because the price for natural gas is increasing every year and the efficiency of proposed case is higher than the references system.

- System price- S_P, Fig. 5a, the figure shows the financial cost of the investment for the proposed system in the considered zones.

- Reduction of greenhouse gases emissions- R_{GHG}, Fig. 5b, if we used the proposed system instead of references system, we make a considerable reduction o GHG emission and values depends on which zone is placed the proposed system.

- Internal rate of return- IRR, Fig. 6a, it is an indicator of the efficiency for the investment, and the figure shows that the system have more than 5% the limit for a new investment in Romania.

- Payback period-P_P, Fig. 6b, the figure shows the period in which the investment is recovered and has different values for considered zones.

- Net present value-NPV, Fig. 7a, the indicator has positive values for all four zones and for that the investment can be make.

- Cost benefit-CB, Fig. 7b, the indicator has values greater than 1(the limit for project investments) for all four zones and for that the investment can be make.

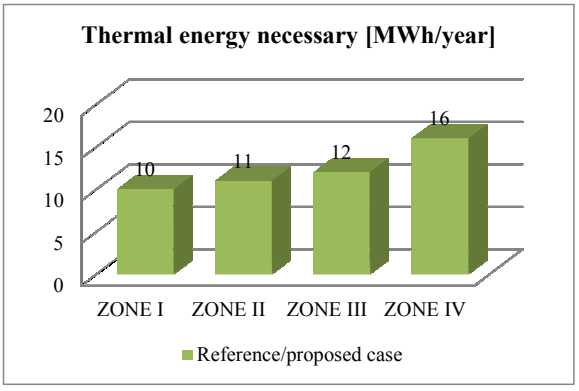

a)

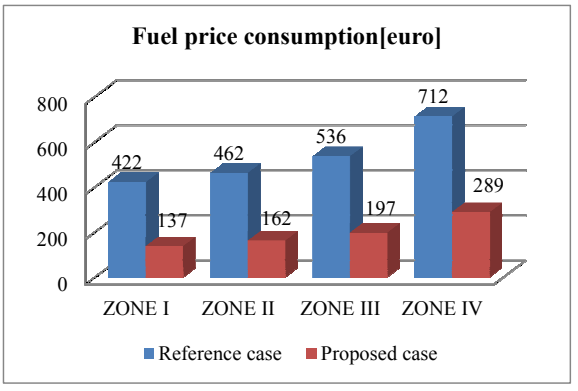

b)

Fig. 3.(a) Thermal energy necessary, (b)Annual fuel consumption reference case

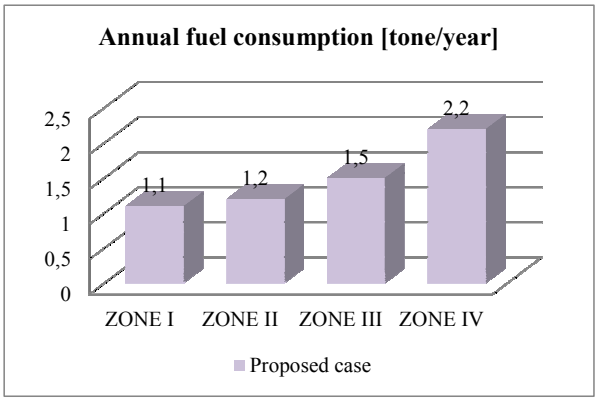

a)

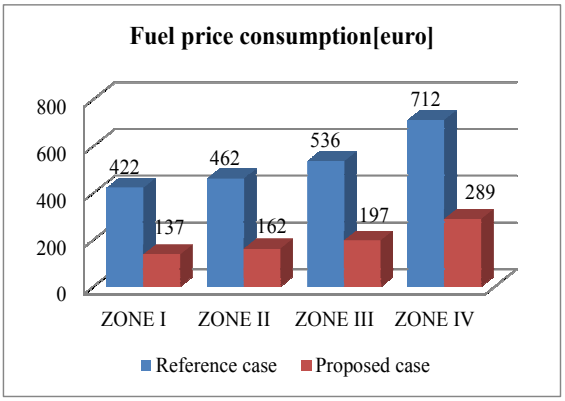

b)

Fig.4.(a) Annual fuel consumption proposed case, (b) Fuel price consumption

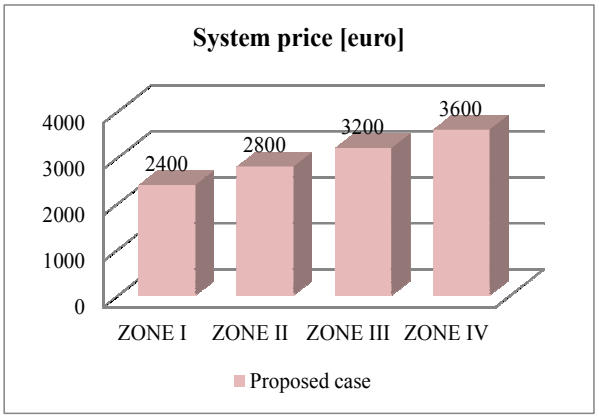

a)

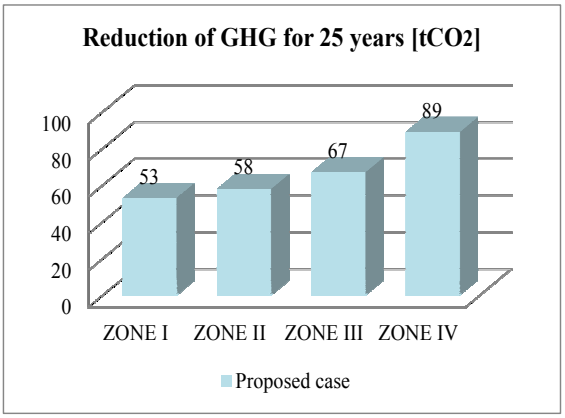

b)

Fig. 5.(a) Proposed system price, (b) Reduction of greenhouse gas emission for 25 years

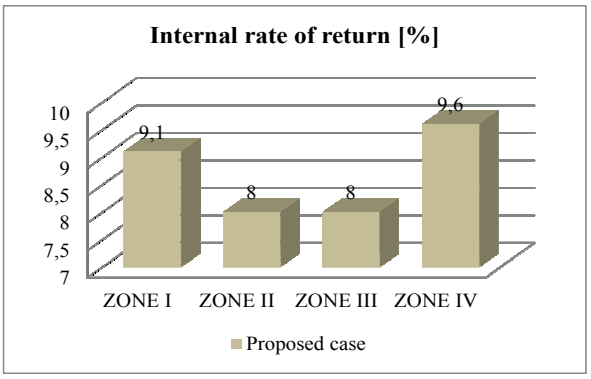

a)

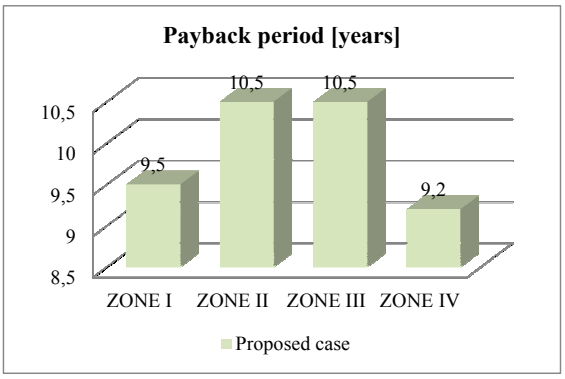

b)

Fig. 6.(a) Internal rate of return, (b) Payback period

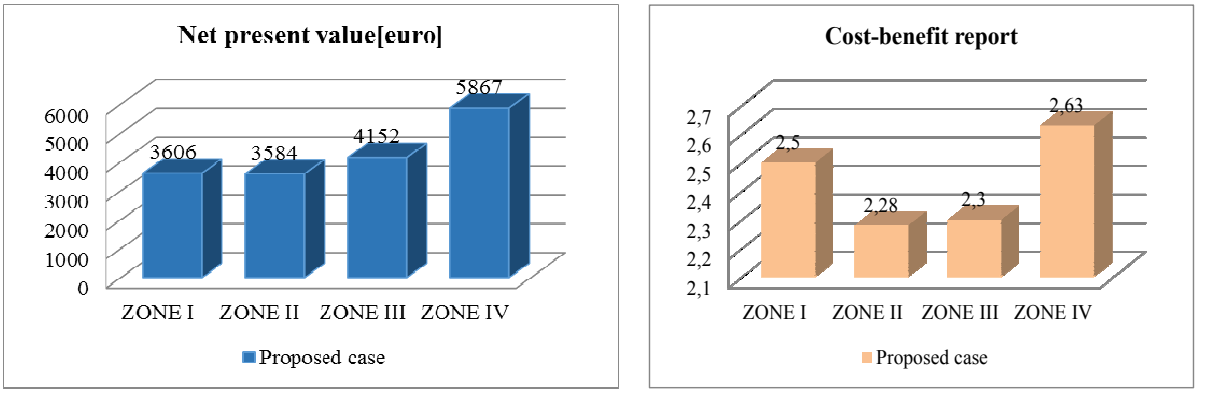

Fig. 7.(a) Net present value, (b) Cost-benefit report

Starting from the four climate zones of Romania we make a map (Fig. 8.) where we transpose the indicators of the proposed system disposed in each zone.

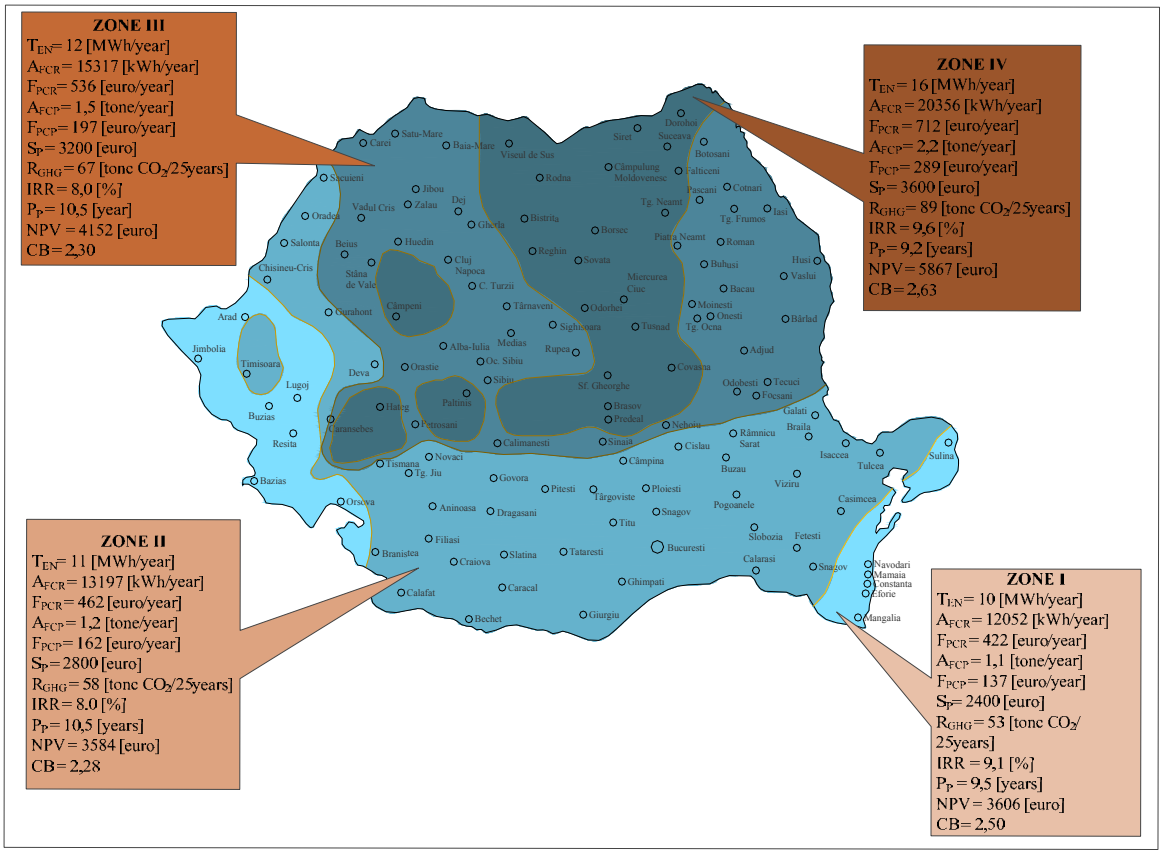

Fig. 8. Map of Romania with technical, economical and financial indicators for the proposed system

5. Conclusion

Valorization of renewable energy forms is one of the goals in the medium and long term energy strategy adopted in the European Union and in our country.

Starting from this reality, the transition to energy systems based on renewable sources is increasingly necessary, given the fact that, over time, their costs decrease and fuel classics costs continues to grow. In the last 30 years solar energy equipment's sales increased because the cost of capital and the production of electricity decreased, while improving their performance.

By implementing biomass central with thermal solar panels would get the following:

- annual fuel consumption of the proposed system is diminished compared to the reference system and also the purchase fuel price of the proposed case will be lower than the reference case;
- this system contributes a significant share to reduce greenhouse gas emissions;
- amortization period is variable, with values ranging from 11-15 years, depending on climate zone.

References

[1] Balan, MC, Şerbanoiu I. Management of the systems to ensure energetical independence of an locality, Phd Thesys, (2012).
[2] Balan, MC, Verdeş M, Ciocan V. Comparative study on the use of unconventional resources for production of heat and hot water, Buletinul Institutului Politehnic din Iaşi, Secţia Construcţii. Arhitectură. Tomul LVII(LXII) Fasc. 1, 2012.
[3] Carrilho G, Augusto AM, Lerer M. Solar powered net zero energy houses for southern Europe: Feasibility study, 2011; 86: 634–646.
[4] Ragwitz M, Resch, G, Hoogwijk, M. Economic analysis of reaching a 20% share of renewable energy sources in 2020, European Commission DG Environment ENV.C.2/SER/2005/0080r.
[5] Al-Ali AR, El-Hag A, Bahadiri M, Harbaji M, Ali El Haj Y. Smart Home Renewable Energy Management System, Energy Procedia, 2011, 12: 120 – 126.
[6] Blaga CA, Panea C, Gligor E. Monoagent heating system for solitary consumers, using heat from biomass burning, Journal of sustainable energy, 2011; II(2): 36 – 42.
[7] Carrilho G, Augusto A, Lerer M. Solar powered net zero energy houses for southern Europe: Feasibility study, Solar Energy, 2011; 86: 634–646.
[8] Garfia, M, Laia FM, Velob E, Ferrera I. Evaluating benefits of low-cost household digesters for rural Andean communities, Renewable and Sustainable Energy Reviews, 2012; 16: 575– 581.
[9] Li HS, Ma WB, Wang XL, Lian YW. Estimating monthly average daily diffuse solar radiation with multiple predictors: A case study, Renewable Energy, 2011; 36: 1944 – 1948.
[10] Veeraboina P, Ratnam GY. Analysis of the opportunities and challenges of solar water heating system (SWHS) in India: Estimates from the energy audit surveys & review, Renewable and Sustainable Energy Reviews, 2012; 16: 668– 676.

Studiu comparativ privind asigurarea energiei electrice din surse neconvețională de energie pentru o clădire rezidențială*

Comparative study for ensuring electrical energy from unconventional sources for a residential building

Marius-Costel Balan[1], Marina Verdeş[1], Vasilică Ciocan[1], Alexandru Verdeş[1]

[1]Universitatea Tehnică "Gheorghe Asachi" din Iaşi, Facultatea de Construcţii şi Instalaţii
Bd. Prof.dr.doc. Dimitrie Mangeron, nr. 1, mun. Iaşi, cod 700050, Romania
E-mail: balanmariuscostel@gmail.com, verdesmarina2003@yahoo.com, vciocan2005@yahoo.com, alexandruverdes@ymail.com

Rezumat. ***Prezenta lucrare ilustrează un studiu comparativ între două sisteme de producere a energiei electrice: clasic şi neconvențional. Studiul se concentrează asupra analizei tehnico – economice pentru cele două sisteme analizate şi care au rolul de a asigura energia electrica pentru o locuință unifamilială.***
Necesitatea acestui studiu se impune, în contextul în care, utilizarea surselor neconvenționale de energie prin tehnologiile actuale se realizează – este adevărat - într-un ritm foarte alert dar, cu investiții inițiale foarte mari.

Cuvinte cheie: energie electrică, sistem, energie neconvențională, energie fotovoltaică, analiză.

Abstract. ***This paper illustrates a comparative study between two power generation systems: classical and unconventional. The study focuses on technical - economic analysis of the two systems which are designed to provide electricity for a single-family residence.***
The need for this study is required, given that the use of unconventional energy sources by current technologies is achieved - it is true - in a very alert rhythm but with very large initial investment.

Key words: electricity, system, unconventional energy, photovoltaic, analysis.

1. Introducere

Dezvoltarea societății umane la nivel global a cunoscut o creştere continuuă dar, odată cu aceasta, a crescut consumul de energie sub diferite forme.

---

* Lucrare inclusă în programul conferinței "Romanian Conference on Energy Performance of Buildings (RCEPB 2013)"

Sursele de regenerabile de energie precum biomasa, energia solara, energia hidro si geotermala pot asigura necesitățile energetice bazate pe utilizarea resurselor locale disponibile. Pornind de la aceasta realitate, tranziția catre sisteme energetice bazate pe surse regenerabile este, tot mai sigură, ținând cont de faptul că şi costurile acestora se diminuează, în timp ce, prețul țițeiului şi gazelor naturale continua să fluctueze. In ultimii 30 de ani vanzarile de echipamente care valorifică energia solară şi eoliană au crescut deoarece, atât cheltuielile de capital cât si cele pentru producerea electricitatii au scazut, simultan cu îmbunatatirea performantelor.

2. Surse neconvenționale de energie

Informații oficiale asupra potențialului "regenerabil" al României arata că ierarhia teoretică este dominata de biomasa 65%, potențialul eolian exploatabil ocupând locul 2 cu 17% din întreg, în timp ce, energia solară prezinta o pondere de 12%.

Conversia energie solare în energie electrică cu ajutorul panourilor fotovoltaice este în continua creştere, ajungând în anul 2012 la o putere instalată de aproximativ 2000 MW, însumând atât centralele electrice fotovoltaice în funcțiune cât şi cele cu aviz tehnic de racordare sau cu contract de racordare, figura 1.

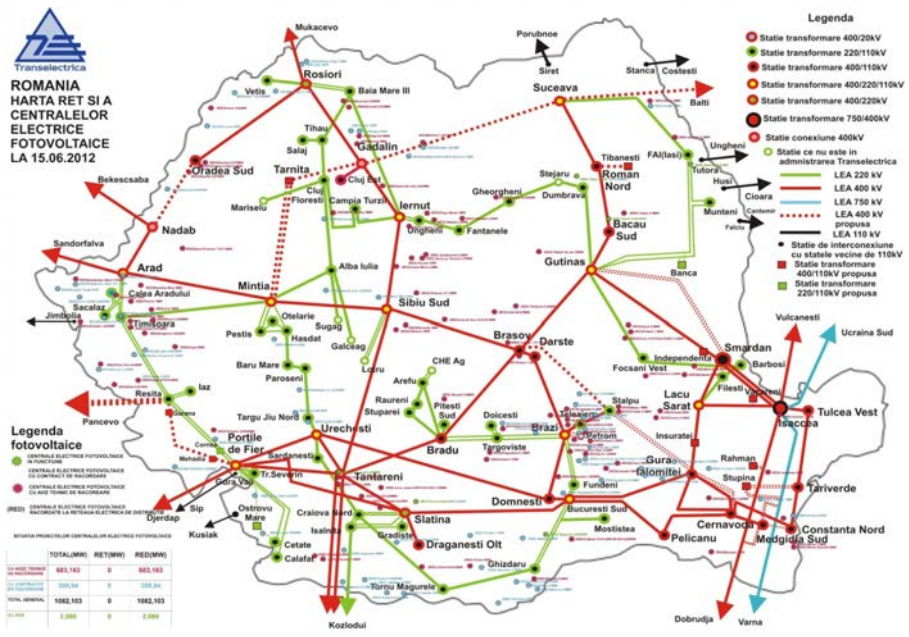

Fig. 1 – Harta centralelor electrice fotovoltaice în 2012
Sursa : Transelectrica

Pe plan internațional capacitățile instalate pentru producerea de energie electrică sunt într-o continuă creştere.

Puterea instalată totală a turbinelor eoliene la nivelul Uniunii Europene este de 84.762 MW la nivelul anului 2010, cu 9755 MW mai mult față de nivelul anului 2009.

Conform Institutului German de Energie Eoliană (DEWI), Germania este prima țară din Uniunea Europeană în ceea ce priveşte implementarea de turbine eoliene cu o putere instalată de 1551 MW în anul 2010 şi o putere totală instalată de 27.215 MW.

Conversia energie solare în energie electrică prin intermediul centralelor fotovoltaice cunoaşte o creştere semnificativă a puterii instalate, de la 5739 MWp în anul 2009 la 13.392 MWp în anul 2010.

Producerea energiei electrice din energie solară este concentrată în mare măsură la nivelul câtorva țări (Germania, Spania, Italia) demonstrat prin faptul că puterile instalate în acestea acoperă 88,9 % din puterea generată.

3. Sistem propus de producere a energiei electrice cu panouri fotovoltaice

Sistemele conectate la rețea, figura 2, alimentează cu energie consumatorul casnic iar surplusul este livrat în rețeaua publică, prin intermediul unor invertoare. Aceste sisteme pot fi de dimensiuni mici, aşa numitele sisteme distribuite, de regulă, montate pe acoperişuri, cu puteri de ieşire de câțiva kW sau, pot fi sisteme de dimensiuni mari, cu puteri de ieşire de ordinul MW. Sistemele distribuite folosesc pentru montarea panourilor fotovoltaice, structuri deja existente, precum acoperişurile sau fațadele sau, se fixează pe suporturi de sine stătătoare, montate în exterior.

Avantajul acestor sisteme este acela că, nu este necesară stocarea energiei care, poate fi folosită oriunde şi, drept urmare, se reduce încărcarea rețelei convenționale.

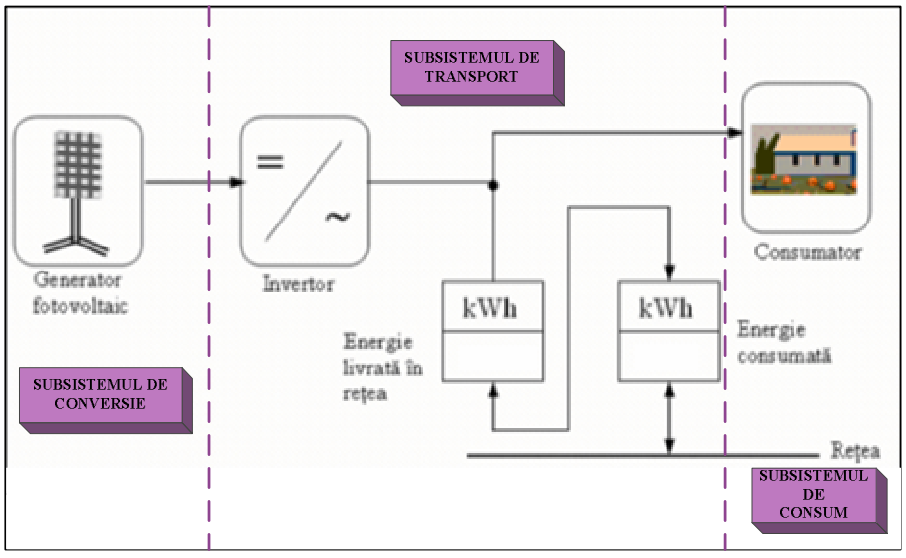

Fig. 2 – Sistem cu panouri solare fotovoltaice pentru producerea energiei electrice

În zilele însorite, acestea furnizează energie electrică consumatorilor casmici, iar excesul de energie este livrat în rețea şi contorizat. Dacă vremea este nefavorabilă, consumatorii sunt alimentați din rețeaua convențională.

4. Analiza tehnico-economică a sistemului de producere a energiei electrice din surse neconvenționale

Analiza funcționării din punct de vedere tehnic, economic şi financiar a sistemului integrat de producere a energiei electrice s-a realizat cu ajutorul programului de calcul RETScreen.

Pentru efectuarea acestui calcul s-au formulat următoarele ipoteze :

- Sistemul cu panouri fotovoltaice se va amplasa în cele cinci zone ale intensității radiație solare (Suceava – zona V, Timişoara – zona IV, Iaşi – zona III, Constanța – zona II, Galați – zona I);
- Necesarul mediu de energie electrică este de 1 MWh/an pentru clădiri de locuit ;
- Costul energiei electrice la nivelul anului 2012 este de 0.131 euro/kWh.

În figura 1.3 este prezentat evoluția prețului energiei electrice începând cu anul 2002:

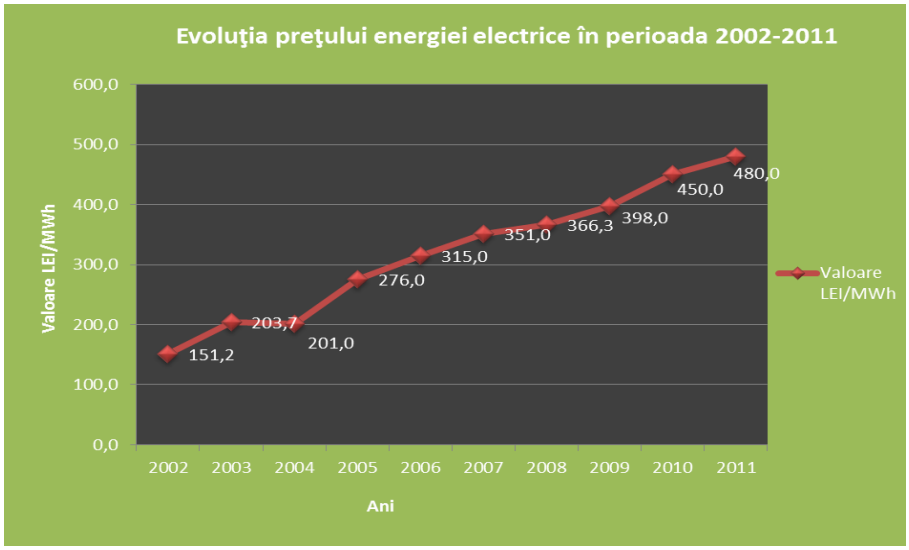

Fig. 4 – Evoluția prețului energiei electrice în perioada 2002-2011

- Pentru o locuință unifamilială s-a utilizat un sistem fotovoltaic cu puterea electrică 1,5 kWp având un preț estimativ de 2600 de euro/kWp ;
- Panourile fotovoltaice utilizate sunt alcătuite din celule monocristaline cu un randament de 18 %.
- Sistemul de referință este considerat ca fiind rețeaua de distribuție a energiei electrice.

Analiza tehnico-economica a sistemului de producere a energiei electrice din surse neconvenționale s-a efectuat prin prisma următorilor indicatorilor de performanța:

- economii anuale – Ea;
- reducerea emisiilor de gazer cu efect de seră - RGES;
- rata internă de rentabilitate – RIR;
- perioada de amortizare - PA;

- valoarea actualizată netă – VAN;
- raportul cost beneficiu - RCB.

Rezultatele analizei sunt prezentate în următoarele diagrame :

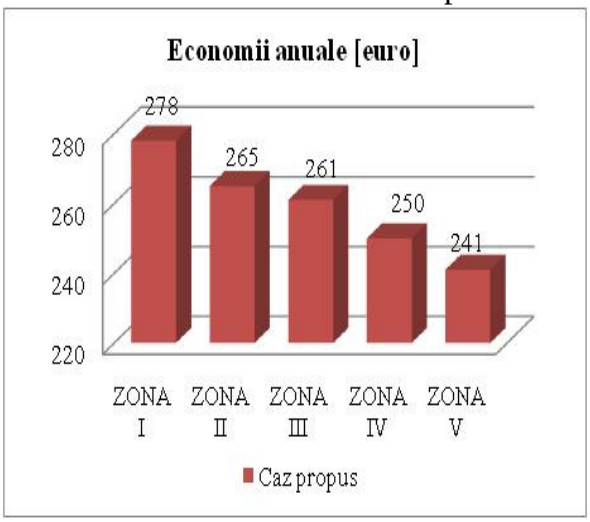

Fig. 5 – Economii anuale generate de sistemul propus

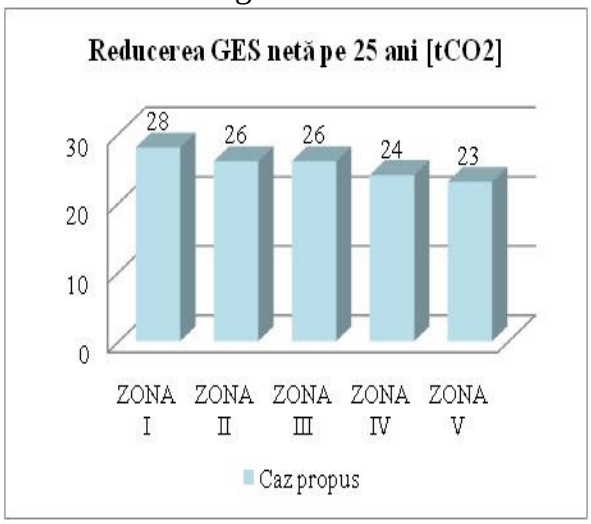

Fig. 6 – Reducerea gazelor cu efect de seră

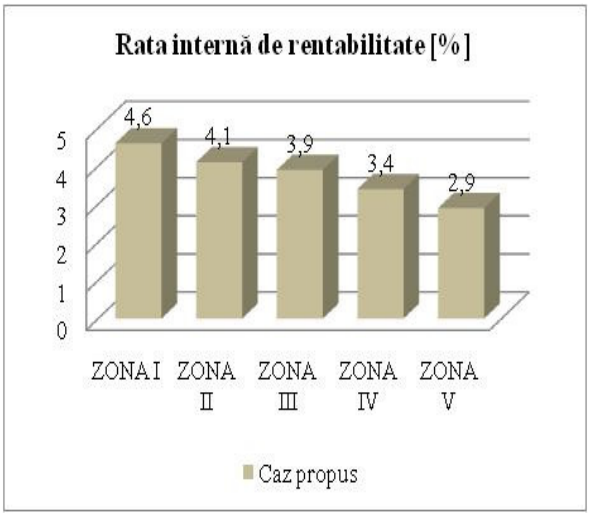

Fig. 7 – Rata internă de rentabilitate

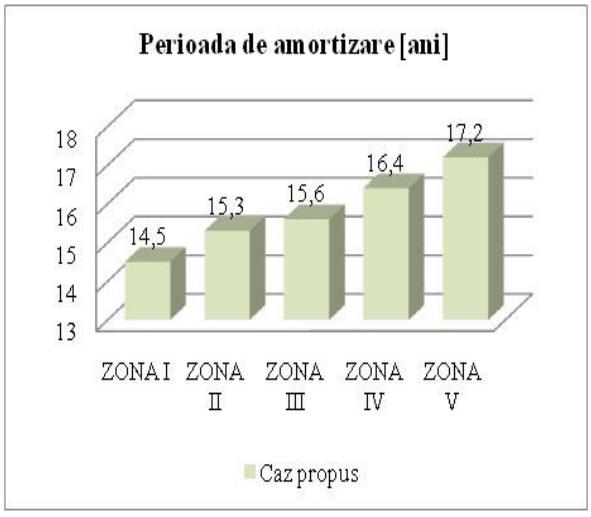

Fig. 8 – Perioada de amortizare a sistemului propus

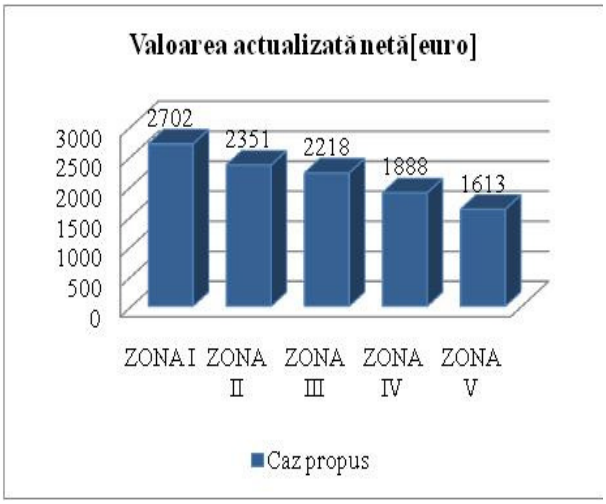

Fig. 9 – Valoarea actualizată netă

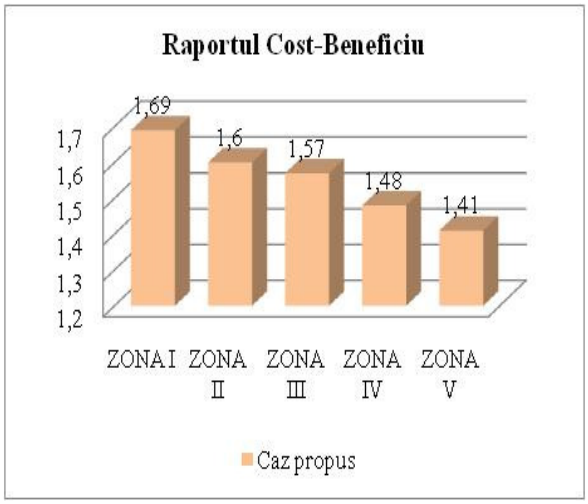

Fig. 10 – Raportul cost – beneficiu

6. Concluzii

În consens cu dezvoltatrea durabilă, sursele regenerabile de energie reprezintă alternativa optimă de rezolvare a problematicii energetice, în ipoteza diminuării sau, chiar a epuizării resurselor clasice.

Utilizarea sistemului de producere a energiei electrice cu panouri fotovoltaice este avantajoasă în toate zonele climatice, deoarece asigură sarcina internă şi livrează în rețea surplusul de energie. De asemenea asigură o reducere a emisiilor de gaze cu efect de seră iar perioadă de amortizare este cuprinsă între 14 – 17.2 ani, perioadă care se situează sub durata de viață considerată.

Analizând sistemul prin prisma valorii actualizate nete, se pate spune că, sistemul fotovoltaic propus se poate implementa în toate zonele, deoarece valoarea acestuia este pozitivă iar, raportul cost-beneficiu are o valoare mai mare ca 1.

Referințe

[1] M.C. Balan**,** „Managementul sistemelor pentru asigurarea independenței energetice a unei localități”, Teză de doctorat, 2012.

[2] Brian Snyder, B., Kaiser, J, M., „Ecological and economic cost-benefit analysis of offshore wind energy”, Renewable Energy, Vol. 34, pp. 1567–1578, 2009.

[3] Campoccia, A., Dusonchet, L., Telaretti, E., Zizzo, G., „Comparative analysis of different supporting measures for the production of electrical energy by solar PV and Wind systems: Four representative European cases”, in Solar Energy, Vol. 83, pp. 287–297, 2009.

[4] Javier, F., Wang, X., Barnett, A., „Energy production of photovoltaic systems: Fixed, tracking, and concentrating”, Renewable and Sustainable Energy Reviews, Vol. 16, pp. 306– 313, 2012.

Bulletin of the *Transilvania* University of Braşov
CIBv 2014 • Vol. 7 (56) Special Issue No. 1 - 2014

IMPROVEMENT OF THE INDOOR CLIMATE CONDITIONS INSIDE ORTHODOX CHURCHES

V. S. HUDISTEANU[1] A. I. BARAN[2] M. BALAN[3]
N. C. CHERECHES[3] T. MATEESCU[3] M. VERDES[3]
V. CIOCAN[3]

Abstract: *In this paper is presented a numerical approach of the improvement of indoor climate conditions inside Orthodox churches. First step was to propose a solution to reduce the risk of condensation for an implemented hot air heating system at Three Holy Hierarchs Monastery in Iasi. The improved case consisted in introducing local ventilation at towers level that activates air circulation in these zones. This configuration was a good one and the numerical results are highlighting this effect. The proposed local ventilation was also studied for two other heating solutions that are largely used in this type of buildings, under floor heating and static heaters. The comparative results showed that the local ventilation is the most appropriate combined with the hot air heating.*

Key words: *place of worship, indoor climate, heating strategies, numerical modeling*

1. Introduction

Churches constitute an inestimable wealth, consisting of sacred and liturgical items as well as the patrimony preserved in museums and historical buildings. They also preserve many kinds of valuable artworks, each of them with a specific vulnerability: paintings on canvas and wooden panels are subject to cracking, swelling, blistering, and soiling; frescoes mostly to efflorescence and blackening; wooden artifacts to cracking; metals to corrosion; textiles to fading and soiling [1]. Therefore, the HVAC system has an important role in order to preserve these values.

The thermal indoor climate is defined by:

- Air temperature
- Surface temperatures
- Relative humidity
- Air movements

In order to control the indoor climate we need a physical and quantitative understanding of the complex interaction in the building between air, the building structure, objects and interiors and people.

The proper indoor climate is determined with respect to:

- **Comfort** is a subjective parameter that

[1] PhD student, eng. "Gheorghe Asachi" Technical University of Iasi
[2] M.Sc. student, eng., "Gheorghe Asachi" Technical University of Iasi
[3] "Gheorghe Asachi" Technical University of Iasi

describes to what extent humans find the indoor climate acceptable. People are very sensitive to temperatures, but not so sensitive to relative humidity. The comfort temperature range depends mainly on clothing, activity and duration of stay in the building; a typical range is 18–22°C. Relative humidity matters for humans only when it is very high, over 80%, or very low, fewer than 30% [2].

• **Conservation** of materials in the building requires an indoor climate that minimizes ageing and degradation of the materials that are to be preserved. This depends on the materials and the type of degradation processes that are prevalent in the building. For materials, relative humidity is often the most important climate parameter [2].

• **Costs** are always a limiting factor and we must consider this from the beginning. A solution that is too expensive is useless [2].

Ulf Christensen from Norway said that after developing some theories he and his team got some experiences with the following types of heating systems and products:

• Direct electrical heating with traditional pipe-heaters under benches, low temperature electrical sheets or cables built in ceilings and floors and panel-heaters at walls or newer types of bench-heaters and mobile radiant heaters

• Gas radiant heating in older and in newer churches

• Water-based heating with some different types of heating centrals and distributions [3].

Also, **Diana Piksriene from Lithuania** presented the peculiarities of heating-ventilation systems installed in 4 Lithuanian churches and their impacts.

The principle of ***blowing out warm air*** with gas heat has been applied for heating-ventilation process at the Cathedral of Sts. Apostles Peter and Paul. A gas boiler-room, ventilation pipes and other equipment for air intake, warming and warm air sending have been installed in the unemployed space of the cathedral's attic. The automatic control of the system allows warming up the Cathedral premises objectively to the temperature desired before the service or other ceremony, and later to keep it to a minimum and to maintain the standard relative air humidity as well. Thus the economic effect has been achieved and the damages in this church were minimally [4].

Electrical under-floor heating has been installed at the church of St. Virgin Mary's Visit Convent and the church of St. Trinity. On the first case the maintenance of this heating system was extremely expensive and has not been used for several years, until they have found some sponsors. They intend to use the heating system the following winter adjusting the intensity of heating accordingly to the rites and ordinary periods of time. On the second case the church was heated during the cold season continuously and the economical effectiveness has been achieved controlling heating intensity during events and by heating separate floor areas according to the demand. In both cases the electrical under-floor heating system has not damaged the space of interiors of the churches [4].

Radiant heating using gas has been installed at the church of St. Virgin Mary. The glass pipe of the heating device, which has been fitted in a pad of curve of arch in central nave, gives warmth while the gas is burning. This heating system has damaged the space of the interior of the church and did not produce the desired thermal effect in local places of people's presence. For these reasons this heating system has not been used in the church [4].

The present paper presents a Romanian place of worship: "Sfinţii Trei Ierarhi" (Three Holy Hierarchs) Monastery from

Iasi – demonstrates the concerns in this regard since the 1880s when, during the capital restoration was equipped with hot air central heating system, which is partially functional in present.

The solution has been designed in the Engineering Office of F.R. Richnowski of Lemberg, between 1885 and 1886. Indoor premises heating was made with air heated in a central station powered by wood, located in a specially designated place in the church basement. The fresh air intake and the flue were located outside the building. Air circulation is achieved gravitationally, through channels of stone and brick masonry laid under the floor to which air intake and discharge ports are connected, arranged on a perimeter basis at the floor level and distributed evenly in the middle of the church ("pronaos"), in front ("naos") and inside the altar. The importance of ventilation and heating system, from an operational point of view and especially for the conservation of unique ceremonial objects and works of art housed inside the cathedral, is such as to justify the technical interest in the cutting-edge solution proposed by the restorer as well as for its efficiency.

Unfortunately, the lack of written documents does not allow us to obtain further information on the subsequent operation of the installation

2. Case Description

The problem studied in the base case is taking into account the present HVAC system of the Three Hierarchs Monastery. This situation is presented in Figure 1.

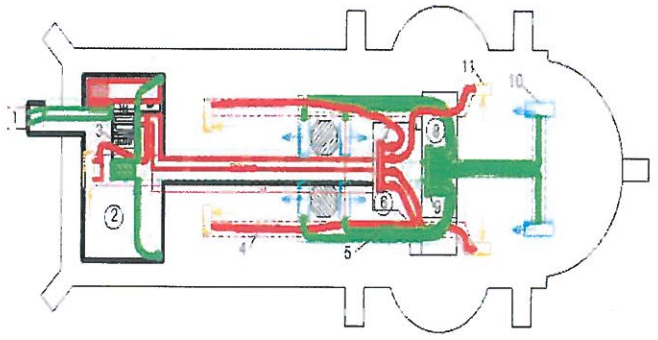

Fig. 1. *Networks existing air channels under the floor: 1-fresh air intake channel; 2-basement of porch; 3- air handling unit; 4-flexible pipe connected to the suction grid; 5- flexible pipe connected to the outlet grid; 6- suction chamber;7- exhaust air collector; 8- pressure side chamber; 9- treated air collector; 10-outlet grid; 11-suction grid*

The second one is obtained by improving the actual situation. The third and fourth cases are created in order to compare another two largely used heating systems for this type of building.

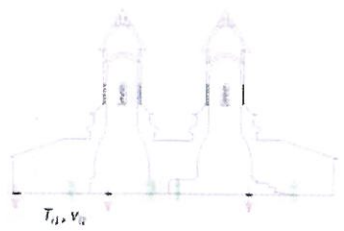

Fig. 2. *Base case: air heating system - without tower ventilation*

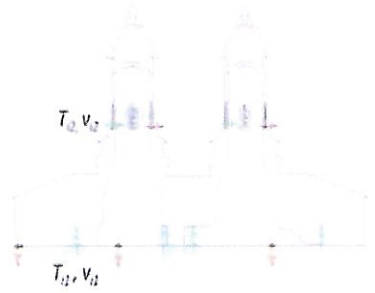

Fig. 3. *Improved case: air heating system - with tower ventilation*

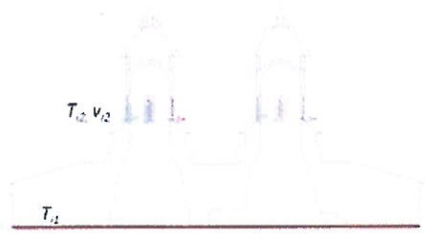

Fig.4. *Under floor heating*

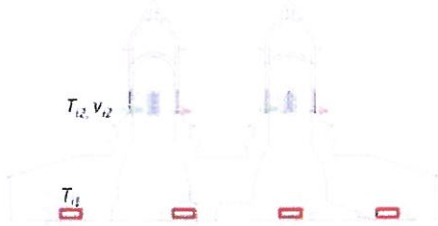

Fig.5. *Static heaters*

3. Numerical modeling

The numerical model is realized using ANSYS-Fluent software, in steady state regime. The type of flowing is the turbulent one: - k- ε RNG model.

A 2D model was created for the longitudinal section of the building. The geometrical dimensions used were those of the real building. The external conditions imposed to the walls and windows in simulations were the temperature of air of -18 °C and the convective heat transfer coefficient of 24 W/m^{2}K.

4. Results

The numerical results were obtained as temperature and velocity spectra and profiles. The qualitative information on the flowing can be observed in the following images - Figures 6-10.

For obtaining the quantitative data in figure 10 are concentrated the values of velocity at 1 m height from the floor in the studied cases.

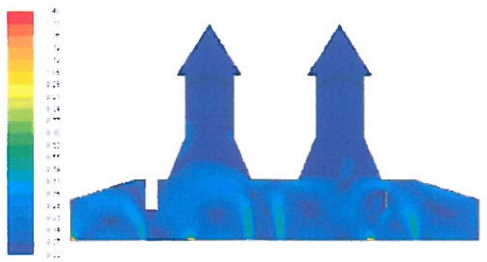

Fig. 6. *Velocity spectrum – base case*

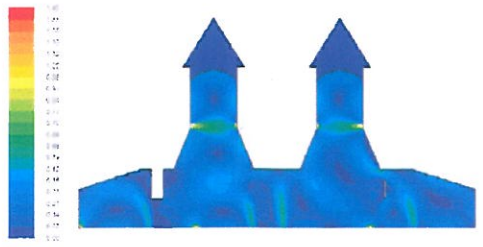

Fig. 7. *Velocity spectrum – proposed case*

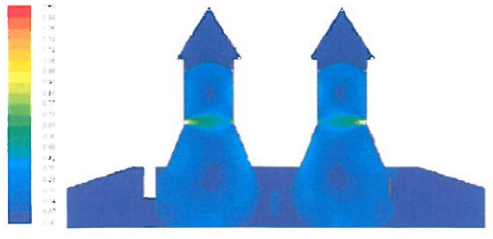

Fig. 8. *Velocity spectrum – under floor heating*

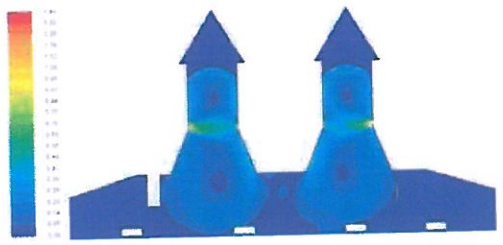

Fig. 9. *Velocity spectrum – static heaters*

Analyzing the velocities in the studied cases some particularities can be remarked. In the base case is presented the currently implemented solution that consists of heating and ventilation of the church by air. In this case the air recirculation at the inferior zone leads to a homogenous temperature.

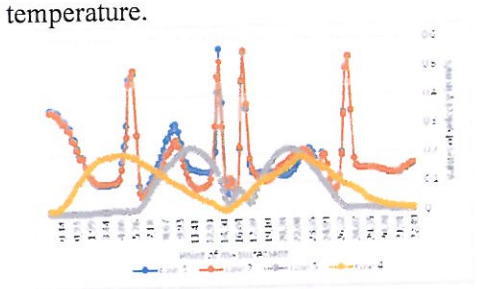

Fig. 10. *Profiles of velocities at 1 m height*

Analyzing the velocities in the studied cases some particularities can be remarked. In the base case is presented the currently implemented solution that consists of heating and ventilation of the church by air. In this case the air recirculation at the inferior zone leads to a homogenous temperature.

The 4 air inlets can be observed with velocities of 0.5 m/s and the two outflows with velocities of maximum 1.4 m/s. In the same time, the poor circulation of the air inside the two towers is affecting that zone, with a high risk of condensation.

Therefore, a local ventilation of the towers is proposed in order to evacuate humidity and eliminate condensation. This configuration is presented in Figure 7 of the presented study. Under the effect of ventilation the velocities rise inside the towers and evacuate the excess of humidity.

The other two cases studied are taking into account two heating solutions that are largely used in churches: Figure 8 – Under floor heating and Figure 9 – Static Heaters, combined with the solution of ventilation the towers. With respect to the air circulation, the two solutions are almost the same.

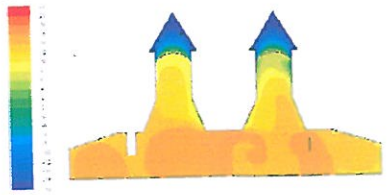

Fig. 11. *Temperature spectrum – base case*

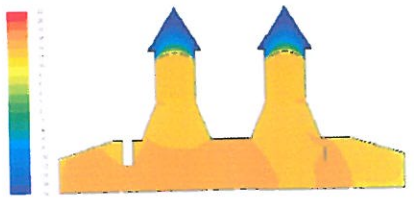

Fig. 12. *Temperature spectrum – proposed case*

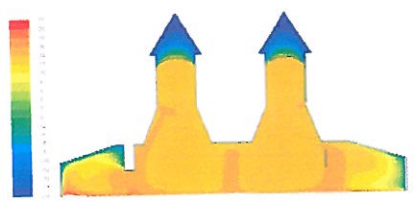

Fig. 13. *Temperature spectrum – under floor heating*

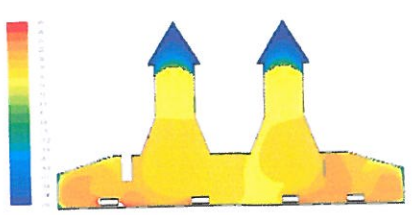

Fig. 14. *Temperature spectrum – static heaters*

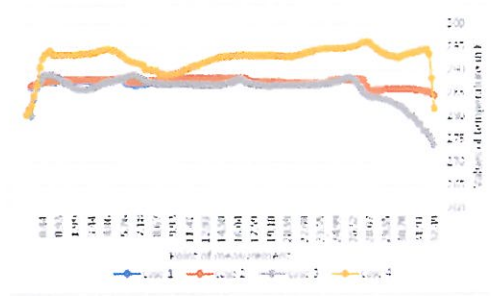

Fig. 15. *Profiles of temperatures at 1 m height from the floor*

The distribution of temperatures underlines the effect of air flow for each configuration. In this way, the main problem is detected for the base case, where is recorded a low temperature of the air in the towers and their walls. For the second case, the effect of using the local ventilation can be seen in the raise of temperatures in these zones.

In case of using under floor heating the low velocities at both extremities of the church determine the decrease of the temperature near the walls.

When static heaters are used it can observed a non-uniform distribution of temperatures, especially in the occupation zone.

In the first three cases – Figure 15, the temperature at 1 m height has similar values of approximate 15 °C. The chart of temperatures in case of static heater is influenced by their presence, but as average value, the temperature in the occupation zone is almost 15 °C.

5. Conclusions

The solution of local ventilation in towers enhanced the evacuation of humidity and reduces the risk of condensation.

In the occupational zone, the use of ventilation in towers does not affect the distribution of temperatures and velocities;

With under floor heating system and static heaters, the use of ventilation in towers generates two recirculation of air below them which creates a gradient of temperatures rising towards the sides of the church;

The second case, with hot air heating, is the most appropriate for keeping the comfort parameters in the occupational zone.

References

1. Dario Camuffo and Antonio della Valle: "*Church heating: A balance between Conservation and Thermal Comfort*", Experts Roundtable on Sustainable Climate Management Strategies held in Tenerife, Spain in April 2007
2. Tor Bronström (Sweden): "*Fundamentals of indoor climate" at the seminar in Riga regarding "Indoor Climate in Churches – Problems and solutions"*, November 2004
3. Ulf Chriestensen (Norway): "*Heatin strategies in Norway" at the seminar in Riga regarding "Indoor Climate in Churches – Problems and solutions*", November 2004
4. Diana Piksriene (Lithuania): "*Heating devices and their influence on the interiors of cold churches" at the seminar in Riga regarding "Indoor Climate in Churches – Problems and solutions*", November 2004
5. Theodor Mateescu: "*Ensuring the microclimate in religious buildings – Historical testimonies-*", XXIVth National Conference Building Services and Energy Economy, Iaşi, 3-4 July 2014, vol. I